

# Auditory Processing in the Binaural Brainstem in a Mouse Model of the Fragile X Syndrome

Inaugural-Dissertation  
to obtain the academic degree  
Doctor rerum naturalium (Dr. rer. nat.)  
submitted to the Department of Biology, Chemistry and Pharmacy  
of Freie Universität Berlin

by

Nikodemus Geßele  
from Haag in Oberbayern

2017

Supervisor: Prof. Dr. Ursula Koch

Second expert appraiser: Dr. Daniela Vallentin

Day of the oral defense: 04.04.2018





*Für Theresa und Vincent*



---

# 1 Contents

1	Contents.....	7
2	Summary .....	11
3	Zusammenfassung.....	13
4	Introduction .....	15
4.1	The auditory system of mice as a model to study altered neuronal processing in a neurological disorder.....	15
4.1.1	An evolutionary drive for the formation of sensory systems .....	15
4.1.2	The nature of sound and its perception .....	16
4.1.3	The general organization of the auditory system of mammals.....	16
4.1.4	Characteristics and adaptations of hearing in mice .....	18
4.1.5	Interaural level differences are initially processed in the lateral superior olive.....	19
4.1.6	LSO circuitry as a model to quantify the balance of inhibition and excitation.....	20
4.1.7	Temporal fidelity is a prerequisite for basic auditory processing .....	21
4.1.8	LSO neurons are tuned to a limited range of frequencies .....	22
4.1.9	Spatial arrangement of cells depending on their characteristic frequency .....	22
4.2	Fragile X syndrome.....	26
4.2.1	Auditory processing in a genetically engineered mouse model of FXS.....	26
4.2.2	The lack of FMRP enhances excitatory signaling.....	28
4.2.3	Adaptation to repetitive sensory stimulation is affected in FXS.....	29
4.2.4	Enhanced excitability is already reflected at the level of the LSO.....	30
4.3	Hypothesis.....	32
4.4	Aim of this study .....	32
4.5	Statement of significance .....	32
5	Material and methods .....	33
5.1	Animals .....	33
5.2	Breeding .....	33
5.3	Genotyping.....	33
5.4	Immunohistochemistry.....	34
5.5	Confocal microscopy.....	34
5.6	<i>in vivo</i> recordings .....	35
5.6.1	Preparations and anesthesia.....	35
5.6.2	Surgery .....	35
5.6.3	Animal monitoring .....	36

5.6.4	Sound generation and delivery .....	36
5.6.5	Sound stimuli and recording protocol .....	38
5.6.6	General stimulus presentation parameters.....	41
5.6.7	Data acquisition.....	42
5.6.8	Iontophoretical labeling and histological reconstruction of recording sites.....	42
5.7	Data Analysis .....	43
5.7.1	Regression analysis .....	43
5.7.2	Ratio of responsiveness .....	44
5.7.3	ILD values .....	44
5.7.4	Q values.....	44
5.7.5	Assessment of temporal precision.....	45
5.7.6	Statistical tests .....	46
6	Results .....	47
6.1	The lateral superior olive of mice.....	47
6.1.1	Anatomy and neurotransmitter distribution is comparable to other rodents .....	47
6.1.2	Monaural features of a binaural nucleus.....	48
6.1.2.1	LSO principal cells respond to acoustic signals with pronounced onset firing....	50
6.1.2.2	Subtle differences in onset firing are categorized by the ratio of responsiveness	50
6.1.2.3	Auditory neurons are spatially organized regarding their characteristic frequency . .....	51
6.1.2.4	LSO cells respond reliably with short latencies and small jitter .....	54
6.1.2.5	Rapid stimulation with click trains induces an effect of adaptation.....	55
6.1.3	Response characteristics of binaural stimulation.....	58
6.1.3.1	Rising contralateral sound intensity gradually suppresses ipsilateral excitation..	58
6.1.3.2	Minor effect of adaptation is based on postsynaptic mechanisms.....	60
6.2	Altered auditory processing in the LSO of FXS mice.....	62
6.2.1	LSO cells of FXS mice show slightly elevated responses.....	63
6.2.2	Frequency tuning is broadened in FXS animals.....	64
6.2.3	First spike latency and jitter are affected only for particular stimulation.....	65
6.2.4	Increasing the stimulation rate cause a faster decrease of temporal precision in <i>Fmr1</i> KO animals.....	66
6.2.5	ILD processing of pure tones is shifted in KO animals.....	68
6.2.6	A loss of FMRP does not change the response following excessive stimulation....	70
7	Discussion .....	73
7.1	General firing patterns of mouse LSO cells show differences to other mammals .....	73
7.2	Characteristic frequencies are spatially organized with spectral limitations.....	74
7.2.1	Distribution of CFs covers only a part of the perceptible frequencies .....	74

---

7.2.2	Tonotopic arrangement is less pronounced in comparison to other mammals.....	75
7.3	A differential examination of the temporal fidelity of neuronal responses.....	75
7.3.1	Small jitter portrays a temporally precise nucleus with promoted click processing in FXS .....	76
7.3.2	Repetitive click stimulation reveals recessive temporal accuracy for increasing activation in <i>Fmr1</i> KO animals.....	76
7.3.3	Elevated responses of <i>Fmr1</i> KO animals are contrasted by fewer multiple spikes .	77
7.4	Frequency tuning is broadened in FXS mice .....	78
7.4.1	Balance of excitation and inhibition could be disturbed .....	78
7.4.2	Impaired tonotopic refinement during ontogeny could reduce spectral resolution ..	79
7.4.3	Tuning bandwidths of other auditory nuclei show contradictory Q values.....	80
7.5	A lack of FMRP causes a shift in the processing of interaural level differences.....	81
7.5.1	Smaller ILD values for pure tones could reflect enhanced excitability in <i>Fmr1</i> KO animals .....	81
7.5.2	Suppression efficacy is reduced in FXS.....	82
7.5.3	ILD values are scattered across the behaviorally relevant range .....	83
7.5.4	ILD values depend on spectral content .....	85
7.6	Processing of pure tones after repetitive stimulation is not affected in FXS .....	86
7.6.1	Artificial adaptation results from strong activation of LSO cells.....	86
7.6.2	Altered cortical adaptation in FXS is not reflected at the level of the LSO .....	87
7.6.3	Ion channel interactions of FMRP have no effect on response strength .....	88
7.7	Concluding remarks .....	89
8	References .....	90
9	Abbreviations .....	105
10	Acknowledgments.....	107



## 2 Summary

The fragile X syndrome (FXS) is the most common inherited cause of autism and intellectual disabilities in humans. A mutation of the *Fmr1* gene on the X chromosome leads to a reduced or abolished expression of the protein FMRP and induces a broad spectrum of symptoms. Amongst different features related with autism, a large number of patients report impairments in the processing of sensory information, including hypersensitivity to acoustic stimuli, audiogenic seizures and decreased habituation and adaptation. Using genetically engineered *Fmr1* KO mice, an altered transmission of neuronal signals could already be shown in higher centers of the auditory pathway. These results illustrate a general increase of neuronal activity. However, it remains unclear if this is a result of excessive excitation or reduced inhibition and where the origins are to be found.

The lateral superior olive (LSO) is the first nucleus to receive and process binaural information. Principal cells compare sound intensity differences between both ears to help localizing a sound source in space. Excitation from the ipsilateral ear becomes gradually suppressed by contralateral inhibition when a sound source is moving from the one side of the head to the other. This characteristic allows to assess the excitatory drive alone and the interplay of excitation and inhibition at the same time by presenting acoustic stimuli to one or both ears of the animal. Using *in vivo* extracellular single unit recordings, we aimed to discover, if either excitation or inhibition is altered in FXS mice already at this basic nucleus of the auditory pathway. A comparison of wildtype and *Fmr1* KO animals helped to identify, which features of auditory signal transduction are affected at this early stage of sensory processing. As to date only very limited *in vivo* data of the LSO of mice is accessible, we initially had to characterize the response properties of its principal cells.

The expected basic features showed to be comparable to other mammals, with some minor adaptations regarding accentuated firing patterns and spectral limitations. A lack of FMRP as a consequence of the *Fmr1* knock-out, however, showed to affect the general firing pattern. Neuronal responses to stimulation with white noise bursts, click sounds and pure tones were slightly increased, including enhanced firing and differences in timing. Response bandwidth of frequency tuning was significantly broadened and the processing of intensity differences between ears was shifted. These results indicate an enhanced excitability in *Fmr1* KO animals already at the level of the auditory brainstem. Yet, characteristic features of FXS like reduced adaptation or delayed responses were not significantly affected. This implies that cortical impairments as a result from a lack of FMRP are already formed at the beginning of the auditory path as a model of the signal cascade in central processing. However, most observed differences are only mildly altered, leading to the conclusion for a gradual augmentation of impairments throughout the course of signal transduction.



### 3 Zusammenfassung

Das Fragiles-X-Syndrom (FXS) stellt die häufigste Ursache für erblich bedingten Autismus und geistige Behinderung beim Menschen dar. Hierbei führt eine Mutation des *Fmr1*-Gens auf dem X-Chromosom zu einer Fehlproduktion des Proteins FMRP und verursacht somit ein breites Spektrum an Symptomen. Neben Ausprägungsformen des Autismus berichten viele Patienten von Problemen in der Verarbeitung sensorischer Informationen. Dazu zählen unter anderen Überempfindlichkeit von Hörwahrnehmungen, akustisch induzierte Epilepsien und beeinträchtigte Habituation und Adaptation. Mithilfe von *Fmr1* knock-out Mäusen konnten bereits Veränderungen der Signalübertragung in unterschiedlichen Hirnregionen demonstriert werden. Diese Ergebnisse zeigen eine generell erhöhte neuronale Aktivität. Dabei ist unklar, ob dies eine Folge von verstärkter Erregbarkeit oder verminderter neuronaler Hemmung ist. Zudem ist der Ursprung dieser veränderten Verarbeitung weitgehend unbekannt.

Die laterale superiore Olive (LSO) des Hirnstamms ist die erste Station der aufsteigenden Hörbahn, die Signale von beiden Ohren verarbeitet. Hier werden Intensitätsunterschiede von Schallen zwischen beiden Ohren verglichen und tragen somit zur Lokalisation einer Schallquelle bei. Exzitatorische Eingänge des ipsilateralen Ohres werden durch ansteigende Inhibition des anderen Ohres graduell unterdrückt, je weiter sich eine Schallquelle von der einen auf die andere Seite des Kopfes bewegt. Dank dieser Eigenschaft kann sowohl die Exzitation allein als auch das Zusammenspiel von erregenden und hemmenden Eingängen mittels akustischer Stimulation und gleichzeitiger extrazellulärer Einzelzelleitungen *in vivo* untersucht werden. Ein Vergleich zwischen Wildtyp- und *Fmr1* Knock-out-Mäusen diente hierbei zur Klärung, welche Merkmale bereits in dieser frühen Stufe der Signalübertragung bei FXS betroffen sind. Da bislang so gut wie keine *in vivo* Daten zur LSO von Mäusen vorliegen mussten wir im Vorfeld die Antworteigenschaften der Hauptzellen untersuchen.

Mit Ausnahme des Feuerverhaltens und spektraler Anpassungen zeigten sich hier keine Unterschiede zu bisher untersuchten Säugetieren. Ohne FMRP, als Folge des *Fmr1*-Knockouts, zeigte sich das generelle Feuerverhalten allerdings verändert. Auf die Präsentation von weißem Rauschen, Clicks und Reintönen reagierten die Zellen mit leicht verändertem Antwortverhalten, was sich unter anderem in verstärktem Feuern und Unterschieden im Timing zeigte. Die Bandbreite des Frequenztonings war vergrößert und die Verarbeitung von Intensitätsunterschieden zwischen beiden Ohren beeinträchtigt. Die meisten Aspekte der Adaptation waren in beiden Genotypen hingegen zu vernachlässigen. Diese Ergebnisse legen nahe, dass die Signalverarbeitung bei FXS als Folge einer verstärkten Erregbarkeit bereits auf der Ebene des auditorischen Hirnstamms verändert ist. Veränderungen scheinen damit bereits sehr früh in der Signalverarbeitung aufzutreten, wenn auch in

abgemilderter Form. Dies lässt den Schluss zu, dass die Beeinträchtigungen entlang der auditorischen Bahn schrittweise zunehmen.

## 4 Introduction

### 4.1 The auditory system of mice as a model to study altered neuronal processing in a neurological disorder

Innumerable ways emerged in the history of science to investigate the fundamentals of diseases and their physiological processes. In the course of such research, it is commonly not feasible to directly examine the origin of a disorder. For technical or ethical reasons, it is often necessary to design strategies to evade this inaccessibility. In the present case, we aimed to study the physiological basics of the fragile X syndrome (FXS), a prevalent inheritable cause for mental retardation and autism in humans. Among a large number of other symptoms, it is known that this disorder is associated with sensory processing deficits. This emanated the idea to elucidate neurophysiological changes in this phenotype using the auditory system as a model. However, neurological research in human patients is mostly limited to noninvasive approaches. The possibility to generate genetically engineered mice with the same genetic and a comparable phenotypical background to human FXS patients offered the possibility to investigate neuronal processes in closer detail. In this study, the auditory system of such mice served as a model to illuminate the basics of altered neuronal processing in FXS.

#### 4.1.1 An evolutionary drive for the formation of sensory systems

One feature of living organisms is the ability to detect information from their environment and respond to it. Protozoans recognize changes in temperature or pH and try to avoid critical values by flagellar locomotion. Trees notice the position of the sun and orientate their leaves towards it for a maximal yield of light. And seagulls returning from fishing are able to relocate their offspring in a busy colony only by listening to its individual calls. In the course of evolution, various sensory systems have been developed to survive in the struggle of life. Here, the sense of hearing plays a substantial role for numerous species. Not only prominent representatives such as bats or toothed whales rely on their auditory system, also more unexpected organisms make considerable use of acoustic information. Elephants and giraffes can produce and detect infrasound to communicate across distances of several kilometers. A reasonable number of fish species use sounds for mating and territory defense. And even plants were shown to release more pollen when ensonified with the buzzing noise of approaching bees (Attenborough, 1995). Accordingly, sound detection and processing seems to be beneficial for survival and reproduction. To perform this task, evolution emerged different strategies, fitting to the respective ecological niche and the physical and physiological prerequisites.

### 4.1.2 The nature of sound and its perception

Broken down to the basics, sound is the propagation of pressure changes of a medium, commonly radiating in waves. The velocity and the magnitude of these changes need to be within a certain range to become audible, depending on the considered perception system. Consequently, a hearing organ is a structure being responsive to pressure changes such as a membrane. For the translation into neuronal information, this membrane is typically connected to a mechanoreceptor, e.g. a hair cell. Using sound to collect and transmit information brings a number of advantages: The organism is not dependent on daylight and can thus also act and react at night or in complete darkness. The propagation of sound is much faster compared to other sensations such as olfaction. Moreover, it is possible to gather and exchange information across longer distances than tactile perception or electroreception, up to as far as hundreds of kilometers (Risch et al., 2012). In addition, sound can overcome obstacles and pass through objects or matter, which are impermeable to light. Consequently, it is not surprising that numerous species developed their own strategies to benefit from the perception of sounds. For example, several fish species use their swim bladder to perform this task, many insects developed tympanal organs on their integument and amphibians often show elaborated tympanums (Rossing, 2015).

### 4.1.3 The general organization of the auditory system of mammals

Sound processing in mammals follows the same principal mechanisms as in other hearing animals, but shows some individual adaptations. In general, the propagating waves of a sound source are accumulated and augmented at the animal's pinnae and conveyed to the eardrum via the ear canal. This membrane transduces the pressure fluctuations of air into mechanic oscillation and forms the borderline between outer and middle ear. One apomorphy of mammals, i.e. a common inherited feature only found in the respective taxon, is the development of an elaborated middle ear with three ossicles (Figure 1A). Here, the oscillations of the eardrum are modified and transmitted onto the oval window, a membrane covering the inner ear. This bony structure contains the cochlea and the vestibular system and is filled with endolymph, a fluid with a unique ionic composition. Necessarily, air-born sound has to be transformed into an oscillating fluid. To perform this task and to facilitate translation efficiency, the ossicles serve as an impedance converter. Inside the cavities of the spiral cochlea, the basilar membrane with the Organ of Corti holds hair cells as mechanoreceptors. This membrane is of about 30 mm length in humans and coils up the entire cochlea. As sound is transmitted via eardrum and ossicles onto the endolymph of the inner ear, the basilar membrane responds to the oscillations of the surrounding fluid. Depending on the frequency of the sound and the consistency of the basilar membrane, a certain part of the membrane responds best, or resonates,

resulting in a maximal deflection at this point (Figure 1B). Hair cells at the respective segment of the

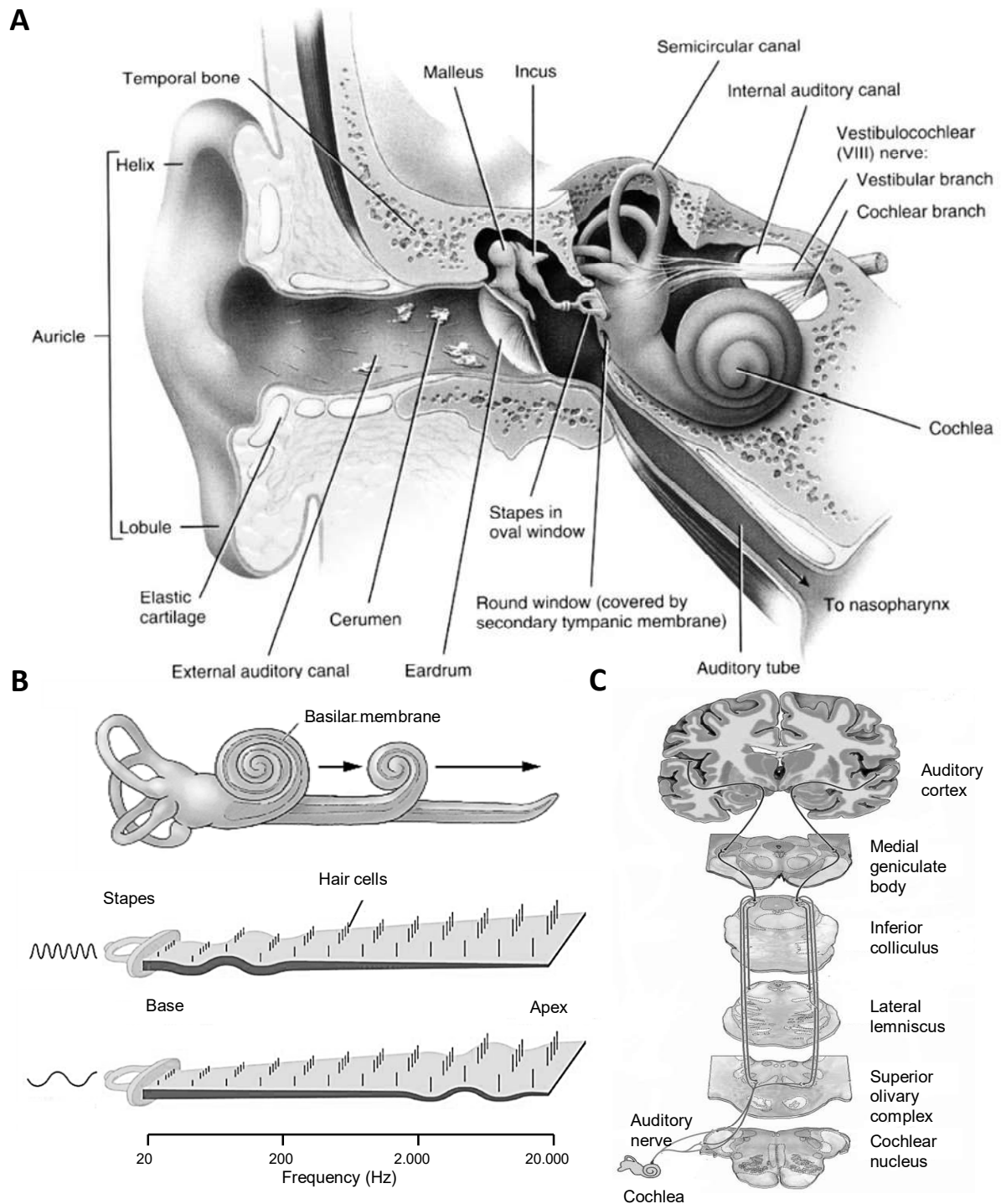


**Figure 1:** The auditory system of humans. **A:** Schematic section of the human ear. Adapted from Tortora and Nielsen, 2013. **B:** Figurative unreeing of the human basilar membrane. Stimulation with low or high frequencies deflects different sections of the membrane. This characteristic is the basic principle for a tonotopic arrangement auf the auditory system. Adapted from Kennedy et al., 2009. **C:** Ascending auditory pathway. Adapted from Purves et al., 2012.

basilar membrane convert this mechanic deflection into neuronal information, comparable to an analog digital converter. From this point, the auditory nerve transmits the deciphered acoustic information to the first relay station of the auditory system in the central nervous system, the cochlear nucleus (Figure 1C). In this brain area, located at the lateral edges of the auditory brainstem, basic filter operations and signal transformations are performed. A prominent feature of this nucleus is the relay function. From here, acoustic information is sent via three major pathways to successive centers of the auditory system. Following one of these pathways, the ventral acoustic stria (VAS), neuronal signals are propagated to a multipartite cellular agglomeration in the ventral part of the ipsilateral pons, the superior olivary complex (SOC). This area is divided into several smaller nuclei, each with distinct functions. Moreover, a subdivision of the VAS crosses the midline of the brain, projecting to the contralateral SOC and other nuclei of the auditory system. Following multiple steps of conversion, filtering and integration in numerous nuclei, the three major streams of the auditory brainstem converge in a prominent structure of the midbrain, the inferior colliculus (IC). This complex brain area mainly combines and integrates the receiving information, in turn projecting to a nucleus of the auditory thalamus, the medial geniculate body. Subsequently, the auditory information is routed to several areas of the auditory cortex, where it is ultimately processed and interpreted as conscious sound impressions. Despite this vast amount of computational steps and a considerable number of intercalated nuclei, the auditory system of mammals is strikingly fast. Studies in humans report a delay of only about 50 ms for a sound reaching the eardrum to conscious perception (Schnupp et al., 2012).

### 4.1.4 Characteristics and adaptations of hearing in mice

Wild house mice (*Mus musculus*) live in hierarchically organized colonies of up to 50 individuals. For intraspecific communication, these animals mainly use olfactory and acoustic signals. Courtship, breeding and warning calls are well documented and show a considerable repertoire of syllables and songs (Sewell, 1972; Haack et al., 1983; Hofer et al., 2002; Holy and Guo, 2005). Accordingly, acoustic communication plays a key role for social interaction. In addition, mice serve as preferred prey for various predators such as cats, weasels and foxes. The best strategy for survival is to quickly detect these carnivores and hide in a safe place. In this case, acute hearing is remarkably beneficial. Moreover, the proportionally large pinnae of mice are an apparent indicator that hearing is of substantial importance for these animals.

Research of the past decades showed a well-developed auditory system in mice. Thresholds for the perception of sound pressure fluctuations are reported to be comparable to other rodents or mammals living in similar environmental conditions and ecological habitats (Fay, 1988; Heffner and Heffner, 2007). Likewise, the ontogenetic development of hearing in mice is consistent with other animals,

showing a hearing onset around postnatal day 12 (Romand, 2012), prior to the opening of the eyes some days later.

The main stages of the auditory system are in accordance with what is known from other mammals, yet few alterations are reported. For example, the spectrum of audible frequencies is adapted to the biologically relevant range. Mice are able to perceive sound frequencies between 2 and 90 kHz (Heffner and Heffner, 2007). Thus, the lower limit is almost five octaves higher compared to humans. At the upper edge of the spectrum, they exceed our hearing range with more than two octaves. The most relevant band of the entire range is suggested to cover frequencies inaudible for humans. This explains the impression that mice do not communicate as sophisticated as it has been shown for other species. In fact, calls of social interaction are reported to range from 30 – 110 kHz, hence entirely located within the ultrasonic frequency range and thus not detectable for human ears (Sewell, 1972; Haack et al., 1983; Hofer et al., 2002; Holy and Guo, 2005). Only few vocalizations of distress and aggression are low enough to become perceptible for the human ear. Thus, it is not surprising that their hearing range is shifted in favor of higher frequencies. In accordance with this distribution of the audible spectrum, adaptations at the level of the central nervous system can be observed. In the mammalian brain, a specialized structure for binaural processing of low frequencies can be found, the medial superior olive (MSO). Consequently, in species with pronounced low-frequency hearing this brain area is commonly well developed. In mice however, this region is of comparably small size. On the other hand, structures known for their preference for the processing of high frequencies are well represented in the auditory pathway of mice. One of these brain areas is the lateral superior olive (LSO), a nucleus primarily known to be involved in the localization of sounds (Pickles, 2008).

#### 4.1.5 Interaural level differences are initially processed in the lateral superior olive

Localizing a sound source in space is a central feature of environmental perception. For both, predator and prey, mastering this challenge is essential for survival and thus for successful reproduction. This evolutionary pressure led to the development of different mechanisms to perform this task. Depending on the laws of physics, different approaches can be used to localize a sound in space. Taking only the azimuthal plane into account, an animal can compute the location of a sound source by using the differences of this sound at spatially separated acoustical sensors as e.g. tympanal organs or eardrums. These could be differences in arrival time, sound intensity or spectral content. For two fairly well separated sensors, such as for example human ears, the different arrival times of a sound coming from one side of the head can be used as a veritable cue to localize a sound in the azimuthal plane. For smaller heads, and thus for closer placed ears, the relative differences in arrival time is decreased, resulting in a less precise resolution. For humans, with an average distance of 17.5 cm between the entrances of both ear canals, the smallest resolvable interaural time difference (ITD) could be measured with about 10  $\mu$ s (Schmidt et al., 1953; Mills, 1958). With either mathematical

modeling or empirical investigations, this results in a minimum distinguishable angle of approximately  $1.8^\circ$  in the azimuthal plane. Transferred to the size of a mouse head, mice were hypothetically only capable of discriminating two points in space of at least  $33^\circ$  displacement. For the precise localization of a hunting predator, this minimal audible resolution would be insufficient.

Especially in the high frequency range, using intensity differences instead of time differences is more effective. Diverging sound pressure levels at both ears result from mainly three different factors: Sound levels of typically radiating sound waves drop when covering a distance, irrespective of frequency or propagation medium. Overcoming an obstacle like an animals head additionally decreases sound intensity at the distal ear and results in a sound shadow. Moreover, the damping influence of air, which plays a comparatively subtle role for sounds of low frequencies like in the human main hearing range, increases dramatically with rising frequency (Blauert and Xiang, 2009). Markedly the latter makes interaural level differences (ILDs) a powerful tool to localize sounds for animals with hearing ranges covering the ultrasonic frequency range.

The integration and computation of ILDs is being performed at several stages of the auditory pathway throughout the mammalian brain (Klug et al., 1995; Irvine et al., 1996; Park et al., 2004). The LSO is the first nucleus in this pathway to receive inputs from both ears and to compare level differences between them (Boudreau and Tsuchitani, 1968; Tollin, 2003). Located in the SOC of the brainstem, this nucleus has been extensively studied in a variety of species for almost 100 years (Hines, 1921; Rasmussen, 1946; Gillaspy, 1958; Opdam et al., 1976; Fech et al., 2017). In anatomical studies, three major cell types have generally been identified using Golgi stainings: principal, marginal and multipolar (Helfert and Schwartz, 1986; Majorossy and Kiss, 1990; Rietzel and Friauf, 1998). Principal cells make up to 75% of the population and show a distinct bipolar or fusiform shape.

### 4.1.6 LSO circuitry as a model to quantify the balance of inhibition and excitation

The LSO receives two major inputs: Fibers from the ipsilateral cochlear nucleus (CN), predominantly originating from spherical bushy cells of the anterior ventral cochlear nucleus (AVCN), run along the ventral auditory stream and form punctuate excitatory, glutamatergic synapses on dendrites of principal cells of the LSO (Wu and Kelly, 1992a; Srinivasan et al., 2004). The second major connections are emanating from the contralateral medial nucleus of the trapezoid body (MNTB), contacting the same principal cells with more widespread glycinergic, inhibitory inputs (Figure 2). The MNTB in turn receives excitatory inputs from globular bushy cells of the AVCN of the same side, forming the largest known synapses in the vertebrate brain, the calyces of Held (Zook and

DiCaprio, 1988). Thus, the MNTB serves as an extraordinary fast and precise converter of excitatory inputs into inhibition.

The great majority of LSO cells is excited by ipsilateral stimuli and inhibited by contralateral ones (Sanes, 1990; Tollin and Yin, 2005). As a result from this circuitry, LSO cells change their response pattern to a sound, when the source of this sound is moving in the azimuthal plane. The strong and reliable response to ipsilateral stimulation becomes gradually inhibited when the sound is moving towards the contralateral side of the head. This characteristic can be mathematically described in a sigmoid

function of the approximated response to ILDs. With help of this function, the balance of inhibition and excitation can be conveniently assessed and quantified.

#### 4.1.7 Temporal fidelity is a prerequisite for basic auditory processing

The sense of hearing is the fastest sensory system in vertebrates. The conscious perception of an acoustic signal takes only 0.05 seconds in humans (Horowitz, 2013). In contrast, detection of a visual stimulus takes about four times longer (Amano et al., 2006). Moreover, the detection of subtle differences in acoustic patterns or the computation of interaural time differences in the microsecond range requires extraordinary fast and precise timing of neuronal signals. Consequently, timing plays a principal role in the auditory system. The transduction speed of neuronal signals is generally more dependent on synaptic transmission than on the absolute conduction distance (Bear et al., 2015). But not only velocity is important for a successful computation. The quality of signal transmission and the faithful conduction are even more decisive parameters. In a neuronal network, the critical points for these tasks are again the synapses. Thus, it is no wonder that the largest known synapses in the mammalian brain are found in the auditory system. The endbulbs of Held, located in the AVCN, and

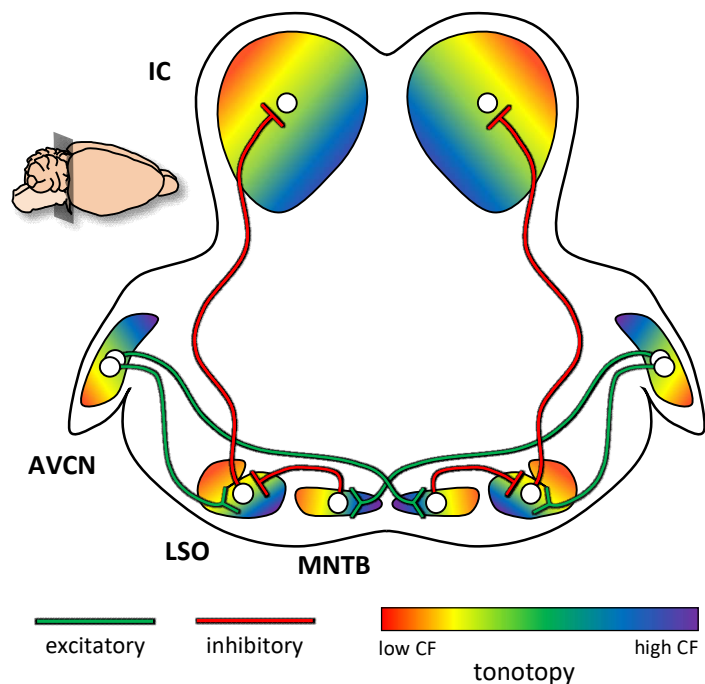


**Figure 2:** Schematic sagittal section at the level of the auditory brainstem illustrating the LSO circuitry. Top-left drawing shows location of section in the mouse brain. Excitatory neuronal connections between nuclei shown in green, inhibitory connections in red. Spatial distribution of characteristic frequencies of single cells is color coded in each nucleus.

the Calyces of Held in the MNTB are well known for their extraordinary fast and precise transduction of neuronal information (Guinan and Li, 1990; Joris et al., 1994; Paolini et al., 2001; Louage et al., 2005; Laughlin et al., 2008). Intriguingly, both nuclei have been shown to project onto principal cells of the LSO. Hence, the LSO is suspected to relay signals with high fidelity, including features such as short latency, good reliability in spike transmission, small jitter and short recovery durations, a prerequisite for the realization of rapid firing rates.

#### 4.1.8 LSO neurons are tuned to a limited range of frequencies

LSO principal cells typically respond to a variety of different sounds, such as white noise, clicks or pure tones. As a common feature of neurons in the auditory pathway and as a result of how different frequencies are translated into neuronal signals in the cochlea, LSO cells respond only to an individual, limited range of frequencies, i.e. are tuned to a certain frequency range. The frequency within this range that still elicits an action potential with the smallest stimulus intensity is called the neuron's characteristic frequency (CF)(Evans et al., 1965). The neuron also responds to higher and lower frequencies adjacent to CF, however higher sound intensities are needed to trigger a neuronal response when stimulating with pure tones at this frequency. Generally, the farther the stimulus frequency is spectrally located from CF, the higher the minimal sound intensity is necessary to elicit an action potential. Plotting of the sound intensity threshold values along a frequency axis thus results in a function, also referred to as tuning curve (Kiang et al., 1967; Javel, 1994). In most cases of mouse LSO cells, the measured tuning curves are roughly V-shaped, typically showing a steep and abrupt cut-off at the high frequency edge of the responsive spectrum. The stereotypic contours of the tuning curves allow for a convenient quantification of the properties of a unit's frequency tuning. CF, bandwidth and intensity thresholds can be easily addressed and compared. Here, a common measure is the bandwidth of the tuning curve 10 or 30 dB above the threshold at CF. This ratio is referred to as the Q value and describes the sharpness of a unit's frequency tuning (Kelly et al., 1991).

#### 4.1.9 Spatial arrangement of cells depending on their characteristic frequency

Commonly, neurons in auditory nuclei are spatially organized according to their CF, also referred to as tonotopic arrangement. This tonotopic distribution is maintained throughout large parts of the auditory pathway (see color code in Figure 2). Here, the cellular arrangement within an auditory nucleus is generally depended on the CF of the neurons. Typically, units tuned to low frequencies are located at one edge of the nucleus, whereas cells with high CF are found at the opposing side of the nucleus. This arrangement and the bandwidth of the frequency spectrum, to which an auditory neuron is sensitive, is a result of various parameters (e.g. Pickles, 2008).

### *Mechanical background of tonotopic organization*

The initial limitation is generated in the cochlea. The flexible basilar membrane inside the osseous cochlea shows a gradient in its physical resonance property. At the basis of the cochlea, next to the oval window, the basilar membrane is comparatively rigid and stiff, thus only susceptible or resonant to high stimulation frequencies. Proceeding towards the apex of the cochlea, the consistency of the basilar membrane is becoming progressively softer. The resonance frequency upon oscillating deflections from a propagating sound wave is consequently decreasing. Stimulation of the basilar membrane with a pure tone thus leads to a deflection of only the particular part of the membrane with the corresponding resonance characteristic. Consequently, only hair cells within this topographical frequency range are excited. Or vice versa, each hair cell is excited by a certain range of frequencies. Emerging from the hair cells, axonal connections project via the spiral ganglion and the auditory nerve onto auditory nuclei in the brain. Here, the location of the targeting neurons is maintained, referring to their CF (Quiroga and Panzeri, 2013).

### *Lateral inhibition shapes tonotopic arrangement*

Supplemental refinement of the tonotopic arrangement is likewise happening at the level of the cochlea. Here, adjacent hair cells display reciprocal effects, or, simply spoken, hair cells inhibit each other. The initial excitation strength of one cell yields the resulting inhibition on the neighboring cells. Consequently, the cells with the strongest excitation, i.e. located at the point of the basilar membrane with the largest deflection, have the strongest inhibitory effect onto the neighboring hair cells. This mechanism is referred to as lateral inhibition and is a common feature of sensory processing (e.g. Békésy, 1967; Sachs and Kiang, 1968; Kral and Majernik, 1996). In the auditory system, it facilitates frequency discrimination and improves the acoustic contrast between different frequencies. Additional refinement is occurring in successive stations of the auditory path. Here, a neuron's frequency response area is shaped in a similar manner (Rhode et al., 1978; Hirsch and Oertel, 1988). Excitatory feedforward effects from basic nuclei as well as inhibitory feedback loops from higher centers furthermore shape a unit's receptive field. In summary, the balance of excitatory and inhibitory inputs eventually defines the spectral resolution of the auditory system.

### *Developmental origin of the auditory brainstem circuitry*

The neuronal foundation for this characteristic is to be located in the ontogeny of the developing mammalian brain. Neuronal progenitors are initially accumulated in loose clusters, forming basic nuclei. Individual cells of these nuclei begin to spread axonal projections in different directions, eventually contacting other brain cells. Here these new axons form first fragile synapses onto dendrites and somata. Despite being directed to the correct brain area, numerous of these surplus connections do not reach their appropriate target. Consequently, these idle connections need to be

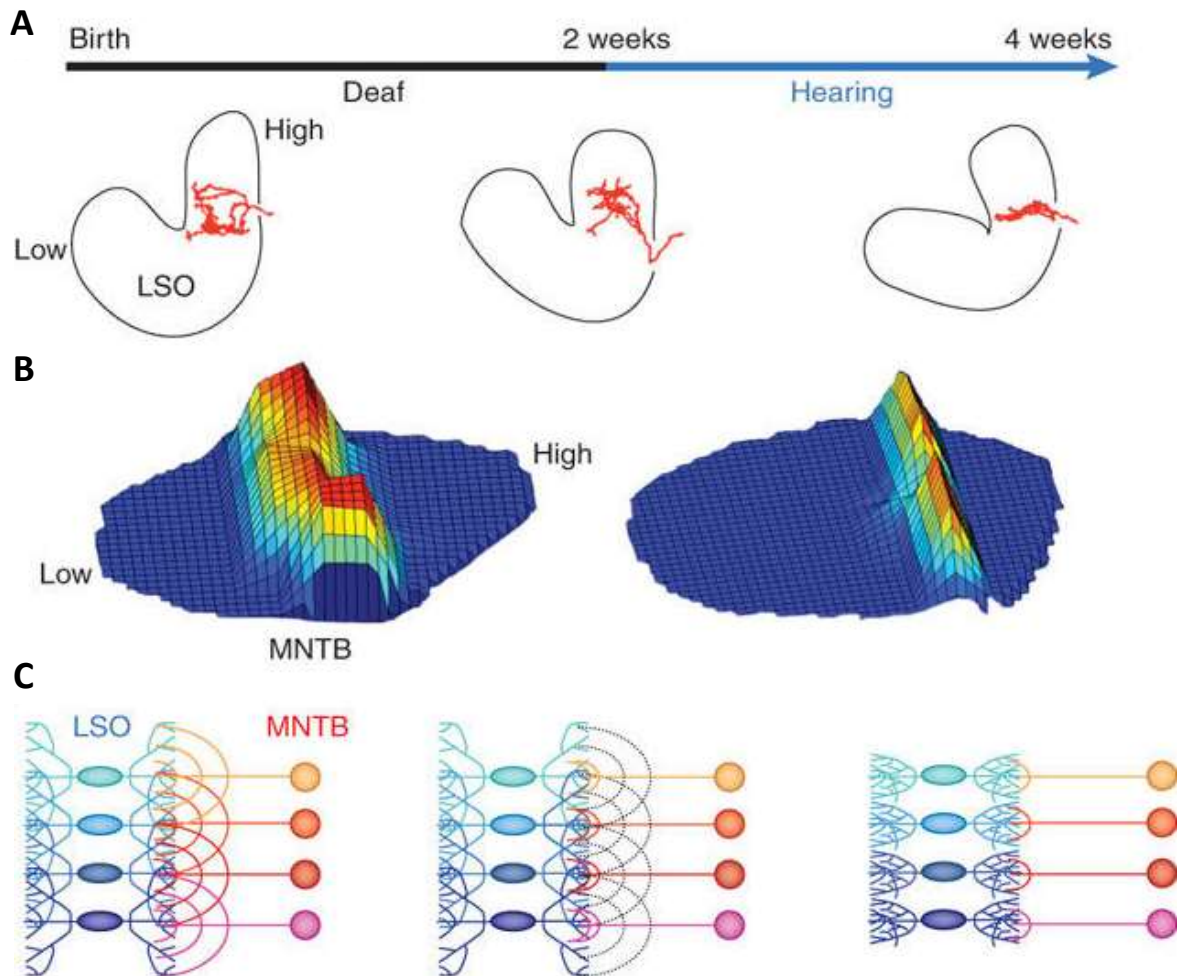


**Figure 3:** Tonotopic refinement of an inhibitory map in the LSO. **A:** Before hearing onset, MNTB axons (red) terminate in topographically restricted areas of the LSO. In the two weeks following hearing onset, the spread of MNTB axons along the tonotopic axis becomes increasingly restricted. Modified from Sanes and Kim, 1991. **B:** Before hearing onset, the area in the MNTB that contains neurons that are synaptically connected to single LSO neurons (MNTB input areas) decreases by about 75% (corresponding to a 50% increase in functional tonotopic precision). This indicates that LSO neurons become functionally disconnected from the majority of their presynaptic partners in the MNTB before sound-evoked neuronal activity is present. Modified from Kim and Kandler, 2003. **C:** Schematic diagram of MNTB-LSO refinement. Before hearing onset, MNTB-LSO connections become silenced (black-dotted axon branches) without being pruned. After hearing onset, pruning of MNTB axons and LSO dendrites occurs, increasing the anatomical tonotopic precision. Adapted from Kandler et al., 2009.

degenerated. On the other hand, correct connections have to be strengthened for fast, reliable and stable transmission of neuronal signals. This synaptic maturation is commonly achieved by neuronal transmission itself. Simply spoken, misrouted connections show a decrease in firing activity. As a result, the synaptic contacts become weaker and eventually degenerate. Contrarily, correct synaptic connections receive and transmit strong and lasting neuronal activity, hence annealing this synapse. In simplified summary, stronger neuronal activity leads to a stronger linkage of axons and their target cell. This mechanism is acknowledged and approved for the stabilization or degeneration of axonal

connections. In a variety of studies, this could be shown for inhibitory neuronal connections in the auditory system, i.e. synapses using GABA or glycine as neurotransmitter (Sanes and Rubel, 1988; Kandler and Friauf, 1995; Sanes and Friauf, 2000; Kullmann and Kandler, 2001; Gillespie et al., 2005). Comparable mechanisms are suspected to be responsible for the maturation of excitatory connections (Case et al., 2011). In case of the auditory system and the tonotopic arrangement of neurons, this maturation can be illustrated as an initially broad distribution of cochlear projections, i.e. cells in auditory nuclei are connected to a wide range of hair cells (Sanes et al., 1989). As misguided projections of neighboring hair cells gradually degenerate, the broad distribution of cochlear projections onto a single neuron becomes more narrow, also known as tonotopic refinement (Figure 3)(Kandler et al., 2009; Rubel and Fay, 2012).

In summary, the LSO circuitry makes this nucleus a valuable model to study the interaction and balance of excitation and inhibition with an immediate possibility to stimulate one or both synaptic inputs conveniently by presenting sounds to the respective ear. Various laboratories used the LSO of mice to study this interplay and its development over the past decades (Harrison and Irving, 1966; Ollo and Schwartz, 1979; Campbell and Henson, 1988; Wu and Kelly, 1991; Walcher et al., 2011). Regardless, little is known about the physiological properties of LSO neurons in living mice. To our knowledge, only one electrophysiological *in vivo* study has been published to date (Karcz et al., 2011). A compelling reason might be the factually small size of a mouse brain and thus the laborious electrophysiological assessment of this comparatively small nucleus within such a brain. Using sophisticated techniques and precise, computer controlled equipment it was now possible to acquire single unit recordings of high fidelity. Accompanied with adequate sound stimulation, separately delivered to either ear, this gave us the possibility to closely investigate the physiological response properties of individual cells in the mouse LSO. Additionally, the use of mice includes another advantage: To date, these animals are the most favorable mammalian species for genetic engineering. Moreover, mice are closely related to humans, with the protein-coding regions showed to coincide by 85% on average (Chinwalla et al., 2002). Together, this offers the possibility to induce a multitude of human genetic disorders and investigate their basic mechanisms. In the present study, we used the LSO of mice as a model to investigate changes in the balance of inhibition and excitation in an inheritable human disorder, the fragile x syndrome.

## 4.2 Fragile X syndrome

Fragile X syndrome (FXS) is a genetic disorder that causes a range of cognitive and physical impairments. It is the most common cause of inherited intellectual disability (Gustavson et al., 1986; O'Donnell and Warren, 2002; Hagerman et al., 2009; Sinclair et al., 2017) and the predominant monogenic cause of autism in humans (Webb et al., 1986; Hagerman et al., 2010). In these studies, the prevalence of FXS is reported to range from 1:4000 up to 1:1500 in males and from 1:8000 to approximately 1:3000 in females. The cause for this disorder is a mutation in the *Fmr1* gene. It is located on the X chromosome and codes for the fragile X mental retardation protein (FMRP). A sequence of this gene, known as the CGG triplet expansion, is commonly repeated about 5 - 40 times in healthy subjects. In patients with FXS, however, this segment is repeated up to 200 times or more and thus silencing the *Fmr1* gene. As a consequence, FMRP synthesis is reduced or abolished (Figure 4A; adapted from Li and Zhao, 2015). Normally, this protein is produced in many regions and tissues of the body and is involved in the regulation of several other proteins. A lack of FMRP can lead to a broad spectrum of symptoms reminiscent of autism spectrum disorder, including deficits in social behavior, delays in language development and intellectual disabilities (Barnes et al., 2009; Berry-Kravis et al., 2007; Hagerman et al., 1986; Roberts et al., 2007). Moreover, physical abnormalities like protruding ears, elongated faces, hyperflexible extremities, prominent foreheads and enlarged testes have been reported. On the molecular level of the central nervous system, *Fmr1* expression is involved in critical processes for early neurodevelopment such as synaptic plasticity and spine growth (Greenough et al., 2001; Irwin et al., 2001). Recent studies have shown sensory processing deficits including hypersensitivity to sensory stimulation (Sinclair et al., 2016), which are suspected to result from synaptic aberrations (Figure 4B; adapted from Ting and Feng, 2011). This is also supported by increased latencies in auditory brainstem response (ABR) measurements, elevated cortical responses and decreased habituation in response to sensory and especially auditory stimuli (Figures 4C,D; adapted from The Dutch-Belgian Consortium, 1994, and Ethridge et al., 2016)(Castrén et al., 2003a; Knoth and Lippe, 2012).

### 4.2.1 Auditory processing in a genetically engineered mouse model of FXS

For a better understanding of the physiological basics of this inheritable disorder, a genetically engineered mouse model was generated. The deletion of the *Fmr1* gene was achieved by insertion of a neomycin resistance gene into exon 5 of the fragile X mental retardation syndrome 1 locus on the X chromosome. As a result, production of FMRP is impaired in heterozygous females and completely suppressed in homozygous animals. *Fmr1* KO offspring show many phenotypic

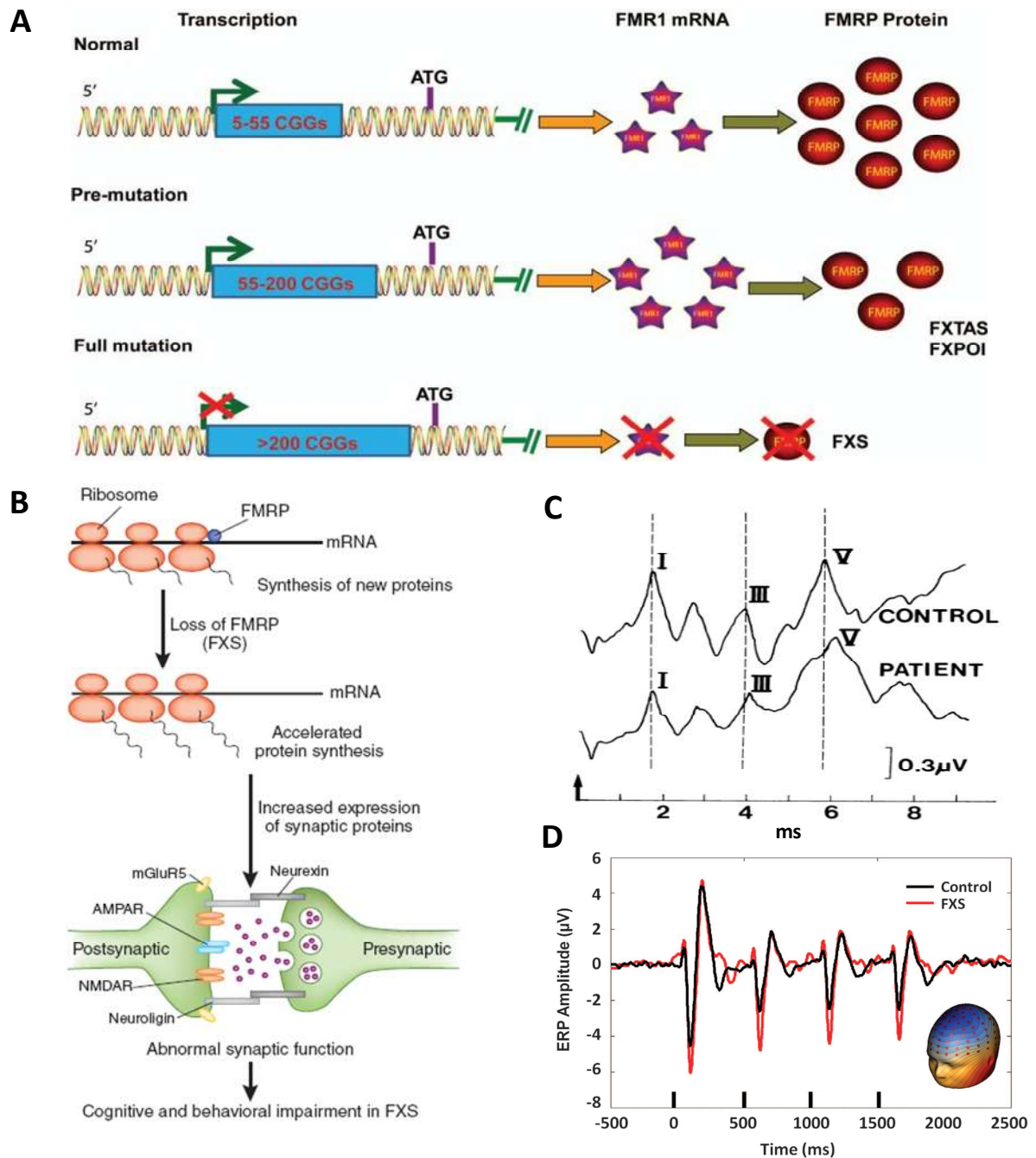


**Figure 4:** Genetic fundamentals of FXS and functional implications of a lack of FMRP. **A:** Normal individuals have fewer than 55 CGG repeats. When CGG repeat length exceeds 200, the so-called “full mutation,” the *Fmr1* gene is methylated and silenced, which is the major cause of fragile X syndrome (FXS). Adapted from Li and Zhao, 2015. **B:** FMRP can function as a translational break to stall new protein synthesis. In the absence of FMRP in FXS, the translation of many synaptic proteins are therefore accelerated, leading to aberrant synaptic function that contributes to cognitive and behavioral impairment in FXS. Adapted from Ting and Feng, 2011. **C:** ABRs in a normal individual and in a patient with FXS. Latency values for these subjects approximate respective group means. Clicks at 70 dBnHL were presented to the right ear, and recordings were derived from vertex and right earlobe electrodes (Cz-A2). Adapted from Arinami et al., 1988. **D:** EEG measurements of FXS patients show less habituation of the N1 ERP compared to healthy controls. ERP grand average PCA-weighted virtual channel plot for FXS and matched controls, with inset PCA spatial component topography. Small black bars indicate presentation of the auditory stimulus. ERP, event-related potential; PCA, principal components analysis. Adapted from Ethridge et al., 2016.

characteristics of the Fragile X Syndrome in humans, including autistic-like core symptoms of altered social interaction and occurrence of repetitive behaviors with additional hyperactivity, reduced anxiety, and increased errors in a learning assay (Consortium et al., 1994). On the level of acoustic sensory processing, elevated cortical evoked responses, defects in startle responses as well as audiogenic seizures were reported (Chen and Toth, 2001a; Knoth et al., 2014; Musumeci et al., 2000; Rotschafer and Razak, 2013a). Accordingly, in the auditory cortex of Fragile X mice both response characteristics and learning rules are altered in line with the observed auditory hypersensitivity, indicating an abnormal development of auditory cortical circuits (Kim et al., 2013; Rotschafer and Razak, 2013a). Previously, high expression levels of FMRP were shown at the level of the auditory brainstem (Wang et al., 2014). This suggests that these deficits might originate from disturbed auditory brainstem circuits and are propagated to superior centers. In FXS patients, the analysis of ABRs revealed prolonged inter-peak latencies, indicating dysfunction in auditory brainstem conduction times (Arinami et al., 1988b; Ferri, 1989; Wisniewski et al., 1991). Moreover, morphological alterations of the superior olivary complex (SOC) nuclei and neurons have been observed in post mortem tissue of subjects with FXS and autism (Kulesza and Mangunay, 2008; Kulesza et al., 2011). In this context, one of the earliest findings in cortical areas of patients and in mouse models of FXS include augmented dendritic spine counts, which are associated with excessive excitatory inputs (Bagni and Greenough, 2005a). Additionally, murine models of FXS display altered ABRs and changes in synaptic input density in SOC neurons (Rotschafer et al., 2015a).

### 4.2.2 The lack of FMRP enhances excitatory signaling

The idea of an increase in excitatory trafficking is supported by the fact that FMRP loss causes deficits in synaptic pruning in sensory cortical areas, leading to axonal overgrowth (Galvez et al., 2005; Galvez and Greenough, 2005). Similarly, FMRP promotes cell to cell pruning of excitatory connections in hippocampal cell cultures and in the neocortex (Patel et al., 2014; Pfeiffer and Huber, 2007). The physiological mechanisms contributing to this enhanced connectivity are still debated. One idea is that alterations in the mechanisms of synapse formation as a result of enhanced glutamate signaling could play an important role in this process. In this context, synaptic long-term depression (LTD) and potentiation (LTP) are substantial for synapse consolidation. The class of metabotropic glutamate receptors (mGluRs) seems to be involved in one of several described mechanism of LTD (Bear et al., 2004). Protein-synthesis-dependent LTD was shown to be exaggerated in the absence of FMRP, a functional consequence of mGluR activation. FMRP is normally synthesized following stimulation of mGluRs (Weiler et al., 1997). According to an approved model, mGluR activation normally stimulates synthesis of proteins involved in stabilization of LTD and, in addition, FMRP (Bear et al., 2004). This protein thus functions as a negative feedback to inhibit further protein synthesis. Therefore, all functional consequences of mGluR-dependent protein synthesis might be

exaggerated in the absence of FMRP. Here, especially the group 1 metabotropic glutamate receptor mGluR5 seems to play a predominant role. It is shown that this mainly postsynaptically expressed receptor type is involved in several mechanisms, which is affected in FXS patients and the corresponding mouse model. Among other indications, mGluR5 activation induces an increase in the excitability of neocortical neurons (Sourdet et al., 2003), which in turn are involved in heightened behavioral responses to sensory stimuli as reported in FXS patients (Castrén et al., 2003b). Pre-pulse inhibition of auditory startle is shown to be impaired in mGluR1/5 KO mice (Brody et al., 2003), a feature that is closely related to what is known from FXS (Chen and Toth, 2001b). Moreover, systemic application of the mGluR5 antagonist MPEP raises the threshold for audiogenic seizures (Chapman et al., 2000), a robust phenotype in *Fmr1* KO mice (Chen and Toth, 2001b). In summary, mGluR5 seems to be a promising candidate for further basic research and future treatment of fragile X syndrome.

#### 4.2.3 Adaptation to repetitive sensory stimulation is affected in FXS

When we enter a room, we immediately recognize the particular smell. After a short time, however, we will not notice it anymore. This phenomenon is called sensory adaptation. The functional relevance for this phenomenon is supposed to enhance contrast between prevailing sensory impressions and new and noteworthy signals. It is commonly understood as a decrease in the response to ongoing or repetitive stimulation. This can happen at the level of the primary receptors, such as desensitization of olfactory sensory neurons, or in the course of the processing of the elicited neuronal response, i.e. a downregulation of neuronal activity. Impairments in this mechanism are suspected to contribute to sensory hyperreactivity. In fact, reduced sensory adaptation was shown in the cortex of *Fmr1* KO mice (He et al., 2017). Additionally, also habituation seems to be affected by a lack of FMRP. Habituation is described to be the simplest form of learning, where an organism adapts its behavior to ongoing or repetitive stimulation. Studies using *Aplysia* and rats explain habituation as a result from homosynaptic depression of excitatory neurotransmission (Kupfermann et al., 1970; Castellucci and Kandel, 1974; Farel and Thompson, 1976; Weber et al., 2002). However, little is known about the underlying cellular mechanisms of habituation, such as short-term depression, depletion of neurotransmitters, receptor desensitization or inactivation of ion channels. To date, a correlation between FXS and reduced or impaired habituation is reported in a number of studies (Castrén et al., 2003a; Van der Molen et al., 2012; Schneider et al., 2013; Ethridge et al., 2016). Interestingly, a habituation phenotype including acoustic sensory processing was reported to be associated with the level of FMRP expression (Miller et al., 1999a).

FMRP was also shown to interact with a number of ion channel complexes. It stimulates the activity of the sodium-activated potassium channel Slack (Brown et al., 2010). A loss of FMRP reduces potassium currents and can thus impair the temporal precision of action potentials. Additionally,

FMRP interacts with a subunit of the calcium activated potassium channel (BK) and increases the calcium-dependent activation of this channel (Deng et al., 2013). The reduction of this channel activity leads to an elongation of action potential duration and affects synaptic short-term plasticity in *Fmr1* KO mice. These interactions are suspected to affect the processing of fast repetitive stimulation. Intriguingly, both channels were shown to be expressed in cells of the LSO of mice (Rizzi et al., 2016; Sausbier et al., 2006).

Taken together, these findings point toward a correlation between FXS and the processing of repetitive stimulation in the context of altered neuronal transmission. As most of these studies use EEG or ABR measurements of brain activity, the physiological mechanisms involved in this process are still unclear. Moreover, reduced adaptation was only shown for cortical areas of sensory processing, the source of these changes remains unclear. Thus, physiological fundamentals and the origin of altered habituation and adaptation in FXS are still elusive.

#### 4.2.4 Enhanced excitability is already reflected at the level of the LSO

Our lab already demonstrated various alterations in the LSO of *Fmr1* KO mice using immunohistochemical procedures and *in vitro* recordings on acute brain slices (Garcia-Pino et al., 2017). This study provided evidence for a strong expression level of FMRP in neurons of the LSO of WT mice, whereas KO animals were lacking this protein (Figures 5A-C). Antibody labeling against presynaptic transporter proteins indicated an increase in excitatory inputs, pointing towards an enhanced synaptic connectivity (Figures 5D-G). Whole-cell patch-clamp recordings revealed larger amplitudes of excitatory postsynaptic currents (EPSCs) in principal cells of the LSO, while inhibitory postsynaptic currents did not change (Figure 5I). Additionally, an increase in the frequency of spontaneous EPSCs (sEPSCs) was observed (Figures 5J). These findings indicate an elevated excitability and overshooting responses in *Fmr1* KO animals in correlation with a lack of FMRP. In addition, the timing of neuronal activity appeared to be affected. The latency of elicited action potentials showed larger fluctuations throughout postnatal development, ranging from delayed responses in P8 KO animals to significantly shorter latencies in adult-like individuals (Figure 5K). The theory of an enhanced synaptic connectivity is further supported by additional unpublished electrophysiological data from our lab, where a gradual increase in stimulation strength of afferent excitatory fibers revealed a larger number of synaptic inputs onto LSO neurons in KO animals. We therefore suggested an elevated number of release sites as the mechanism for the heightened excitatory transmission. However, synaptic development of the inhibitory connections from MNTB neurons onto LSO principal cells remained largely unaffected from a lack of FMRP. In summary, these results strongly support the hypothesis of an increased excitability, a shift in the balance of

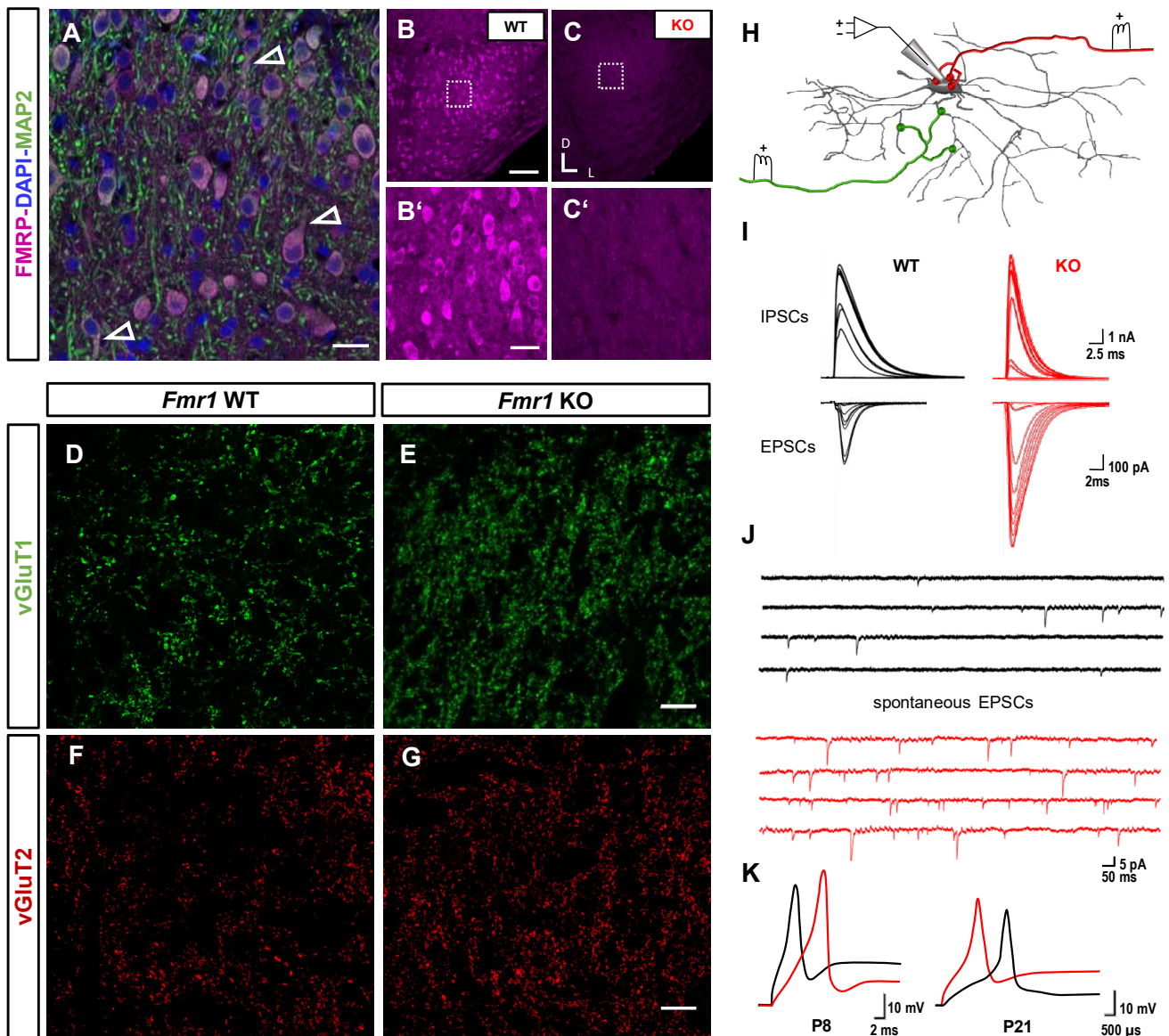


**Figure 5:** FMRP expression pattern and impact of *Fmr1* KO on developing LSO cells. **A-C:** Confocal images of LSO neurons showing immunoreactivity for FMRP with emphasis on somata and proximal dendrites (A, arrowheads). Strong immunolabeling for WT animals, no labeling for KO animals (B,C). FMRP staining in magenta, DAPI staining in blue and MAP2 staining in green. Scale bars: A&B': 20  $\mu$ m and B: 100  $\mu$ m. **D-G:** vGluT1/2 immunolabeled area of LSO coronal sections is increased for *Fmr1* KO mice. **H:** Schematic *in vitro* recording scenario from an LSO principal cell. Stimulation of green excitatory projections from the ipsilateral CN elicits EPSCs, stimulation of red inhibitory fibers from the contralateral MNTB results in IPSCs. **I:** Representative voltage traces show comparable IPSC amplitudes for WT (black) and *Fmr1* KO (red) animals (upper traces), whereas EPSC amplitudes are increased in FXS mice (lower traces). **J:** Frequency of spontaneous EPSC (sEPSC) is increased in *Fmr1* KO mice. **K:** Latency of action potential generation is shifted throughout postnatal development. Young FXS mice show delayed firing, whereas shorter latencies are observed in adult-like individuals. Adapted from Garcia-Pino et al., 2017.

excitation and inhibition and an altered sound processing already at the level of the auditory brainstem. Finally, these findings serve as framework for the present work.

### 4.3 Hypothesis

Based on earlier results in the field of research about FXS and the hitherto findings of our lab, we suppose the approved alterations in FXS at higher stages of the central nervous system to origin already at the basis of neuronal processing. In the present case, we suspect an enhanced excitability, a decrease in adaptation and a shift in the balance of inhibition and excitation observed in cortical regions of the auditory pathway to be a result of changes already at the level of the auditory brainstem.

### 4.4 Aim of this study

In this study, we examined the effect of FXS on sensory processing in LSO principal cells using electrophysiological single unit recordings *in vivo*. Emphasis was set on the investigation of increased excitability and the resulting impact on the balance of excitation and inhibition. Concomitantly, the origin of the reported cortical changes of habituation and adaptation was also subject of this research. To address these questions, LSO neurons of genetically engineered mice comprised an attractive circuit-model to assess the synaptic or somatic alterations underlying auditory hypersensitivity and adaptation processes at the brainstem level in FXS. Moreover, possible changes in the balance of excitation and inhibition as a consequence from the lack of FMRP can be conveniently investigated *in vivo* by differential stimulation of one or both ears. For a thorough investigation, we initially needed to determine the physiological properties of principal cells of the LSO of mice.

### 4.5 Statement of significance

In the past decades, numerous studies of basic and applied research have been conducted to decipher the fundamentals of the fragile X syndrome in humans and to develop effective treatments of this disorder. To date, some symptoms can be mitigated, the underlying mechanisms and the origins of these symptoms, however, remain largely elusive. The revelation of the basic cause of altered sensory processing as a representative model can thus help to understand this disorder in more detail.

## 5 Material and methods

### 5.1 Animals

All experiments were performed in accordance with the German animal welfare legislation and approved by the Landesamt für Gesundheit und Soziales, Berlin (Germany). *Fmr1* KO and wild-type founders were obtained from Jackson Laboratories (FVB.129P2-Pde6b+ Tyrc-ch *Fmr1*tm1Cgr/J, stock no. 004624). This strain was chosen in accordance to the majority of previous scientific work on FXS in mice. Further crossings were done in the animal facility and homozygous *Fmr1* KO and wild-type littermates of both gender were used for the experiments. Mice were housed in the animal facility before experiments, kept on a 12h/12h light/dark cycle and had *ad libitum* access to standard laboratory food pellets and drinking water. Room temperature was set to  $22\pm 0.5^\circ\text{C}$  and relative humidity was maintained at  $50\pm 10\%$ . For animal welfare, cage enrichment like shelters, toys and nesting material was periodically exchanged.

### 5.2 Breeding

For having both homozygous wild-type and KO animals in one litter, only heterozygous females were selected for breeding. Males were alternating of either homozygous genotype. To improve breeding success, only animals older than 12 weeks and up to maximal 25 postnatal weeks of age were used. Breeding pairs were chosen to have approximately the same age. Generally, females were placed in the male's cage for fourteen days to enhance fecundity. Pups were weaned and separated by gender and genotype at postnatal days 21-28.

### 5.3 Genotyping

Since all possible genotypes were available in one litter, but only homozygous animals were used, pups were genotyped prior to experiments. At postnatal days 3-5 pups were tattooed and tails cuts were collected. DNA of tail cuts was extracted overnight in polyethylene glycol at room temperature. Master mix was prepared immediately prior to PCR, containing 10x Taq buffer B, 2.5 mM  $\text{MgCl}_2$ , 0.15 mM 4dNTP,  $0.375\ \mu\text{M}$  *Fmr1* primer wt forward,  $0.375\ \mu\text{M}$  *Fmr1* primer mutant forward,  $0.375\ \mu\text{M}$  *Fmr1*

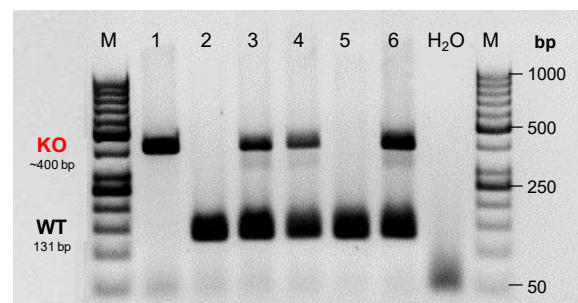


**Figure 6:** PCR used for genotyping of *Fmr1*-KO mice. Mouse tail DNA was amplified with primers for WT (131 bp) and KO (~400 bp) products. Separated by gel electrophoresis on a 1,5 % agarose gel. M, markers; H<sub>2</sub>O, no DNA.

primer reverse, 5 U/ $\mu$ l Taq polymerase (all from Bio&Sell, Feucht, Germany). Protocol for master mix and cycler settings were adapted from Jackson Laboratory. A gel containing 1x TBE buffer (8.9 mM Tris buffer, 8.9 mM boric acid, 2.5 mM EDTA (all from Carl Roth, Karlsruhe, Germany)), 1.5% agarose and 0.0015% Ethidium bromide (Carl Roth) was loaded with the probes and 6x Loading Dye (Fermentas, Thermo Fisher Scientific, Waltham, MA, USA) and run for approximately 25 minutes at 140 V until bands were clearly separated (Figure 6). To minimize the risk of confusion, each animal was genotyped a second time following the final experiment.

## 5.4 Immunohistochemistry

For immunohistochemical experiments, mice were used at postnatal days 8 – 21 or 37 – 40, respectively. Animals were anesthetized by an intraperitoneal injection of Fentanyl (Janssen-Cilag, Neuss, Germany), Medetomidin (Ratiopharm, Ulm, Germany) and Metformin (Pfizer, NY, USA). They were perfused transcardially with 0.1 M phosphate buffer (PB; pH 7.4) for 3 min followed by paraformaldehyde (PFA, Carl Roth; 4% in 0, 1 M PB; pH 7.4) for 15 min. Immediately after perfusion, brains were dissected and post-fixed overnight in 4% PFA at 4°C. Brains were thoroughly washed at room temperature with 0.1 M phosphate buffered saline (PBS; pH 7.4). Coronal brain sections of 50  $\mu$ m were obtained using a vibratome (VT1200, Leica Biosystems, Nussloch, Germany). Sections including the LSO were collected. Unspecific binding was blocked incubating the sections in solution containing 10% normal donkey serum (NDS; GeneTex, Irvine, CA, USA), 0.2% Triton X-100 (Carl Roth) and 0.1 M PBS, for one hour at room temperature. Slices were subsequently incubated overnight in the primary antibody sera, optionally containing rabbit  $\alpha$ -vGluT1 (Synaptic Systems; dilution 1:1000), guinea pig  $\alpha$ -vGluT2 (Synaptic Systems; dilution 1:1000), guinea pig  $\alpha$ -GlyT2 (Millipore; dilution 1:1000), chicken  $\alpha$ -MAP2 (Neuromics; dilution 1:1000), 3% NDS, and 0.2% Triton X-100, in 0.1 M PBS.

Slices were washed in 0.1 M PBS and incubated for 2 h at room temperature in secondary antibody sera, respectively containing 3% NDS, 0.2% Triton X-100, Alexa 488 donkey  $\alpha$ -rabbit (life technologies; dilution 1:250), Cy3 donkey  $\alpha$ -guinea pig (Dianova; dilution 1:250) and Alexa 647 donkey  $\alpha$ -chicken (Dianova; dilution 1:300). Negative controls were obtained by omitting the primary antibody. Sections were washed several times in 0.1 M PBS, mounted and covered with homemade anti-fading mounting media (Indig et al., 1997).

## 5.5 Confocal microscopy

Fluorescent micrographs were acquired using a confocal laser scanning microscope (TCS SP8, Leica Microsystems, Wetzlar, Germany) equipped with a 5x HCX PL FLUOTAR objective (NA 0.15), a 20x HC PL APO Imm Corr objective (0.75 NA) and a 63x HCX PL APO immersion oil objective

(1.4NA). The pinhole was set to 1 Airy unit for each channel. Illumination and detection pathways were separated for each fluorophore and individual color channels were sequentially acquired to avoid bleed-through artifacts. The acquisition settings were adjusted to cover the entire dynamic range of the detectors and remained unchanged during the course of imaging process. Z-stacks of confocal images were obtained and maximal projections of 4-6 single optical sections were used for high magnification figures. Stacks of confocal images were further examined and processed with ImageJ (NIH, USA).

## 5.6 *in vivo* recordings

### 5.6.1 Preparations and anesthesia

For *in vivo* experiments, animals were chosen blindfolded to avoid bias by the experimenter. Age of animals ranged from postnatal days 37 – 98. Animals were genotyped a second time after the end of an experiment. Hearing of the selected animal was briefly confirmed by startle response to several handclaps, presented invisibly to the animal. General anesthesia was initiated with an intraperitoneal injection using a mixture of xylazine (Rompun 2%, 5 mg/kg, Bayer AG, Leverkusen, Germany) and ketamine (Ketavet 10%, 100 mg/kg, Pfizer, NY, USA) until an areflexive state was reached. An intraperitoneal access was placed for consecutive dosage of the anesthetic. Additional doses were administered when needed, at least every 40 minutes, and the open eyes of the mouse were covered with eye ointment (Bepanthen Augen- und Nasensalbe, Bayer AG).

Sedative, analgesic and anxiolytic drugs commonly act upon neuronal transmission, e.g. block receptors or interfere with the production of second messengers. Accordingly, they have a significant influence on the firing patterns in neuronal networks, such as the auditory system (Capsius and Leppelsack, 1996; Hoffmann et al., 2008; Duque and Malmierca, 2014). The point of action of most anesthetics is at the inhibitory receptors (Evans and Nelson, 1973; Brownell et al., 1979; Kuwada et al., 1989). Ketamin and xylazine, however, act on NMDA-mediated excitatory transmission. At cells of the LSO, excitation has been shown to be mediated by non-NMDA receptors (Caspary and Faingold, 1989; Wu and Kelly, 1992b). Additionally, this mixture was tested to be the preferred anesthetic for recordings in the auditory brainstem (Kaltenbach and Saunders, 1987) and was used in numerous *in vivo* studies in the auditory brainstem of mice (Sonntag et al., 2009; Felix et al., 2013; Wang et al., 2015).

### 5.6.2 Surgery

The fur of the animal's scalp was removed and a sagittal incision was placed from the occipital bone to the beginning of the nasal bone. The pericranium rostral of *Bregma* was removed using a micro curette. The surface of the underlying skull was etched (iBOND Total Etch, Heraeus-Kulzer, Hanau,

Germany) and light cured with an UV light source (Superlite<sup>75</sup>, M+W Dental, Bidingen, Germany). A custom made head post was attached to the skull using dental cement (Charisma, Heraeus-Kulzer). Dental cement was light cured for one minute, considering not to expose the animals eyes to the UV light. Subsequently, the animal was transferred into a sound-attenuating chamber (Desone, Berlin, Germany) and fixed in a computer-controlled stereotaxic frame (Neurostar, Tübingen, Germany) using the mounted head post. Tilt and scaling of the animals head were calibrated using *Lambda* and *Bregma* as landmarks, and a marker was placed on the skull overlying the penetration site. A craniotomy of about 2x2 mm around the marker was performed using a scalpel. The underlying meninges were carefully removed, considering not to injure the large vessel covering the commissure of cortex and cerebellum. Excessive blood and ruptures of small vessels were treated with coagulating gelatin sponges (Equispon, Equimedical BV, Zwanenburg, Netherlands). The exposed brain tissue was covered with warm saline to prevent dehydration.

### 5.6.3 Animal monitoring

The physical condition of the animal was continuously monitored. Body temperature was measured with a rectal probe, displayed on a computer screen and maintained using a heating pad (TC01, MCS, Reutlingen, Germany). The state of anesthesia was frequently assessed using toe pinch and corneal reflexes. Cardiac function, respiration and tentative movements of the animal were monitored via a custom-built ECG: Electrodes were placed on the right foreleg and the left hind leg and connected to an amplifier (P55, Grass Technologies, Warwick, RI, USA). For acoustical supervision, a standard computer loudspeaker was coupled to the output of the amplifier. Using the soundcard of the setup computer, the amplified ECG signal was digitized and displayed on a computer screen. Hydration status of the animal was periodically controlled via skin retraction. In case of dehydration, warm isotonic saline was administered using the intraperitoneal access.

### 5.6.4 Sound generation and delivery

All stimulation sounds were designed using the Real-Time Processor Visual Design Studio (RPvdsEx, version 76; Tucker Davis Technologies (TDT), Alachua, FL, USA). Sequence and parameters of the sounds were controlled with Brainware (TDT). Stimulus generation was performed at 195.3 kHz sampling rate using the digital signal-processing hardware of an RZ6 Auditory Processor (TDT). Acoustic signals were calibrated using a ¼ inch measurement microphone (40BF, G.R.A.S., Holte, Denmark), custom written MATLAB software (The MathWorks, Natick, MA, USA) and TDT's SigCalRP calibration software. Signals were produced by magnetic full-range speakers (MF1, TDT) with a membrane diameter of 38 mm. Binaurally presented signals needed to be shielded and delivered separately from the speaker to the respective eardrum of the animal.

Loudspeakers were enclosed with an aluminum housing and sealed with a covering plate. The distance between the membrane of the speaker and the covering plate could be adjusted with acoustically insulating rubber gaskets. A tight-seal funnel was placed upon the orifice outlet of the speaker housing, connected to plastic tubing (outer diameter: 3.2 mm, inner diameter: 1.9 mm) and inserted into the animal's pinna. The length of the plastic tubing needed to be adjusted to flatten the frequency response of the sound at the end of the tubing. Propagating sound waves are dampened when travelling through space. This effect is enhanced for high frequencies, especially in the ultrasonic range. As a result, the farther a sound wave propagates, the stronger the frequency response is shifted towards low frequencies. Additionally, constraining a sound wave to a narrow environment such as a plastic tubing results in multiple interferences, attenuating some frequency bands whereas others become amplified. To counterbalance these effects, a digital finite impulse response (FIR) filter needed to be applied to the stimuli before sending them to the transducers. Simply spoken, this filter is the reciprocal of the speaker's, or respectively the setting's basic impulse response. Amplification of underrepresented frequency bands is not applicable, as this would result in distortions or is impossible *a priori* due to destructive interference. Flattening of a speaker's frequency response is thus achieved by modification of mainly two variables: On the one hand by prevention of interferences, e.g. via adjustments in the transduction path of the acoustic signal. In this case, this is a combination of loudspeaker housing, distance of the covering plate, position of the connected funnel and length and diameter of the delivery tubes. On the other hand by attenuation of excessive frequency bands. Consequently, the maximal practicable sound intensity of the entire frequency range of an ideally flattened frequency response is limited according to the frequency band with the lowest intensity. This leads to the simplified equation: The shorter the tubing, the louder the signal and the broader the suitable frequency range. The arrangement of the setup required a minimal tubing length of 60 mm, empirical tests revealed an ideal length of 75 mm. Following repeated calibration routines for adjustment of the digital FIR filter in SigCalRP, a maximal fluctuation of the frequency response of  $\pm 4$  dB over the required stimulation range from 2 kHz to 50 kHz and a maximal sound pressure level of 90 dB SPL (re. 20  $\mu$ Pa) could be achieved.

The acoustic path from generation at the speaker's membrane to perception at the animal's eardrum was thoroughly insulated to avoid cross talk from the speaker to the other, contralateral eardrum. However, empirical tests revealed cross talk from the ipsilateral speaker to the contralateral ear at signal intensities of more than 40 dB in respect of the animal's individual hearing threshold and the recorded unit. As a consequence, ipsilateral stimulation intensities were set to 20 dB above threshold, if not stated other. At this level, neurons commonly respond with the typical firing pattern and with high reliability, whereas cross talk remains irrelevant.

### 5.6.5 Sound stimuli and recording protocol

#### *Search for LSO neurons*

Pseudorandom, correlated white noise bursts of 100 ms duration were presented every 250 ms at an intensity of 60 dB SPL to search for auditory neurons. Signals were cosine gated with a 5 ms rise-fall time to avoid artifacts caused by the transducers. For a rapid approach of auditory regions within the brainstem, binaural stimulation at equal intensity was used since most nuclei in the auditory brainstem respond to binaural acoustic signals. Once the area of the SOC was encountered, the search routine was switched to exclusively ipsilateral stimulation. Firstly, the neuronal activity from ipsilateral excitation of numerous LSO cells is already inhibited to a certain extent when contralateral stimuli are of equal intensity. Thus, binaural stimuli may cause a miss of LSO activity as many LSO neurons do not fire during binaural stimulation with equal intensities. Secondly, in the vicinity of the LSO no other area of ipsilateral excitability is known. Consequently, a response to ipsilateral stimulation serves as a first indication for the location of an LSO neuron. Following the isolation of a unit matching these criteria, a switch to contralateral and finally binaural stimulation was performed as an additional verification. If the unit showed no spike response to contralateral stimulation and no or at least reduced activity on binaural sound presentation, this neuron was considered as an LSO principal cell and subsequent recordings were performed.

#### *Spontaneous firing rate*

Spontaneous activity of the isolated unit was recorded, omitting any acoustic stimulation. These measurements were conducted prior to other recordings, as auditory neurons can exhibit a transient increase of spontaneous firing rates following elevated neuronal activity.

#### *Noise threshold*

Next, the response to either ipsi- or contralateral 100 ms noise bursts from 0 to 90 dB SPL in steps of 10 dB was recorded. On the one hand, these recordings served as a documented verification of the exclusively ipsilateral excitation. On the other hand, they were used to assess the unit's individual intensity threshold for white noise.

#### *nILD and proof for IE characteristic*

Ipsilateral intensity of the noise bursts was then fixed at 20 dB above threshold. Contralateral noise bursts were presented simultaneously at  $\pm 30$  dB in steps of 5 dB to examine the unit's response properties to interaural level differences of white noise (nILD). Moreover the resulting ILD function of this trial provided final evidence, that the recorded neuron was an LSO principal cell.

### *Determination of characteristic frequency range*

Subsequently the characteristic frequency was determined. 100 ms tone pips with 5 ms rise-fall time, logarithmically spaced in 50 steps from 2 kHz to 50 kHz, were presented exclusively via the ipsilateral transducer at 60 dB SPL.

### *Tuning curves and threshold determination*

In 12 experimental sessions detailed ipsilateral frequency tuning curves were generated. Upper and lower cut off frequency were taken from the previous trial, logarithmically spaced in 20 steps and permuted with the stimulation intensity from 0 dB SPL to 60 dB SPL in 5 dB increments. Characteristic frequency (CF) and intensity threshold were assessed from the resulting frequency response area. In 13 experimental sessions, CF was approximated from the previous trial and intensity threshold was determined for this particular frequency in steps of 5 dB.

### *Pure tone ILD functions*

Next, an ILD function using pure tones was generated (pILD). The ipsilateral stimulus was set to CF, 20 dB above the cell's individual threshold for this frequency. The contralateral stimulus was set to the same frequency and presented simultaneously at  $\pm 30$  dB in steps of 5 dB.

### *Click sounds*

Noise bursts and pure tones with a duration of 100 ms and a rise-fall time of 5 ms represent comparably long signals with smooth on- and offset. A core feature of sound localization in the azimuthal plane with strong evolutionary impact might be the detection of prey or predators. Brief and abrupt sounds like a breaking twig of an ambushing fox could thus be a behaviorally highly relevant stimulus for mice. In the experimental condition, these signals are mimicked by click sounds. In theory, a click is an infinitely short impulse of sound waves, simultaneously carrying all frequencies at equal intensity. In practice, due to technical limitations, presented clicks were of 0.1 ms duration and 10  $\mu$ s rise-fall time. This duration was chosen as a compromise between realizable stimulus intensity and frequency range of the signal. The spectral content of a click is defined by its duration, such as the first spectral zero occurs at the inverse of its duration. An ideal and frequently used click of 50  $\mu$ s therefore shows a spectral gap at 20 kHz. This is negligible for e.g. psychoacoustic experiments with human subjects, as the human hearing range is limited to a maximum of 20 kHz. However, about 50% of all recorded LSO neurons showed a CF between 15 and 25 kHz, disqualifying the use of 50  $\mu$ s clicks. The duration of a click is further accompanied by its effective intensity, as shorter clicks transmit less total sound pressure. Hence, applying clicks shorter than 50  $\mu$ s to circumvent spectral issues would result in clicks with insufficient maximal intensity. On the other hand, inordinate distortions are a result of clicks succeeding a certain duration.

Intensity thresholds differed between units and single cells in turn showed diverging thresholds for the three applied stimuli. Hence, intensity thresholds were determined individually for each cell and examined stimulus type. Consequently, the ipsilateral threshold for click sounds was assessed in 5 dB steps. Threshold was defined when more than 50 % of the unit's response was correlated with the stimulating clicks.

### *Monaural adaptation trials*

In order to measure effects of habituation, the use of pure tones or noise bursts was limited due to the onset response characteristic and the 5 ms rise times. Thus, to achieve an effect, LSO cells needed to be periodically stimulated with click sounds at different repetition rates. 600 ms ipsilateral click trains were presented with a recovery period of 1400 ms between trials at 20 dB above the respective threshold. Repetition rate of the clicks was realized as inter-click intervals of 10, 7, 6, 5, 4, 3, 2 and 1 ms, resulting in stimulation rates of 100, 143, 167, 200, 250, 333, 500 and 1000 Hz, respectively.

### *Binaural adaptation trials*

In preparation for the binaural adaptation trial, an ILD function for clicks was evaluated. In accordance to the previously recorded ILD functions, ipsilateral click intensity was set to 20 dB above threshold, whereas contralateral intensity was varied  $\pm 30$  dB in steps of 5 dB. As previously introduced, LSO cells are not only sensitive to ILDs, also differences in timing play a significant role for the balance of excitation and inhibition. In order to define comprehensively the accounting parameters for the interplay of excitation and inhibition, influence of interaural time differences (ITDs) was approximated. Pilot experiments showed a sufficient coverage of the required ITD range, when contralateral click delay was varied between 0 and 1 ms in steps of 0.5 ms. These measurements were interlaced with the evaluation of the ILDs to reveal the combination of ILD and ITD at which the unit was most sensitive, i.e. inhibition via contralateral stimulation was most effective.

To quantify the impact of either ipsilateral excitation or contralateral inhibition in case of FXS, binaural adaptation trials were performed. In order to maintain sufficient adaptation power, general parameters were assessed in pilot experiments. Here, a click presentation rate of 200 Hz showed to be the best compromise between strong excitation from fast repetitive stimulation and a still faithful response to almost every single click, even for long presentation durations. Additionally, several units of *Fmr1* KO animals showed a stronger response to a subsequent pure tone, compared to WT mice. Accordingly, duration of the adapting click train was set to 1000 ms at a repetition rate of 200 Hz. In 50 % of all trials, a monaural, ipsilateral click train, 20 dB above the previously determined threshold for clicks was presented (see Figure 18A, upper stimulation trace). In the remaining trials, the adapting click train was presented binaurally. Contralateral intensity was set to a value, where almost complete inhibition of the ipsilateral excitation was achieved (see Figure 18A, lower

stimulation trace). Subsequent to the adapting click train, with a delay of 10 or 50 ms, a 100 ms monaural, ipsilateral pure tone at CF and at 20 dB above the unit's individual threshold was presented. Each combination was repeated 10 times, with a 1000 ms recovery time between trials.

#### *Assessment of intrinsic properties*

The circuitry of the LSO allows to test for differences of intrinsic properties from a lack of FMRP of only LSO cells *in vivo*. Using the paradigm in figure 18A, the contribution of ion channel activity only at LSO cells was addressed. FMRP interacts with a number of ion channel complexes and two of which were shown to be expressed at LSO cells (Rizzi et al., 2016; Sausbier et al., 2006). A lack of FMRP was associated with a reduced activity of the sodium-activated potassium channel Slack (Brown et al., 2010) and a decreased activation of the calcium-activated potassium channel BK (Deng et al., 2013). As a functional consequence, synaptic short-term plasticity and the precise temporal processing of action potentials is affected in *Fmr1* KO mice. A reduced activation of these potassium channels could thus be reflected in the processing of auditory stimuli at LSO cells.

The response to a monaural pure tone was compared following either mon- or binaural strong acoustic click stimulation. Monaural click trains caused the cell to strongly fire. Contralateral inhibition suppressed this firing in the binaural condition and thus also the strong activation of potassium channels. The excitatory inputs to the successive pure tone, however, were identical in both conditions. A difference in the response to this pure tone between WT and *Fmr1* KO animals would then reflect changes of the intrinsic properties of only the respective LSO cell and was independent of propagated changes from lower stages.

#### 5.6.6 General stimulus presentation parameters

The sequence of any recording trial was randomly presented to prevent adaptation of the cell's response. All applied stimuli were extensively analyzed for various parameters such as effective levels, frequency content, duration, repetition rates, rise/fall times and possible interferences. Depending on the focus of the experiment, not all mentioned above procedures were applied to limit the required time for a complete set of recordings. This helped to maintain a constant recording quality, as signal intensity and signal-to-noise ratio (SNR) tend to fluctuate with increasing recording duration. In addition, shorter recording protocols reduce the risk of losing a cell before the set is completed. The most relevant parts of a recording protocol were the final ones, as the required parameters for the respective trials had to be determined in the first place. Thus, limiting the essential recording time improves the chance of accomplishing a complete set of data of high fidelity.

### 5.6.7 Data acquisition

Recording electrodes were pulled from borosilicate glass capillaries (10-15 M $\Omega$ , BioMedical Instruments, Zöllnitz, Germany) on a PC-10 puller (Narishige, Tokyo, Japan) and filled with 2 M NaCl, containing 2% horseradish peroxidase (HRP; Type II, Sigma-Aldrich, St. Louis, MO, USA). Neuronal activity was amplified and filtered (300-3000 Hz) using a Model 3000 amplifier with regular headstage (A-M Systems, Carlsborg, WA, USA). Analog signals were digitized at 24.4 kHz sampling rate and fed into a computer via an RZ6 Auditory Processor (TDT, Alachua, FL, USA). Real time spike data were displayed and selected using Brainware (TDT). To ensure that recorded data originate from a single unit, wave shape of selected spikes was continuously cropped, plotted for different criteria and stored separately for post-hoc analysis. Trigger for recognition and recording of single action potentials was manually adjusted and set to approximately 2/3 the size of the negative voltage deflection. In extracellular recordings, action potentials of LSO cells commonly showed a larger negative amplitude (see example traces Fig. 17B, upper inset). Setting the trigger threshold to the negative side of the voltage trace thus facilitated the reduction of artefacts due to a too low trigger threshold. At the same time, loss of occasional spikes with a small total amplitude was reduced. Both analog voltage traces and action potential event times were simultaneously recorded. Analog traces were collected with 12-bit resolution at 50-kHz sampling frequency.

### 5.6.8 Iontophoretic labeling and histological reconstruction of recording sites

Following each successful recording of a cell, stereotactic coordinates were stored. Once per experimental session, typically after recording of a highly representative unit, a small amount of horseradish peroxidase (HRP) was iontophoretically applied. A +90 V DC current for 3 minutes ejected an adequate amount of HRP for labeling after subsequent histological processing. With this labeling, clear verification of the recording site was accomplished. Moreover, all other

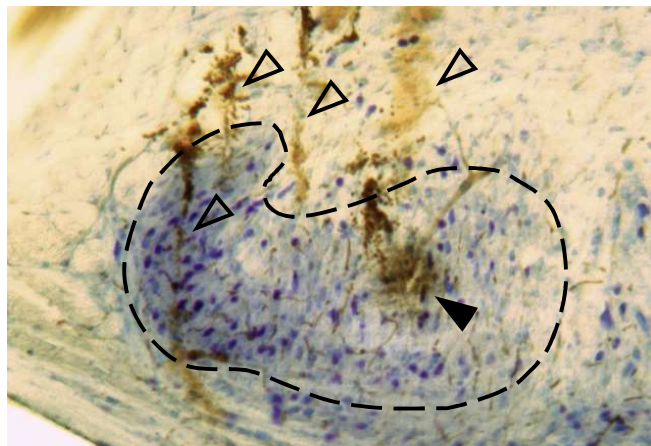


**Figure 7:** Verification of a recording site in a Nissl-stained coronal section of the LSO. Solid arrowhead shows HRP labeling of recording site. Hollow arrowheads indicate electrode tracks. Broken line represents border of LSO. Scale bar: 100  $\mu$ m

recording sites could be subsequently reconstructed. Experiments were terminated with a lethal dose of the anesthetic. After decapitation, the brain was carefully removed and immersion fixed for 24 hours at 4°C in a solution of 4% paraformaldehyde (PFA) and 0.1 M phosphate buffer (PB). Brains

were washed thoroughly in 0.1 M PB and embedded in 4% warm, low-melting agarose in 0.1 M PB. 70  $\mu\text{m}$  thick coronal sections containing the LSO were obtained using a vibratome (VT1200, Leica Biosystems, Nussloch, Germany) and mounted on object slides. HRP injection was made visible by a 35-minute application of a diaminobenzidine reaction kit (D7304, Sigma-Aldrich, St. Louis, MO, USA). Brain slices were rinsed with *aqua bidest* and counterstained for 7 minutes in a cresyl violet solution. Object slides were differentiated for approximately 30 seconds in acetate buffer, dehydrated for 30 seconds in 99% ethanol and cleared for 2-3 minutes in xylol. Slides were covered with mounting medium (Roti®-Histokitt, Carl Roth) and stored at 4°C. Labeling sites were located using a transmission light microscope (CH30, Olympus, Tokyo, Japan) and digitally captured with a CMOS camera (ISH300, Tucsen, Fuzhou, China)(Figure 7). Stereotactic coordinates were read out according to a standardized mouse brain atlas (Paxinos and Franklin, 2004). Atlas coordinates and corresponding experimental coordinates were compared and the difference was subtracted from the remaining recording site coordinates of this experimental session. This helped reducing the initial calibration bias and provided for a well-suited 3D-reconstruction of the recording sites.

## 5.7 Data Analysis

Analysis of recorded data was performed in MATLAB and GraphPad Prism version 5.01 (GraphPad Software, San Diego, CA, USA).

The characteristic frequency (CF) of a neuron is defined as the frequency at which the unit responds with the lowest threshold. In experiments, where a detailed tuning curve was recorded, threshold was determined when more than 50 % of correlated neuronal activity was observed. In the remaining experiments, CF was approximated from the initial frequency sweep at 60 dB SPL. Here, CF was defined as the response with the smallest latency, as pilot experiments showed a suitable correlation of latency and CF.

### 5.7.1 Regression analysis

For regression analysis, linear regression was calculated using the formula

$$r^2 = 1 - \frac{\sum_{i=1}^n (y_1 - \hat{y}_1)^2}{\sum_{i=1}^n (y_1 - \bar{y}_1)^2}$$

where  $r^2$  is the coefficient of determination,  $\hat{y}$  is the predicted value of  $y$  and  $\bar{y}$  is the mean of the observed data.

### 5.7.2 Ratio of responsiveness

Sensory neurons can be categorized by means of their firing pattern. In this context, they are often referred to as onset, sustained or chopper units. For a detailed characterization and quantification of a unit's response properties, a quality measure beyond a classification of onset and sustained activity was needed. Analysis of all recorded units revealed that 90 % of the neuronal activity upon stimulation with a 100 ms pure tone at the cell's CF, 20 dB above perception threshold, occurred within the first 10.2 ms, with respect to the unit's FSL. Accordingly, cells showing correlated response exclusively within the first 10 ms were considered strong onset neurons and therefore this time window was used to evaluate response behavior. A ratio was calculated of the number of elicited action potentials within the first 10 ms, divided by the number of spikes of the total stimulation period. Consequently, if all neuronal activity occurred within the first 10 ms, a ratio of responsiveness (RR) of 1 was calculated. On the other hand, an RR of 0.5 implied the same number of action potentials in the first 10 ms compared to the remaining 90 ms. Thus, a smaller RR value reflected a stronger sustained firing behavior. This analysis helped to reveal subtle differences in the firing patterns between WT and *Fmr1* KO animals.

### 5.7.3 ILD values

To describe a cell's response to ILDs, a sigmoid function was fit to the data using the formula

$$y = a + \frac{b}{1 + \exp\left(-\frac{h-x}{s}\right)}$$

where  $y$  is the discharge rate,  $x$  is the ILD,  $h$  is the ILD of the half maximal inhibition (point of inflection, respectively),  $s$  is the slope at the point of inflection and  $a$  and  $b$  are free parameters. Decreasing values of the half maximal inhibition ILD reflect a shift of the ILD towards the ipsilateral ear, i.e. higher contralateral sound intensity is needed to achieve an inhibitory effect.

### 5.7.4 Q values

As a measure of tuning sharpness, the Q values for each neuron were determined. The Q10 value is calculated as the ratio of CF over the bandwidth 10 dB above threshold, whereas the Q30 value is 30 dB above threshold. A larger Q value reflects a sharper tuning, i.e. a more narrow frequency response area.

### 5.7.5 Assessment of temporal precision

#### *Vector strength*

The calculation of vector strength (VS) was used to measure the degree of phase-locking, ranging from 0 to 1. Here, 0 indicates no phase-locking, and 1 indicates perfect phase-locking. The conventional discrete definition of VS was applied, initially introduced for the computation and quantification of neuronal phase-locking by Goldberg and Brown, 1969:

$$\text{vector strength} = \frac{\sqrt{(\sum_n \sin \theta)^2 + (\sum_n \cos \theta)^2}}{n}$$

Here,  $\theta$  describes the phase of each spike in radians, and  $n$  is the number of spikes.

The calculation of VS gives an appropriate prediction of a unit's synchronicity, as long as the compared units show matching firing patterns, e.g. strictly onset or sustained firing. For onset cells like LSO neurons of mice, binning of the summed neuronal activity in a histogram results in a well-defined distribution, culminating in a single peak (Figure 8, 250 Hz condition). Less dispersion of the summed spikes and thus stronger agglomeration in a certain point within the considered cycle results in a higher VS. For cells with a regular or occasional response of two or more spikes, addition of all spikes of the repetitive cycle produces more than one peak. Following the applied mode of calculation, VS will decrease significantly, regardless of the factual high synchronicity of the first spike of the cycle (Figure 8, 100 Hz condition & summary below). Granted that the comparative

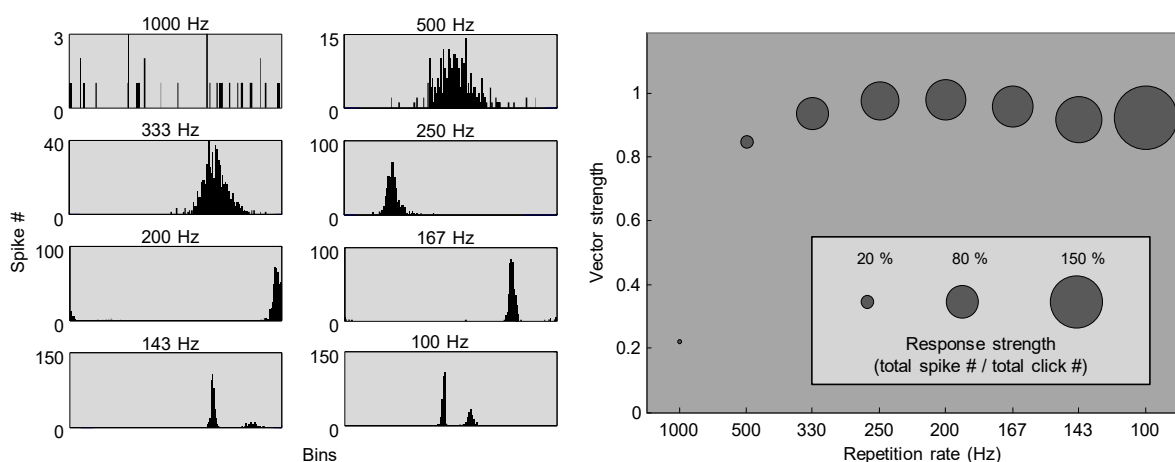


**Figure 8:** Limited significance of vector strength as a measure to describe firing accuracy. The calculation of vector strength (VS) commonly quantifies a neuron's precision to respond to repetitive stimulation. Strongly correlated and well-synchronized responses generate a narrow peak when plotted as a histogram and account for larger VS values. Onset cells occasionally elicit a second action potential upon single stimulation, especially for slower repetition rates. The resulting second peak distorts the calculation of VS (see e.g. 100 or 143 Hz repetition rate). In these conditions, the sharp first peak indicates a remarkably high precision, typically producing a large VS value. The occurrence of a second peak understates the effective VS. Right plot summarizes VS values for separate conditions, size of individual data points indicates general response strength.

groups exhibit similar variability of firing patterns, averaging of the calculated VS values and comparison between groups will give a good approximation of the pooled neuronal activity. However, in the present case, a larger portion of WT cells respond with two spikes upon stimulation with clicks, compared to KO animals. This leads to an erroneous averaged bias towards smaller VS in WT animals, even if the real phase-locking precision of the first spike was higher. Consequently, another method had to be applied to evaluate firing precision.

#### *Single response evaluation*

Neuronal response upon stimulation with click trains was cropped into single cycles, corresponding to the repetition rate of the stimulus. Occasionally, and in particular depending on the repetition rate, latency of the neural response to click trains gradually increased with stimulation duration. Thus, window size of cycles was manually adjusted to ensure that all relevant action potentials were located within the respective window, from the first to the last cycle of the stimulation period. Moreover, this helped minimizing the influence of uncorrelated spontaneous activity between single clicks, which appeared to be relevant especially for slow repetition rates. To assess both, overall and single cycle reliability, the occurrence of a correlating response was examined in every cycle. Likewise, latency and standard deviation of only the first correlating spike were calculated. Additionally, the number of total correlated action potentials and therefore the chance for more than one spike per click were determined. The advantage of this method over the calculation of VS was on the one hand, that a better approximation of the general precision of action potential timing could be achieved. On the other hand, also the changes of parameters like reliability, standard deviation, latency or spike numbers during the progress of stimulation could be examined.

#### 5.7.6 Statistical tests

Data were tested for normality using the Kolmogorov-Smirnov test. Differences between two mean values were assessed with the unpaired two-tailed Student's *t*-test for normally distributed data and with Mann-Whitney-Test for pairwise comparison of non-parametric distributed data. For data sets with significantly different variances, unpaired *t* test with Welch's correction was used to calculate statistics. Groups were compared with Kruskal-Wallis test with Dunn's post-hoc test. Data are presented as mean  $\pm$  SEM. The significance thresholds of  $p < 0.05$  (\*),  $p < 0.01$  (\*\*) and  $p < 0.001$  (\*\*\*) were used.

---

## 6 Results

### 6.1 The lateral superior olive of mice

The LSO of mice has been subject to numerous studies throughout the past decades, including anatomical descriptions, neuronal tract tracing, immunohistochemical examination, behavioral experiments and *in vitro* electrophysiology in acute brain slices (Harrison and Irving, 1966; Ollo and Schwartz, 1979; Campbell and Henson, 1988; Wu and Kelly, 1991; Walcher et al., 2011; Weisz et al., 2016). Yet, the response characteristics to different sound patterns has not been characterized to date. In the present study, we aimed to fill this gap and performed *in vivo* extracellular single unit recordings on anesthetized animals, stimulating the LSO with acoustic signals whilst recording the neuronal response from single cells of this nucleus.

#### 6.1.1 Anatomy and neurotransmitter distribution is comparable to other rodents

We started by investigating the basic anatomical properties of the LSO in the used mouse strain, such as location, extent within the brainstem and synaptic connectivity. As in all other mammals, the LSO of mice is located in the superior olivary complex, a predominantly auditory region of the ventral brainstem. With both Nissl and immunohistochemical antibody stainings, a well-defined border to adjacent brainstem nuclei can be delineated (Figures 9A,B). In coronal brain sections, it appears as a bean-shaped accumulation of cells and is mainly comprised of fusiform cells with an average soma diameter of 12-15  $\mu\text{m}$ . The LSO of adult FVB mice spans 400  $\mu\text{m}$  in the mediolateral plane, in dorsoventral direction 500  $\mu\text{m}$ , and about 700  $\mu\text{m}$  in the rostrocaudal plane.

Immunohistochemical labeling of transporter proteins showed the expected expression patterns of neurotransmitter distribution known from other mouse strains (Figure 9C). Studies in a variety of species have shown excitatory glutamatergic inputs emerging from the ipsilateral ear and inhibitory glycinergic projections from the contralateral side (Wu and Kelly, 1992a; Srinivasan et al., 2004; Ito et al., 2015). Here, antibody staining against the vesicular glutamate transporter 1 (vGluT1) revealed punctuate glutamatergic inputs, predominantly expressed on dendrites of principal LSO cells. In contrast, antibodies against the glycine transporter 2 (GlyT2) labeled large areas of the somatic surface, indicating prevalent glycinergic presynaptic terminals. No obvious spatial gradient in neurotransmitter distribution, cell size or shape was observed, demonstrating a fairly homogenous nucleus. These results are in agreement with findings from other mouse strains, or rodents in general, and confirmed our expectations.

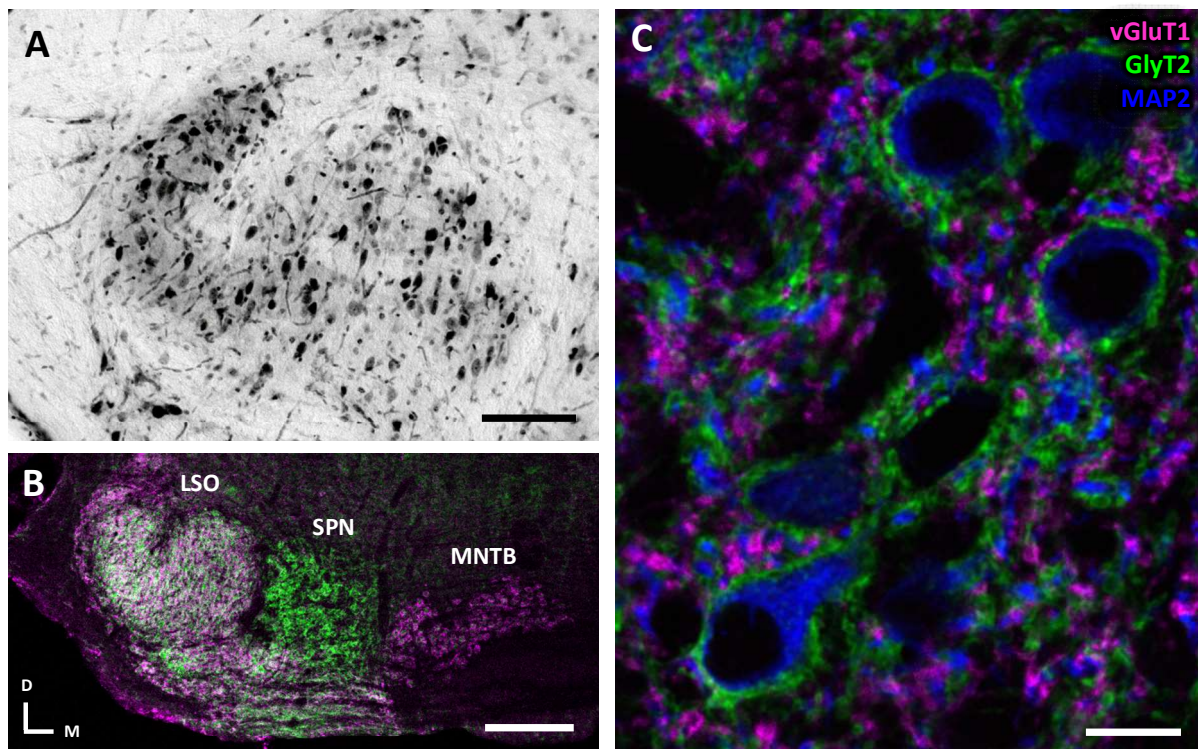


**Figure 9:** Anatomical and neurochemical features of the mouse LSO. **A:** Bright-field photomicrograph of a Nissl-stained LSO of an *Fmr1* WT mouse showing representative shape and cellular arrangement. Scale bar 100  $\mu\text{m}$ . **B:** SOC overview in the auditory brainstem. Vesicular glutamate transporter 1 (vGluT1; magenta) and glycine transporter 2 (GlyT2; green) served as reference markers to identify different substructures. MNTB is exclusively positive for glutamatergic labeling, SPN showed only glycinergic inputs whereas the LSO typically was immunoreactive for both transporters. Contours of minor nuclei like LNTB, VNTB and MSO showed to be ambiguous using this approach. Dorsal and medial directions are indicated and apply for the entire panel. Scale bar: 200  $\mu\text{m}$ . **C:** Maximal projection confocal image of five optical sections, showing punctuate, glutamatergic synaptic inputs (vGluT1; magenta), typically contacting dendritic regions of LSO principal cells. Extensive glycinergic inputs (GlyT2; green) cover large areas of somatic surfaces. Neurons are counterstained with MAP2 (microtubule associated protein 2; blue), labeling cell bodies and dendrites. Scale bar: 10  $\mu\text{m}$ .

### 6.1.2 Monaural features of a binaural nucleus

Most neurons in the LSO receive binaural inputs. In natural environmental conditions, this nucleus will typically receive and process inputs from both ears. However, for a comprehensive characterization of isolated ipsilateral input properties it is mandatory to eliminate any influence from the contralateral ear. Hence, the results of the following section are all obtained from exclusively monaural stimulation of the ipsilateral ear.

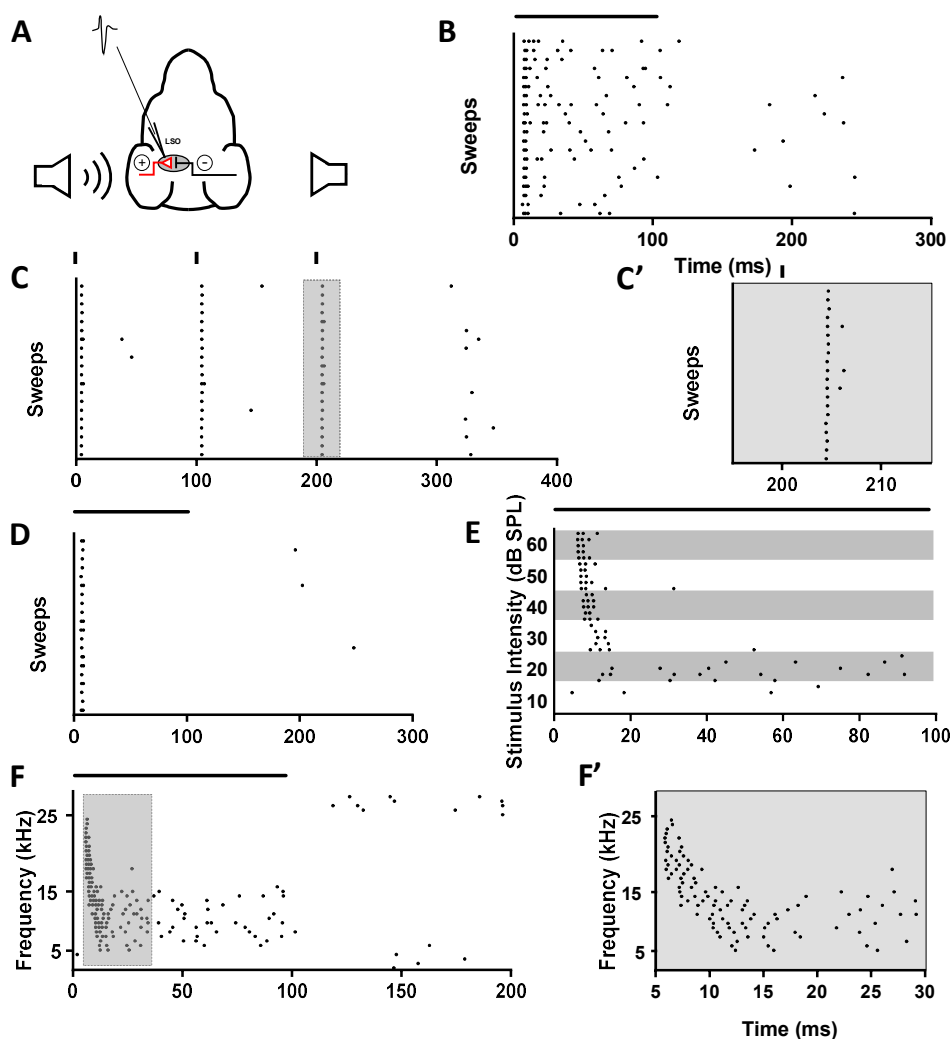


**Figure 10:** Raster dot plots of basic firing patterns upon stimulation with different sounds. Representative firing patterns of LSO principal cells. Each dot represents a single action potential. Black bars indicate duration of sound stimulation. Sound signals are presented 20 dB above perception threshold for individual cell and stimulus type, if not stated other. **A:** Typical recording scenario. LSO principal cells are excited via ipsilateral stimulation, contralateral sound delivery inhibits neuronal activity. Sound stimuli are delivered separately to each ear. **B:** Stereotypic neuronal response to monaural, ipsilateral presentation of a 100 ms white noise burst. A strong onset response with few spikes is followed by scarce firing. **C:** Firing pattern upon stimulation with click sounds. LSO cell responds with typically one action potential and with high reliability on single clicks. Magnification in **C'** reveals small jitter and sporadic occurrence of a second spike. **D:** Response to 100 ms pure tone stimulation at the cell's characteristic frequency (CF). Most cells respond with one or few spikes only at signal onset. **E:** Firing pattern changes for pure tone stimulation at CF, depending on signal intensity. First spike latency and jitter increases for decreasing sound levels. **F:** Firing pattern changes for pure tone stimulation with different frequencies. At the lower spectral edge, LSO cells show delayed sustained activity. With rising frequency, firing changes towards more onset-like response, in combination with decreasing FSL. At CF, cell shows strong and exclusive onset firing, enclosing the smallest FSL. Onset behavior persists for frequencies above CF, yet FSL increases again. Magnification in **F'** illustrates this characteristic in detail.

### 6.1.2.1 LSO principal cells respond to acoustic signals with pronounced onset firing

LSO neurons of mice respond to a variety of different stimulation signals. In this part of the study, we tested for the response patterns to stimulation with white noise, pure tones and click sounds. All recorded IE cells responded reliably to all three types of stimulation signals.

To ipsilateral stimulation with pseudorandom white noise, most LSO cells responded with an onset burst of action potentials, followed by sparse sustained activity throughout the whole stimulation period (Figure 10B). Presentation of click sounds caused a highly precise and reliable response with typically one action potential per click and a sporadic, scattered offset response (Figure 10C). Occasionally, a second action potential was elicited (Figure 10C'). Searching for the units preferred pure tone frequency, a typical response pattern was observed: A large number of LSO cells showed a brief and precise onset response to its characteristic frequency (Figure 10D), commonly ranging from one to few initial spikes per stimulation. The average number of action potentials did not change within a wide range of stimulus intensities, only a delay of the first spike with decreasing sound pressure level was observed (Figure 10E). When the sound intensity reached, and eventually fell below the perception threshold, the firing pattern of most LSO cells changed from onset to sparse and random neuronal activity throughout the whole stimulation period. Increasing the frequency resulted in an abrupt inhibition of firing. In contrast, a decrease of the frequency caused a delayed response, gradually shifted to a sustained firing pattern (Figures 10F,F').

Intensity thresholds differed between single units within one recording session, ranging from -10 dB SPL to 60 dB SPL. Likewise, fluctuations of intensity thresholds between different stimuli of single units was observed. Consequently, for each recorded cell, the individual stimulus threshold had to be determined. Typically, thresholds for pure tones at the neuron's preferred frequency were smallest with  $14.8 \pm 1.63$  dB SPL, averaged across all recorded LSO cells. 64.6 % of all neurons showed a higher threshold for click stimuli compared to pure tones ( $25.5 \pm 2.25$  dB SPL), whereas for 78.3 % a higher threshold for noise bursts was measured ( $22.9 \pm 2.85$  dB SPL). Recorded spontaneous firing rates ranged from 0 – 65 Hz with 70.2 % of all cells showing less than 10 Hz. 22.4 % revealed no spontaneous activity during the recording session (Figure 11A). Spontaneous firing did not correlate with the cells preferred frequency (Figure 11B,  $p = 0.8876$ ,  $r^2 = 0.0003$ ). Generally, these findings are in accordance to what is known from other species.

### 6.1.2.2 Subtle differences in onset firing are categorized by the ratio of responsiveness

The majority of LSO cells displayed a strong onset firing behavior on pure tone stimulation at the cells preferred frequency. The remaining neurons showed a progressive gradient of sustained activity, ranging from only a few more spikes following onset activity to strong sustained firing throughout the whole stimulation period. For a closer characterization and a quantification of a unit's

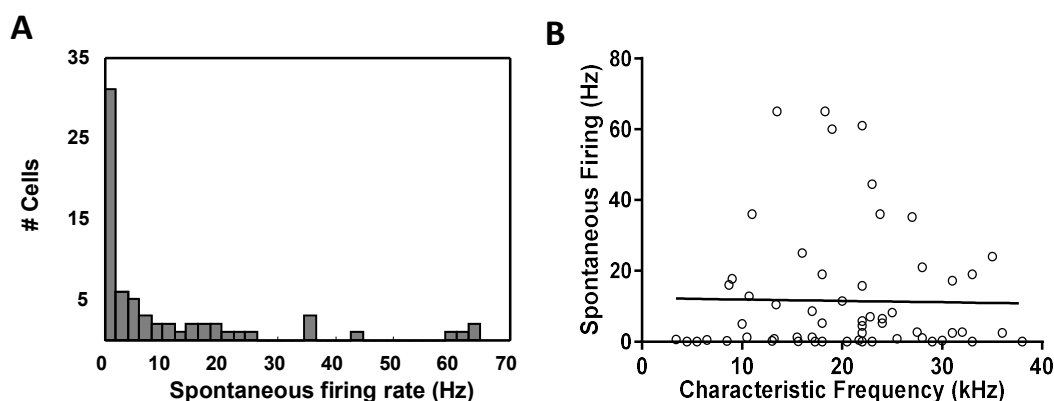


**Figure 11:** Scarce spontaneous firing shows no correlation with characteristic frequency. **A:** Histogram of all recorded spontaneous firing rates. The great majority of LSO cells shows no or little spontaneous activity. **B:** Spontaneous firing rates are not correlated with the unit's CF.

response properties, the ratio of responsiveness (RR) was assessed. This calculation was required to correlate the firing pattern with additional parameters of relevance for this study. Especially for the latter comparison with *Fmr1* KO animals, the conservative classification in onset and sustained firing showed to be insufficient in the present case. This yielded the development of an additional measure. 62.3 % of all recorded LSO neurons returned RR=1, revealing a strong onset response exclusively within the first 10 ms of response (Figure 12B). The remaining cells showed RRs across the whole range, with a minimal value of 0.087, indicating a strong sustained activity during stimulation with only 8.7 % of all action potentials occurring within the first 10 ms of response. Commonly, cells with an RR between 1 and 0.5 would have been classified as onset neurons, with help of the calculation of RR, these subtle differences in firing pattern were revealed. Moreover, these differences in response characteristics were suspected to be associated with the basic neuronal activity level. Yet, no correlation of spontaneous activity and firing pattern were observed (Figure 12C,  $p=0.4687$ ,  $r^2=0.0079$ ). Firing patterns of auditory neurons can be linked to their characteristic frequency, a result of how the primary discharge pattern of hair cells and auditory nerve fibers is transformed in the cochlear nucleus (Sullivan, 1985). However, this is mainly relevant for low frequency neurons, where pronounced phase locking is observed. In order to examine, if differences in firing patterns are dependent on the characteristic frequency, the correlation of frequency and RR was analyzed. However, frequency tuning was not correlated with a unit's RR (Figure 12D,  $p=0.2207$ ,  $r^2=0.0277$ ).

### 6.1.2.3 Auditory neurons are spatially organized regarding their characteristic frequency

Most neurons in the ascending auditory pathway are tuned to a certain frequency at which they respond best, i.e. with the highest firing rate (best frequency, BF). Occasionally, this best frequency deviates to some extent from the frequency at which the cell still responds at the smallest stimulus intensity (characteristic frequency, CF). The majority of LSO cells show onset firing with constant firing rates across wide ranges of stimulation frequency or intensity, thus making BF an inappropriate measure to characterize a neuron's preferred frequency. Measured CFs ranged from 3.4 to 40 kHz,

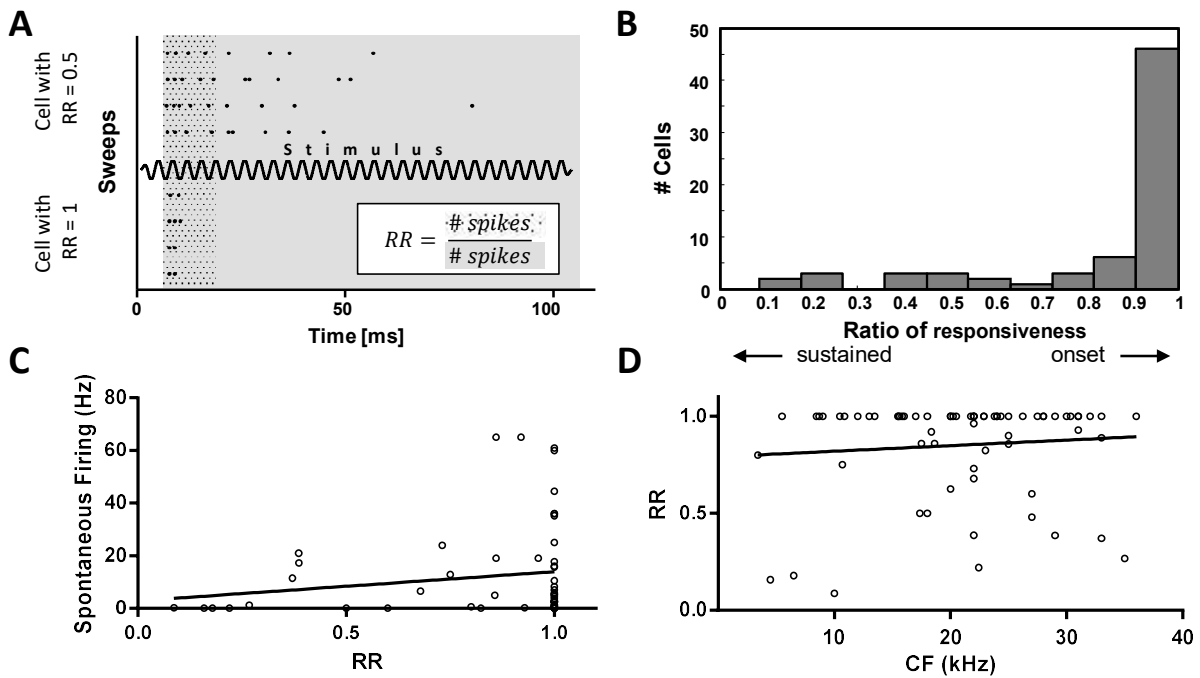


**Figure 12:** Classification of response characteristics. **A:** Raster dot plots of the response pattern of two representative cells to illustrate the calculation of the ratio of responsiveness (RR). Following conventional categorization, both units would account for onset cells. Application of RR allows for a more detailed classification. The number of elicited action potentials within the first 10 ms after response onset is divided by the total number of spikes. **B:** Quantification of neuronal response to stimulation with pure tones. Ratio of responsiveness (RR) classifies firing pattern into more refined categories than onset and sustained to reveal subtle changes in the neuronal response. More than half of all recorded cells show strong onset response, however a gradual tendency towards more sustained firing is observed. Correlation analysis revealed no significant relationship between RR and spontaneous firing (**C**) or CF (**D**).

showing a Gaussian distribution across this frequency range when plotted as a histogram (Figure 13A, KS distance=0.07803). Studies of the past decades described the hearing range of mice to approximately cover frequencies from 2 kHz to 90 kHz (Ehret, 1976; Heffner and Masterton, 1980; Zheng et al., 1999; Heffner and Heffner, 2007; Radziwon et al., 2009). This shows that only a part of the available spectrum is used for sound localization in the azimuthal plane. Moreover, as almost 50 % of all recorded cells show CFs between 15 kHz and 25 kHz, this frequency band seems to be of major behavioral relevance. This is in agreement to audiograms of mice, where a peak in sensitivity is shown for the same frequency range (Garcia-Lazaro et al., 2015). However, the great majority of vocalization calls has been proven to cover frequencies between 30 kHz and 80 kHz (Sewell, 1972; Hofer et al., 2002; Holy and Guo, 2005). This indicates that only few cells of the LSO are suited to process vocalizations.

Commonly, neurons of auditory nuclei are spatially organized within the nucleus' boundaries depending on their preferred frequency, also referred to as tonotopic organization. In a variety of other species, it has already been shown that neurons of low CF tend to be located in the lateral part of the LSO, whereas high frequencies are represented in the medial part. Plotting of all recorded

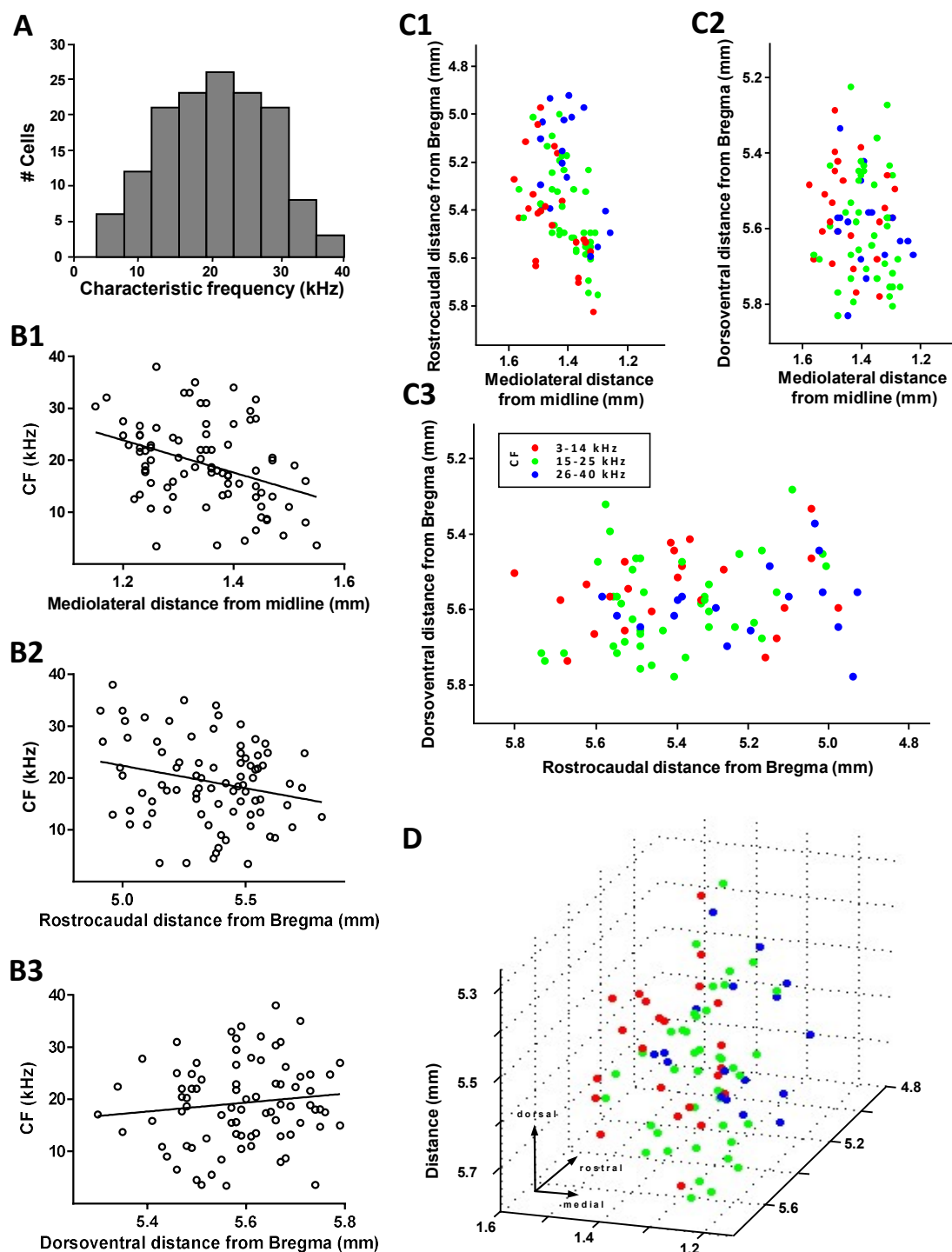


**Figure 13:** Distribution of characteristic frequencies and tonotopic arrangement. **A:** Proportional distribution of CFs of all recorded LSO cells, ranging from 3.2 to 40 kHz. Gaussian-like dispersion predominantly represents behaviorally relevant frequencies for ILD computation. **B:** Topographic reconstruction of recording sites and the corresponding CFs revealed a correlation regarding the mediolateral (B1) and the rostrocaudal axis (B2). No relationship is observed for the dorsoventral dimension (B3). **C1-3:** 2D-plots showing reconstructed recording sites. Each dot represents one LSO neuron. Colors code for CF (red: low, green: intermediate, blue: high CF). Most recording sites are located within the boundaries of the LSO, referring to the stereotaxic mouse brain atlas, Paxinos and Franklin, 2004. **D:** 3D-reconstruction reveals mediolateral and rostrocaudal gradient of tonotopic arrangement. High frequencies tend to be located in the medial and rostral divisions of the LSO, low frequencies in the lateral and caudal parts.

neurons in the mediolateral dimension revealed a significant regression of CFs with units of low CF located in the lateral limb of the nucleus (Figure 13B1,  $p=0.0006$ ,  $r^2=0.1371$ ). Also in the rostrocaudal axis, CFs tend to be tonotopically arranged (Figure 13B2,  $p=0.0006$ ,  $r^2=0.0550$ ). In this dimension, neurons with low CFs were commonly found in the caudal division of the LSO. However, no significance was found for the dorsoventral extent (Figure 13B3,  $p=0.2891$ ,  $r^2=0.0139$ ). Visualizing all recorded CFs in a two-dimensional plot confirmed these findings (Figures 13C1-3). Consequently, the tonotopic arrangement of neurons in the LSO of mice is not restricted to a tonotopic spread in the mediolateral axis, but is likewise extended in the rostrocaudal dimension (Figure 13D). This is in accordance to what is known from other mammals and validated our predictions to a large extent. However, a more precise distribution was expected.

#### 6.1.2.4 LSO cells respond reliably with short latencies and small jitter

The auditory system is the fastest sensory system in mammals (Horowitz, 2013). For example, humans are able to detect timing differences of sound patterns as little as 10  $\mu$ s (Blauert, 1996). Delays and variability in timing are therefore critical parameters for auditory processing. Response latency upon stimulation is commonly more dependent on the number of relaying synapses than on the total transmission distance. As the LSO is one of the first nuclei within the auditory pathway, we expected to find small response latencies. Furthermore, transmission reliability in terms of both variability in timing and the probability of correlated neuronal response was suggested to be of high fidelity. For the majority of recorded cells, the response latency was dependent on the stimulus intensity (see Figure 10E). Thus, all latencies were calculated at 20 dB above the neuron's individual threshold for the respective stimulus. Depending on the nature of the acoustic stimulus, first spike latencies (FSL) of  $4.46\pm 0.05$  ms for click sounds and  $7.76\pm 0.30$  ms for pure tones at the neuron's CF were measured. Response to white noise bursts showed a FSL of  $9.01\pm 0.42$  ms (Figure 14A). As not only the delays from sound occurrence to neuronal response is a decisive parameter for temporal processing, also the variability in timing was addressed. Taken the standard deviation (SD) of the FSL as a measure for firing accuracy, the highest precision (SD=0.109 ms; N=40) was achieved by stimulation with click sounds (Figure 14B). More variability in response accuracy was observed for pure tones (SD=0.409 ms; N=70) and white noise bursts (SD=1.249 ms; N=73). However, the large differences in latency and SD between clicks and both other stimuli are mainly an effect of the different rise times between stimuli. Pure tones and noise bursts were presented with 5 ms rise time, clicks with 0.01 ms. Additionally, LSO cells typically respond with high reliability on presentation of single acoustic signals. On the stimulation with an intensity of 20 dB above the respective threshold, the probability of eliciting at least one action potential was at 91.1 % for pure tones at CF, 96.7 % for noise bursts and 97.1 % for single clicks. Considering all recorded cells and all conducted experimental sweeps, 70.3 % of all cells responded to every stimulation sweep on presentation of a

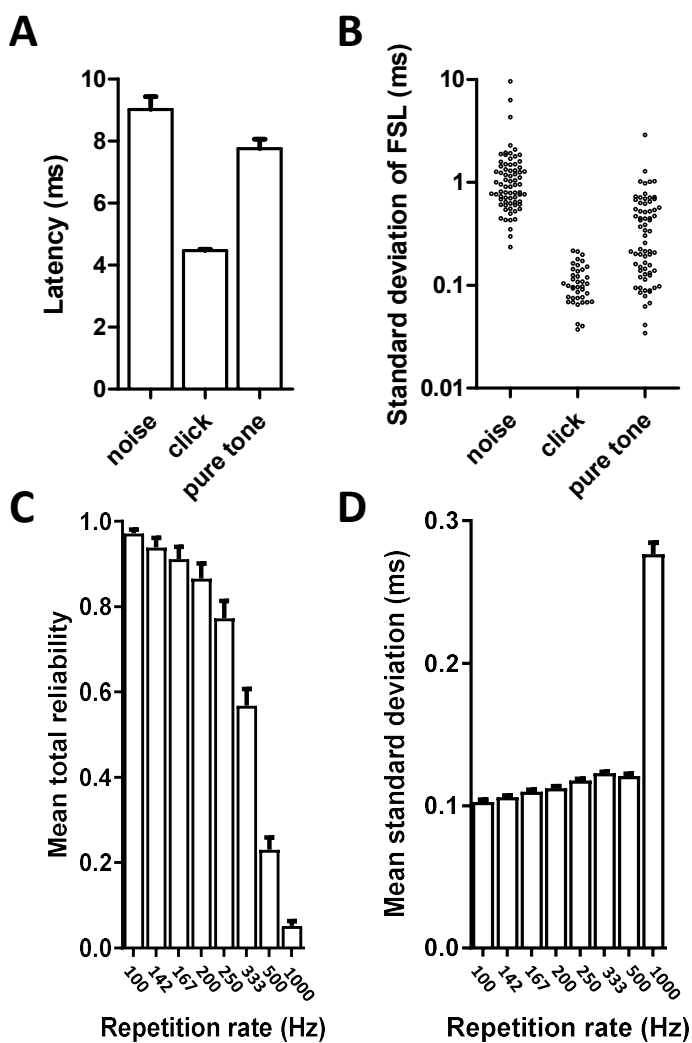


**Figure 14:** Temporal accuracy and reliability of neuronal response. **A:** Mean first spike latencies (FSLs) for the three applied stimuli. Substantial reduction for clicks is caused mainly by shorter rise-times of the stimulus. **B:** Scatter plot for individual standard deviation values of the FSL for each stimulus type. Standard deviation serves as indicator for processing accuracy. Smaller values and dispersion for click sounds are again the result of markedly shorter rise-times of the stimulus. **C:** Averaged mean total reliability for all LSO principal cells to respond on click trains with different repetition rates. A gradual decay in reliability for rising frequencies is observed. **D:** Spiking accuracy on click train stimulation, indicated by the averaged standard deviation, progressively decreases with rising repetition rates. Regardless of the low reliability for the 500 Hz condition, the corresponding standard deviation is still considerably small. This still indicates correlated response, whereas for the 1000 Hz condition, neurons tend to fire at the level of chance. Bar graphs show mean  $\pm$  S.E.M.

pure tone stimulus, 20 dB above response threshold at CF. For noise bursts, 88.0 % of all units elicited at least one action potential. This total reliability was highest on stimulation with clicks, where 89.7 % of all recorded cells showed a response. These results demonstrate a high temporal fidelity for the majority of recorded cells. Additionally, similar values were recorded for repetitive stimulation. On presentation of click trains with increasing stimulation frequency, the mean total reliability and the averaged temporal response fluctuations were assessed. Following a click train with 100 Hz repetition rate, a total response reliability of 97.1 % was shown. Increasing the stimulation rate up to 1000 Hz resulted in a gradual decline of firing reliability (Figure 14C). In addition to the decrease of response reliability, a progressively larger jitter (averaged standard deviation of the response to every single click) as a measure of reduced temporal precision was observed (Figure 14D). These results demonstrate a solid temporal fidelity for the response patterns of LSO cells.

#### 6.1.2.5 Rapid stimulation with click trains induces an effect of adaptation

For a characterization of a cell's behavior throughout the whole stimulation period and thus a determination of adaptation strength, the development of different parameters along the click train

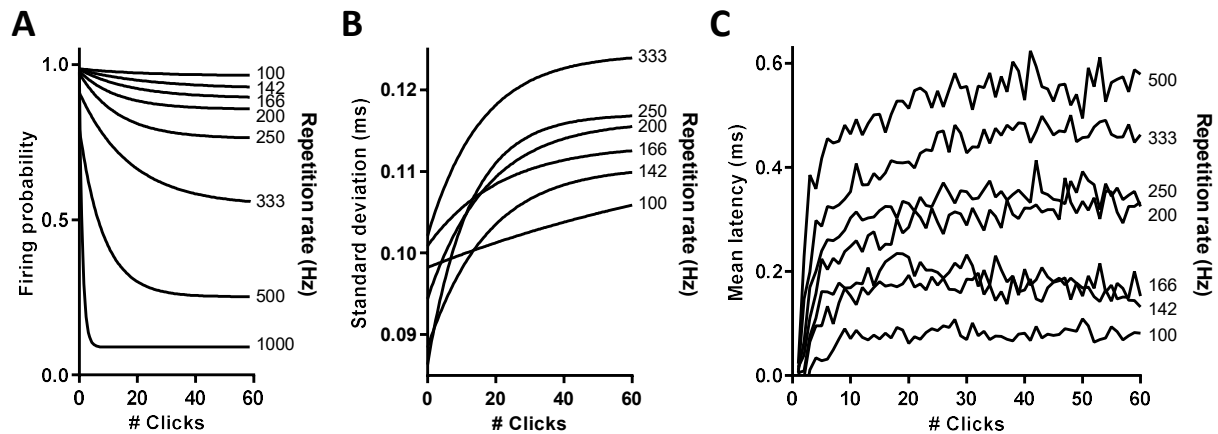


**Figure 15:** Firing probability and jitter increase for rising stimulation rates. **A:** Fitted functions on averaged firing probability for all tested repetition rates. Progress for first 60 clicks of each stimulation frequency shown. For most conditions, a gradual decay is observed, typically reaching a plateau phase after a certain number of clicks. **B:** Averaged standard deviation (SD) functions show a typical increase of the SD for successive click responses, likewise reaching a plateau phase. For most repetition rates, begin of plateau phase is more depended on the number of responses than on time. **C:** Mean latency of all recorded cells, averaged separately for each successive click. Values refer to the individual first spike latency. General progress increases for rising stimulation rates. In accordance to the previous analyses, after an initial increase in latency, a plateau phase is reached after a certain number of clicks, depending on the stimulation frequency.

was analyzed. In this context, an effective impact of adaptation was suspected to be revealed by a change in temporal response characteristics such as firing probability, jitter or latency. To address these parameters, the response to every single click of a click train was calculated.

#### *Changes in firing probability and jitter reflect temporal adaptation*

For the slowest tested repetition rate (100 Hz), no substantial change was seen for the probability of eliciting an action potential. The progress of probability was approximated with an exponential fit to the averaged response function of all recorded units (Figure 15A). Increasing the stimulation rate resulted in a gradual decay of firing reliability. Thus, for example, when stimulating with 333 Hz, after 30 clicks, the average firing probability was decreased to 60 %. Firing precision, assessed with the mean standard deviation for each click, similarly decreased with stimulation progress (Figure 15B). With rising repetition rates, a gradually faster and more pronounced increase in standard deviation was observed. Moreover, the average response latency of action potentials following consecutive clicks increased with higher stimulation rates (Figure 15C). Hence, after 60 consecutive clicks at the lowest measured stimulation rate (100 Hz), the average relative latency increased by 1.7 % from 4.46 ms to 4.54 ms. In contrast, at a stimulation rate of 333 Hz, after the same number of clicks the average latency of all recorded cells increased by 10.5 % to 4.92 ms.

*Decreasing number of spikes indicate adaptation for rising repetition rates*

The changes in firing reliability and accuracy were further reflected by the average number of action potentials following each click. LSO cells typically respond to clicks with a single action potential. Occasionally, a second spike was detected, commonly appearing in the initial segment of the click train. Respectively, the probability for a second action potential decreased during the course of stimulation. This characteristic can be indirectly addressed with the average total number of action potentials following each click (Figure 16A). The change in the number of observed spikes, but also the progress of the measured parameters in figures 16A&C typically reaches a plateau phase after a certain number of clicks. Consequently, a relative effect of adaptation can be assessed when comparing the initial part of a repetitive stimulation train with a segment from the plateau phase. Accordingly, an average number of 1.09 elicited spikes per click for the first 10 clicks of a click train of 100 Hz was observed, whereas this number decreased for the last ten clicks of the spike train to an average number of 1.02 spikes per click. Following this analysis, the total number of spikes to the entire click train serves as an indicator for adaptation. For example with 333 Hz repetition, these

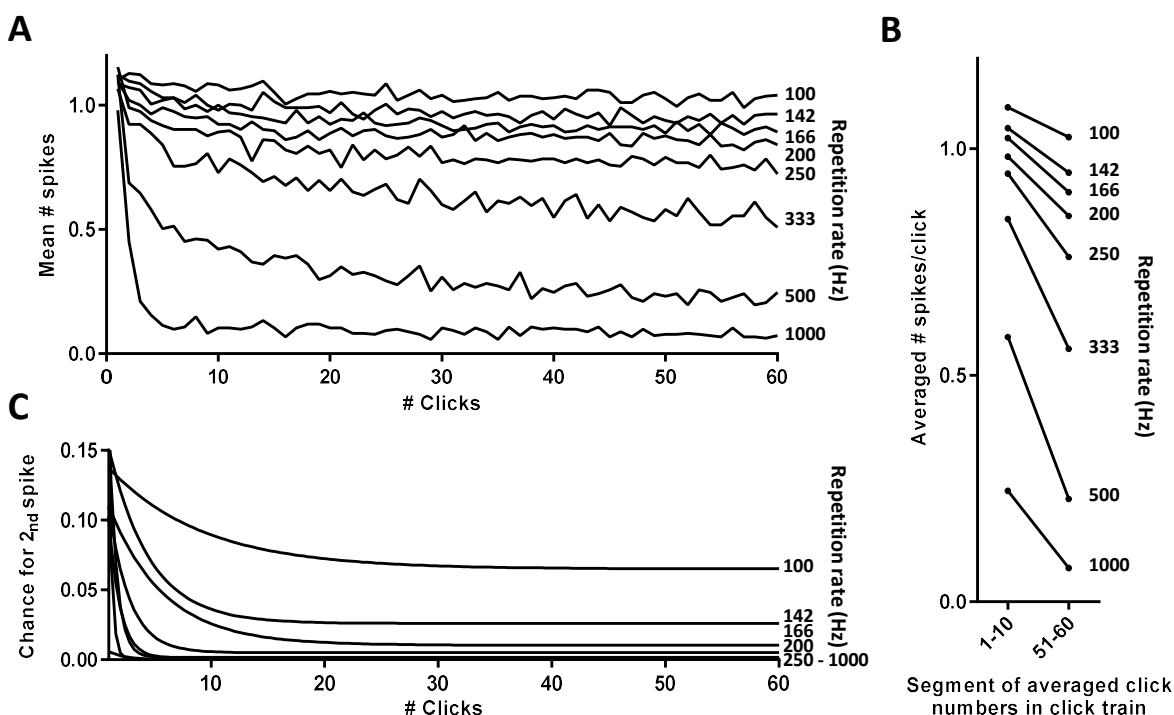


**Figure 16:** Adaptation is indicated by decreasing number of elicited spikes. **A:** Averaged progress for the mean number of elicited spikes per single click. Distinct dependency on stimulation rate is observed. Mean numbers for 100 Hz never drop below 1.0, indicating high reliability and frequent occurrence of more than one spike per click. **B:** For better comparability, averaged segments of the response are correlated for stimulation rates and averaged action potential numbers. Rising repetition frequencies are closely linked to a faster decrease in spike numbers as apparent from steeper slopes. Segment size and position dependent on technical limitations. **C:** Decay functions for the chance to elicit more than one action potential per click, averaged separately for each click. Plateau phase is encountered faster compared to previous measurements. For repetition rates higher than 142 Hz, general chance for multiple APs is almost abolished.

numbers change to 0.84 spikes in the first segment and 0.56 in the last (Figure 16B). As apparent from this figure, the amount of decay between first and last segment and hence the steepness of the conjoints increases for repetition rates from 100 Hz to 500 Hz. This demonstrates an increasing impact of adaptation for these stimulation rates, likewise pointing out the averaged number of action potentials per click as a supplementary measure for adaptation.

Besides, the chance to elicit more than one action potential can be interpreted as an indirect measure for the degree of adaptation, as the comparison of our data for the different repetition rates and the response to single clicks revealed. For the lowest measured stimulation rate of 100 Hz, the chance for eliciting a second spike peaks at the beginning of the presented click train with an overall probability of 14 % and reaches a plateau phase after 15-25 clicks, the chance thereupon fluctuating around 7 % (Figure 16C). With increasing stimulation rates, the initial peak in probability declines, the plateau phase is reached earlier, respectively. Correspondingly, the overall chance of eliciting a second action potential gradually decreases with higher stimulation rates. In summary, these results confirmed or even exceeded our expectations, illustrating the LSO of mice as a highly precise and fast relay station within the auditory pathway. Additionally, this defined the frame conditions for following comparisons with genetically modified animals and served to set the parameters for subsequent binaural adaptation experiments.

### 6.1.3 Response characteristics of binaural stimulation

#### 6.1.3.1 Rising contralateral sound intensity gradually suppresses ipsilateral excitation

The LSO of various vertebrates has been extensively studied and among others the first nuclei where binaural inputs converge. Especially for high frequency acoustic stimuli, this nucleus processes interaural level differences (ILDs) and is the first stage in the auditory pathway to contribute to the localization of a sound source in the azimuthal plane. The temporal and spatial precision how LSO neurons of mice analyze ILDs has not been explored to date. As previously shown, principle cells of the LSO receive excitatory information from the ipsilateral ear. Simultaneously, the contralateral ear projects auditory signals to the contralateral MNTB, from where inhibitory afferents cross the midline and converge on principal LSO neurons. As the contralateral intensity increases, and eventually exceeds a certain value, the ipsilateral excitation is gradually suppressed (Figure 17B). As a first attempt to characterize and quantify this mechanism, all recorded units were tested for ipsilateral excitation with simultaneous contralateral inhibition, in combination with three types of acoustic signals: noise bursts, clicks and pure tones. These stimuli were chosen to examine different aspects of the temporal and spectral processing. Clicks and noise bursts are broadband signal, incorporating many frequencies, whereas pure tones had only one particular frequency. On the other hand, clicks are very brief signals and are thus in contrast to both other long types of stimuli. All

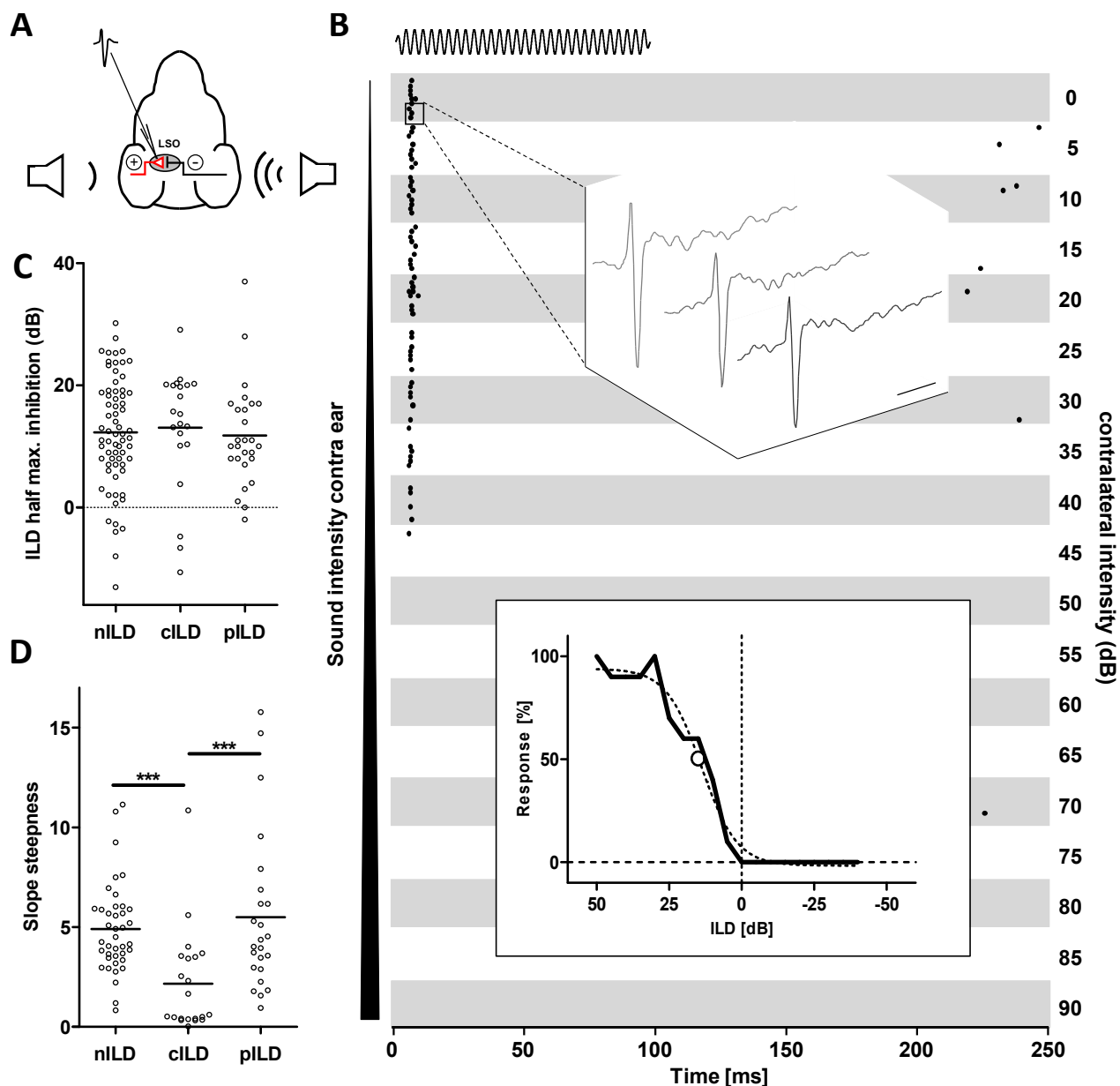


**Figure 17:** Contralateral inhibition gradually suppresses ipsilateral excitation. **A:** Schematic recording scenario. Stimulation of ipsilateral ear triggers excitatory inputs, whereas afferents from the contralateral side inhibit activity. **B:** Raster dot plot of typical ILD processing. Ipsilateral pure tone intensity at unit's CF is kept constant at 20 dB above perception threshold. Contralateral intensity is increased in steps of 5 dB. Ipsilateral excitation is gradually suppressed by contralateral inhibition. The resulting ILD function is approximated using a sigmoidal fit (lower inset). Parameters of fitted function are used for ILD quantification. Point of inflection of sigmoidal fit (hollow dot) indicates ILD of half maximal inhibition. Spike shape comparison of every response guarantees high quality single unit recording with low signal-to-noise ratio (upper inset). Scale bar: 2 ms. Stimulation duration is indicated by sine wave. **C:** Scatter plot for half maximal inhibition ILDs. Comparison for the three stimulus types. No significant differences are observed between conditions. Individual ILD values are distributed across behaviorally relevant range and beyond. **D:** Scatter plot for slopes of fitted ILD functions. Smaller values reflect steeper slopes. Significance for click ILDs is mainly caused by shorter rise-times of the clicks and predominant response with exclusively one spike per click. Lines in scatter plots represent mean values. Mann-Whitney test was used to evaluate differences between genotypes.  $*p < 0.05$  was considered statistically significant.

cells were sensitive for ILDs of all three kinds of signals, showing similar half-maximal inhibition values (i.e. point of inflection of the sigmoidal fit, Figure 17B, lower inset). Mean ILD values for stimulation with pure tones showed half-maximal inhibition at  $11.8 \pm 1.6$  dB. For noise bursts, an average ILD of  $12.3 \pm 1.1$  dB was measured, whereas a mean ILD of  $13.1 \pm 2.2$  dB was recorded for clicks (Figure 17C). As an estimation for the discriminatory power, the slope of the sigmoidal fit at the point of inflection was calculated (McAlpine, 2005). With the applied Boltzmann equation, decreasing slope values reflect a steeper slope of the ILD function, resulting in a faster and more pronounced contralateral inhibitory effect. It was shown that ILD functions from click sounds reveal the steepest slopes ( $2.2 \pm 0.6$ ), followed by noise induced ILD functions ( $4.9 \pm 0.4$ ) (Figure 17D). Pure tone ILDs at the unit's CF showed similar half-maximal ILD values compared to noise ( $5.5 \pm 0.8$ ). The statistically significant difference between click ILDs and both other stimulus types (nILD,  $n=40$ , vs. cILD,  $n=21$ : Kruskal-Wallis with Dunn's post-hoc test:  $p < 0.0001$ ; pILD,  $n=24$  vs. cILD,  $n=21$ : Kruskal-Wallis with Dunn's post-hoc test:  $p = 0.0005$ ) is predominantly a result of the response pattern of LSO cells to these different signals. These cells commonly respond to clicks with only one action potential, whereas for noise bursts and pure tones, one to several spikes are elicited. Increasing the contralateral intensity often gradually suppressed neuronal firing. Thus, the response to noise and pure tones successively decreased from few to no spikes. In case of clicks, there was mostly only one spike which was inhibited. This results in a steeper slope of the ILD function. These results give evidence that the LSO of mice is of comparable function as in other species (Adam et al., 1999; Boudreau and Tsuchitani, 1968; Covey et al., 1991). Moreover, measured ILD values are in accordance to what has been shown in animals of similar size and which share corresponding environmental conditions.

#### 6.1.3.2 Minor effect of adaptation is based on postsynaptic mechanisms

If the auditory system of an animal would be continuously occupied with the processing of perpetual environmental signals such as the rustling of trees in the wind, perception of new and subtle sounds like the cracking of a branch caused by an approaching predator would be impaired. The possibility to adapt to a prevailing stimulus thus helps a sensory system to increase contrast between dispensable enduring input and new and noteworthy signals. In this context, the mechanism of adaptation refers to a cell's ability to reduce its response to ongoing stimulation, e.g. with gradually decreasing firing rates. The majority of LSO principal cells does not respond throughout the entire duration of sustained sounds like pure tones or noise, but show robust onset firing exclusively at the beginning of such sounds. Consequently, the cell's firing pattern does not adapt to ongoing stimulation. On repetitive sounds, LSO cells are able to follow high repetition rates, as previously shown with click sounds. In order to mimic adaptive behavior, a cell can be recurrently and rapidly stimulated and thus repetitively excited. Pilot studies have shown that strong enduring excitation can provoke mild

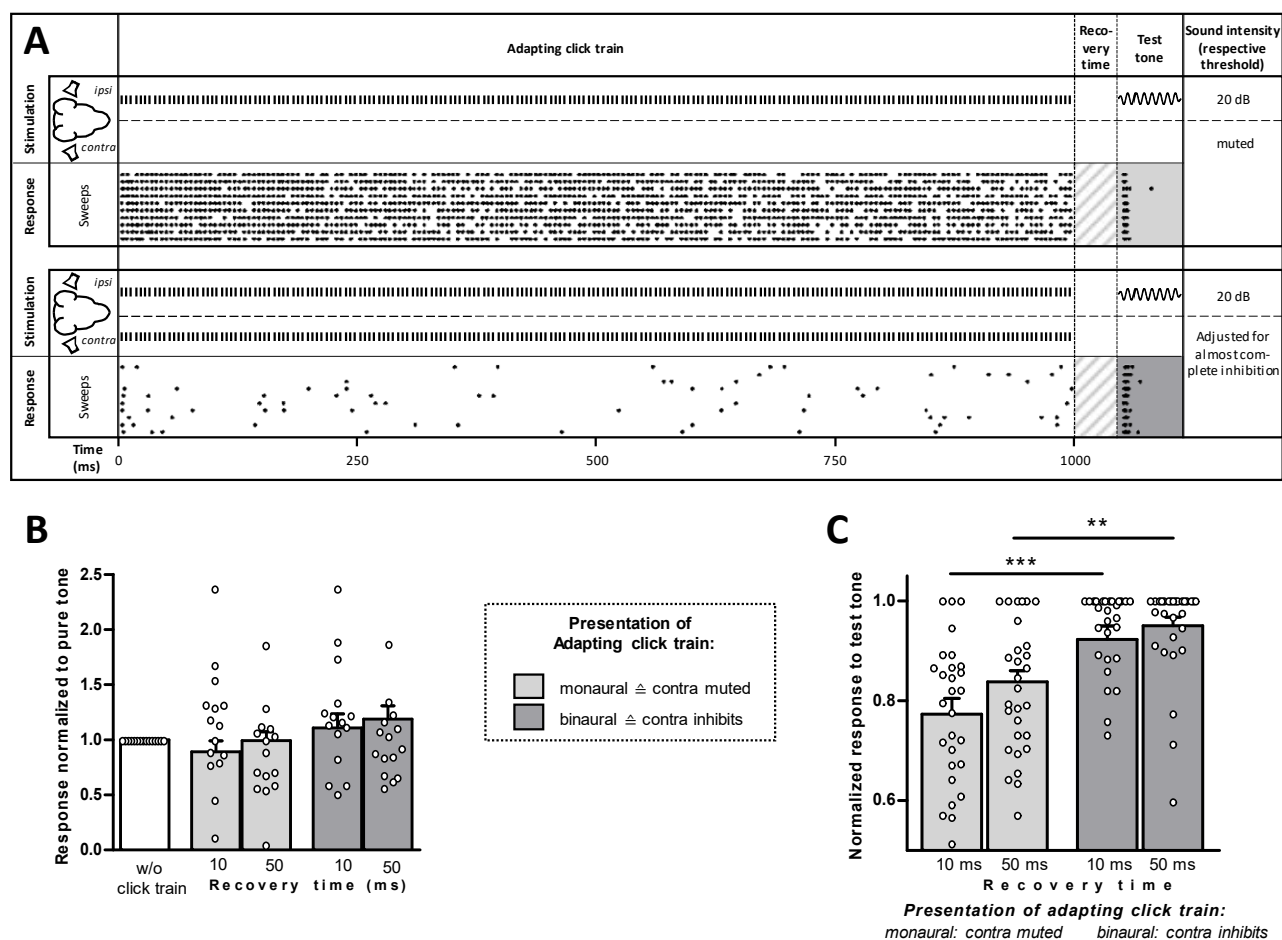


**Figure 18:** Adaptation of LSO cells for pure tones following repetitive click stimulation. **A:** Stimulation paradigm with exemplary response pattern. Cells are excessively stimulated by a 200 Hz click train. Binaural stimulation inhibits most of the neuronal response. Subsequent response to an ipsilateral pure tone at the unit's CF (shaded) is modulated by the preceding click train. Normalized response to pure tone is compared. **B:** Normalization on pure tones without preceding click train serves as baseline response. No significant differences are observed for either mon- or binaural adaptation conditions, as well as for both tested recovery durations between click train and pure tone. **C:** Difference between mon- and binaural click trains reveals effect of contralateral inhibition on subsequent pure tone processing. No significance between recovery durations indicates a minor impact of adaptation at the level of the LSO. Bar graphs represent mean  $\pm$  S.E.M. Kruskal-Wallis test with Dunn's post-hoc test was used to evaluate differences between genotypes.  $*p < 0.05$  was considered statistically significant.

adaptation of the response to consecutive pure tone stimulation in LSO neurons. Following a high frequency click train, serving as the adapting stimulus, a test tone at the cell's CF was presented (Figure 18A). To prevent contralateral inhibition and an influence of crosstalk, the test tone was in any case presented only ipsilaterally and 20 dB above the unit's individual response threshold for a pure tone at CF. The adapting click train was presented either ipsilaterally or binaurally, i.e. ipsilateral excitation was kept constant, contralateral inhibition was toggled. Using this method, we tested the influence of both ipsilateral excitation and contralateral inhibition on a cell's ability to

adapt to a stimulus. Additionally, some conclusions regarding the origin of the adaptation can be drawn. Adaptation could be caused by either intrinsic mechanisms like the modulation of ion channels following strong somatic excitation after ipsilateral stimulation, or could have been presynaptically propagated from previous stages of the auditory path. If adaptation would be observed following binaural stimulation while the unit did not or only marginally respond to preceding repetitive ipsilateral stimulation, this would exclude a mere intrinsic, postsynaptic origin and would support the hypothesis of propagated adaptation. However, no significant changes in firing rates were observed following either ipsilateral or binaural click trains in comparison with the response to a pure tone without preceding click train (Figure 18B). Even if the test tone was presented as briefly as 10 ms after the adapting click train no significant decrease in firing was observed. This indicates that LSO neurons show no adaptive effect after strong and repetitive ipsilateral excitation. Yet, a trend between the responses following either monaural or binaural adaptation can be assumed. Individual data points were scattered across a broad range, suggesting heterogenic response characteristics of the respective cells. Thus, to examine only the effect of adaptation with respect to the synaptic origin, a direct comparison of only the response following click trains revealed a significant decrease in firing rates after monaural stimulation (Figure 18C; 10 ms: Kruskal-Wallis with Dunn's post-hoc test:  $p=0.0002$ ; 50 ms: Kruskal-Wallis with Dunn's post-hoc test:  $p=0.0014$ ;  $n=29$ ). Taken together, these findings indicate a negligible effect of adaptation at the level of the LSO for natural conditions, where sounds typically reach both ears. However, excessive activation of LSO principal cells with only ipsilateral stimulation does effectively suppress the response to a consecutive pure tone. Yet, this kind of adaptation only occurs for the artificial condition of exclusively monaural stimulation, which will hardly occur in a native context. Nonetheless, the results demonstrate an intrinsic and thus postsynaptic origin for this aspect of adaptation.

## 6.2 Altered auditory processing in the LSO of FXS mice

Sensory hyperexcitability is a frequent symptom of FXS patients. Previous studies could already show altered neuronal activity in the auditory and other sensory systems (Castrén et al., 2003b; Rotschafer and Razak, 2014; Sinclair et al., 2017), with emphasis on the cortical level. One aim of the present study was to investigate neuronal responses at an early stage of sensory processing. The LSO represents one of the first nuclei in the auditory system. Additionally, it is the first nucleus to compute binaural information, integrating excitatory and inhibitory inputs from both ears. Hence, this nucleus is the ideal location to study alterations in the balance of excitation and inhibition, encompassing the possibility to control excitatory and inhibitory inputs separately *in vivo*.

### 6.2.1 LSO cells of FXS mice show slightly elevated responses

Spontaneous activity is a fundamental feature of excitable cells like neurons. As a first approach to assess altered neuronal excitability in FXS, the spontaneous firing rates of all recorded LSO units were compared between knockout (KO) and wild type (WT) animals. Firing rates between 0 and 65 Hz were observed, but no significant difference was apparent (Figure 19A). Moreover, about every second recorded cell of either genotype did not show spontaneous activity at all.

As previously shown, most LSO cells respond to white noise, pure tones and click sounds with onset firing, comprised of one to several action potentials at stimulus onset, in a wide range regardless of the stimulus intensity. The majority of LSO cells of *Fmr1* KO animals showed identical response

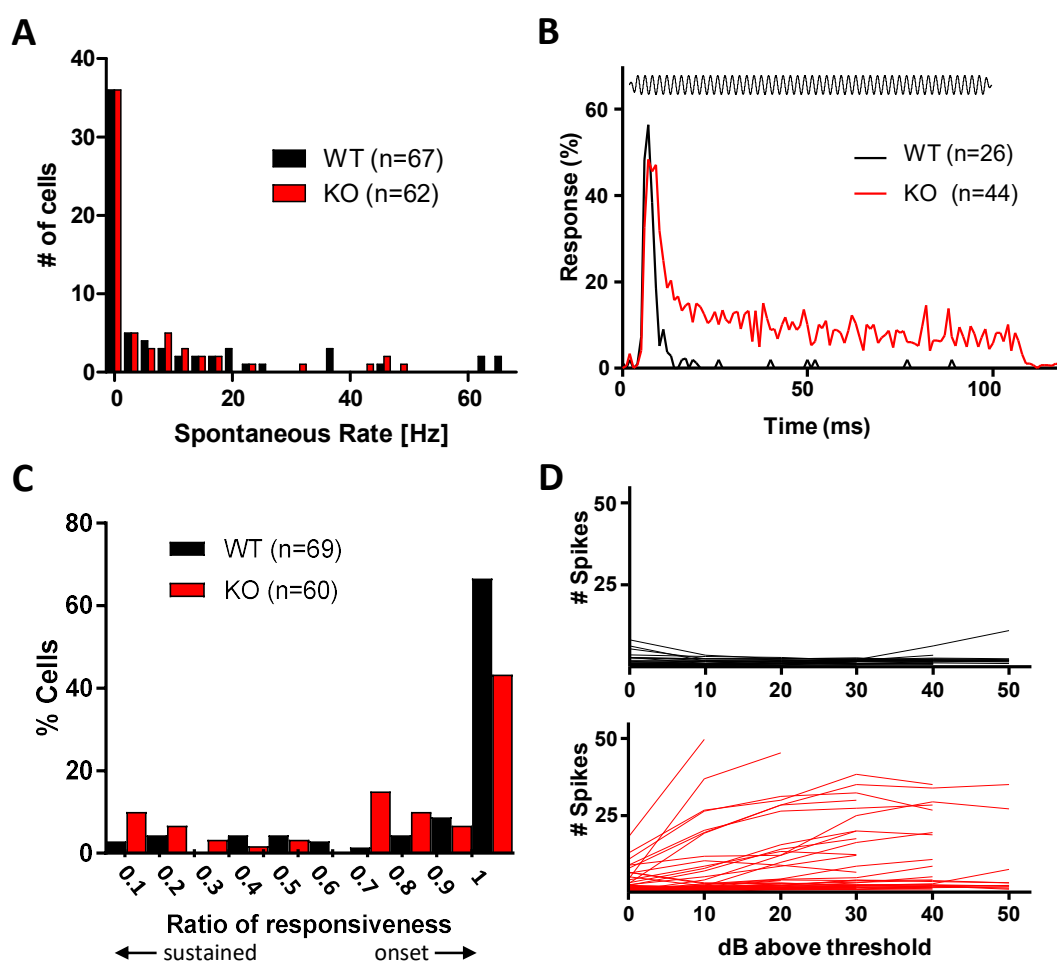


**Figure 19:** Impact of the *Fmr1* knock-out on basic firing properties and monaural sound processing. **A:** Enhanced excitability as a result of the lack of FMRP has no effect on the spontaneous activity of LSO neurons. The vast majority of units exhibits no or little firing rates. **B:** Averaged spike response of WT and KO LSO neurons reveals more sustained activity throughout pure tone presentation in *Fmr1* KO mice. **C:** Ratio of responsiveness quantifies neuronal response pattern and demonstrates a subtle shift in numerous onset neurons of KO animals towards an enhanced activity. **D:** Spike rate dependence on sound pressure level for individual neurons in WT and KO mice, showing no change in the number of spikes for WT neurons with rising sound pressure level at CF, whereas spike numbers gradually increase for several KO neurons. Response threshold is set to 0 dB for each individual neuron.

properties. However, a considerable number of cells was found, which responded with few or several more action potentials and over a longer duration of the stimulation period. Plotting of the summed normalized response to a pure tone at CF revealed an increased general activity (Figure 19B). This finding is likewise reflected when calculating the previously introduced ratio of responsiveness (RR). This ratio helps to quantify the firing pattern beyond the classical categories of onset and sustained firing and reveals subtle differences in the neuronal response. A ratio of 1 represents an exclusively onset responding cell, whereas a value of 0.5 indicated the occurrence of the same number of spikes in the first 10 ms of response compared to the latter 90 ms. In terms of a conventional classification, both mentioned firing patterns would have been considered as onset firing. This approach allowed for a closer determination of a mildly altered firing behavior.

As can be seen in Figure 19C, 67% of all recorded WT units displayed an RR of 1 for a pure tone at CF, 20 dB above threshold, hence indicating strong onset firing. In KO animals, however, only 43% of all cells showed this strong onset firing. Moreover, 32% displayed an RR between 0.5 and 0.9, indicating a change towards more sustained firing cells. In WT animals, however, only 17% of all cells showed an RR in this range. This finding supports the hypothesis of an increased neuronal excitability, reflected in elevated responses. In addition, the vast majority of LSO cells in WT animals responded with a constant number of action potentials in an onset manner over a wide range of stimulus intensities (Figure 19D). While most cells of KO animals showed a comparable behavior, a notable number of cells exhibited rising firing rates with increasing stimulus intensity, pointing towards an elevated neuronal activity. According to the findings in WT animals, RR was not correlated with the spontaneous activity or CF in *Fmr1* KO mice.

## 6.2.2 Frequency tuning is broadened in FXS animals

The bandwidth of a neuron's frequency tuning at different intensity levels is a consequence of various parameters of the animal's auditory system. Aside from monaural factors, such as lateral inhibition at the level of the cochlea, filtering in successive nuclei or the number of converging excitatory afferents, also binaural components like contralateral inhibition and feedback mechanisms shape a neuron's tuning curve. In slice recordings, it was shown that cells of KO animals receive an increased number of synapses converging onto a single LSO neuron (Garcia-Pino et al., 2017). This could indicate that LSO neurons in FXS mice receive inputs from more cochlear nucleus neurons with presumably different frequency tuning. As a consequence, frequency tuning should be broader in *Fmr1* KO compared to WT animals. Figure 20A shows the frequency response area of two representative LSO neurons of WT and *Fmr1* KO animals. Generally, tuning curves of *Fmr1* KO LSO neurons were considerably broader when compared to WT neurons. Tuning bandwidth was quantified by measuring the Q10 and Q30 value (CF/tuning bandwidth at 10 and 30 dB above

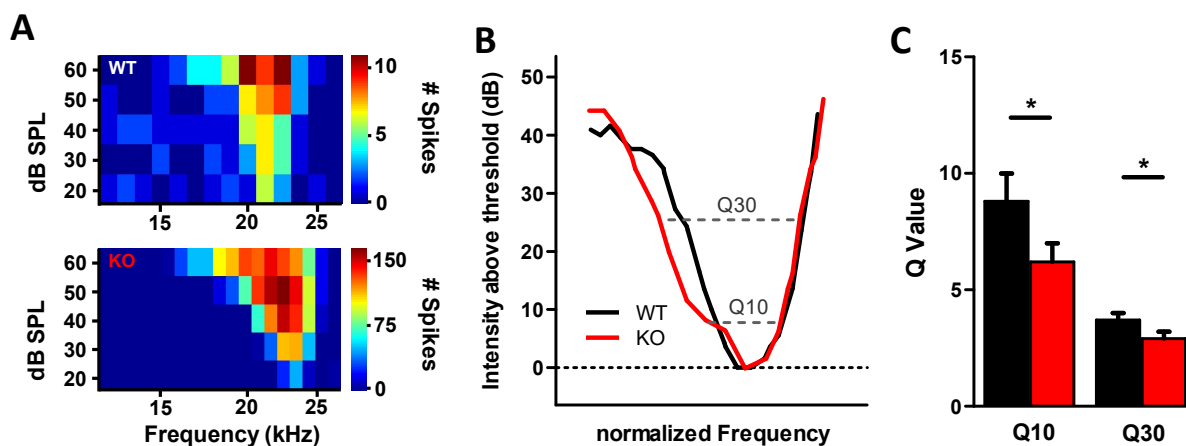
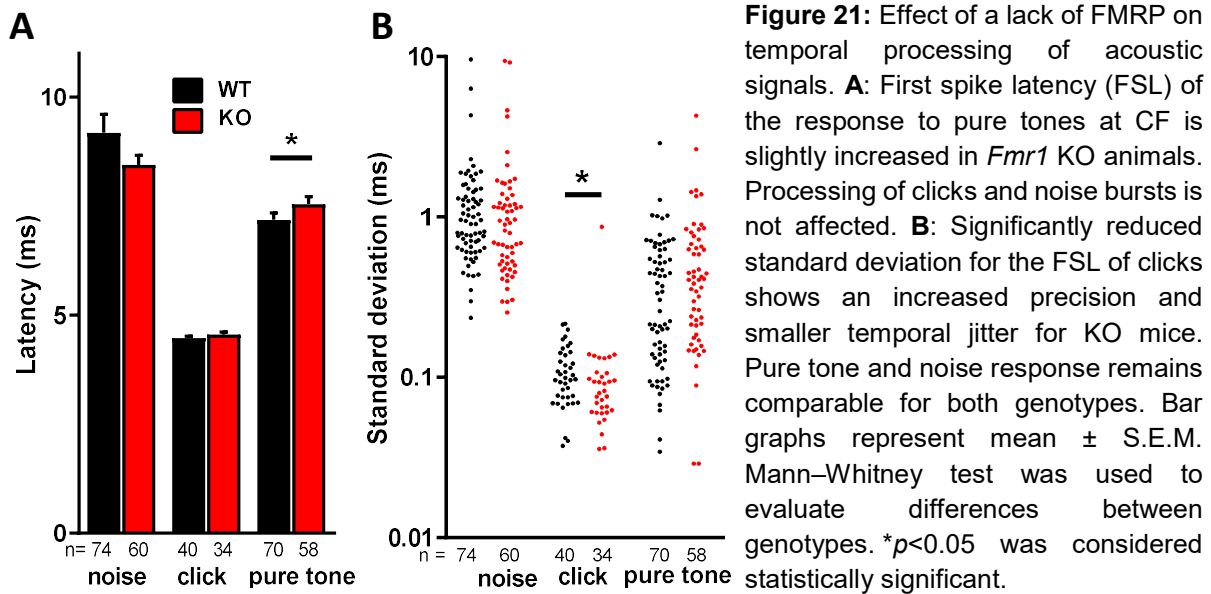


**Figure 20:** Frequency tuning is broadened in FXS. **A:** Frequency response areas of two exemplary LSO neurons, each patch showing the total number of spikes of four repetitions. Warmer colors represent stronger firing. **B:** Schematic tuning curves, illustrating broadening and calculation of Q values. **C:** Q values as a measure for frequency tuning sharpness, expressing the bandwidth of the tuning curve 10 and 30 dB above threshold. Smaller Q10 and Q30 values indicate significantly broader tuning in KO animals. Bar graphs represent mean  $\pm$  S.E.M. Mann–Whitney test was used to evaluate differences between genotypes.  $*p < 0.05$  was considered statistically significant.

threshold, Figure 20B). Pooled data revealed a significant decrease of Q10 and Q30 values in KO mice as a measure for a broadening of bandwidth (Figure 20C; Q10: WT =  $8.8 \pm 1.2$ ,  $n=20$ ; KO =  $6.2 \pm 0.8$ ,  $n=40$ ; Mann-Whitney:  $p=0.0129$ ; Q30: WT =  $3.7 \pm 0.3$ ,  $n=19$ ; KO =  $2.9 \pm 0.3$ ,  $n=37$ ; Mann-Whitney:  $p=0.0186$ ). These findings are also in line with the hypothesis of an increased neuronal excitability, leading to an impaired frequency discrimination.

### 6.2.3 First spike latency and jitter are affected only for particular stimulation

Altered levels of FMRP have been shown to be related with delayed first spike latencies and a subtle increase in jitter on the cortical level (Rotschafer and Razak, 2013b). To answer the question, how strong these temporal aspects of signal transduction are affected already at the level of the auditory brainstem, latencies and jitter were analyzed. A significant increase in FSL for stimulation with pure tones was shown in KO animals (WT:  $7.18 \pm 0.16$  ms,  $n=70$  vs. KO:  $7.54 \pm 0.18$  ms,  $n=58$ ;  $p=0.0316$ ) (Figure 21A). However, no differences of first spike latency in *Fmr1* KO mice were observed for clicks (WT:  $4.47 \pm 0.05$  ms,  $n=40$  vs. KO:  $4.56 \pm 0.06$  ms,  $n=34$ ;  $p=0.6962$ ) and noise bursts (WT:  $9.18 \pm 0.43$  ms,  $n=74$  vs. KO:  $8.45 \pm 0.22$  ms,  $n=60$ ;  $p=0.0569$ ). The discrepancy of mean values between different stimuli is predominantly an effect of the nature of the stimulus and the technical realization. Pure tones and noise bursts had longer rise-fall-times in comparison with clicks to reduce interferences at the level of the transducers. Consequently, this effects the standard deviation in the same manner.



Interestingly, response accuracy for click sounds showed to be significantly more precise in KO animals compared with the WT littermates (WT:  $0.1087 \pm 0.007$  ms,  $n=40$  vs. KO:  $0.1079 \pm 0.024$  ms,  $n=34$ ;  $p=0.0331$ ) (Figure 21B). On the other hand, the standard deviation of the FSL as a measure for a cell's firing accuracy remained unchanged for pure tones (WT:  $0.41 \pm 0.05$  ms,  $n=70$  vs. KO:  $0.57 \pm 0.09$  ms,  $n=58$ ;  $p=0.0623$ ) and noise bursts (WT:  $1.25 \pm 0.16$  ms,  $n=74$  vs. KO:  $1.30 \pm 0.22$  ms,  $n=60$ ;  $p=0.2618$ ). This points towards an even increased temporal precision as a result of a lack of FMRP, at least for the processing of single brief signals like clicks.

#### 6.2.4 Increasing the stimulation rate cause a faster decrease of temporal precision in *Fmr1* KO animals

This finding of subtle changes in temporal processing was further investigated with repetitive stimulation. A click train was presented ipsilaterally to examine the response properties during sustained acoustic excitation. To assess a neuron's firing acuity throughout cyclic stimulation, the vector strength (VS) was calculated according to Goldberg and Brown, 1969. It describes the correlation of a neuronal response to a repetitive stimulus. The response to each single repetition is summed and averaged, resulting in a VS value between 0 for no correlation to 1 for a perfect match of stimulus and response. In the present case of onset neurons with almost exclusively one single action potential following each click, VS can thus be interpreted as the variability or jitter of the neuronal response. For stimulation with clicks at a repetition rate of 100 Hz, a subtle but not significantly higher VS for *Fmr1* KO animals was observed (WT:  $0.977 \pm 0.028$ ,  $n=38$  vs. KO:  $0.984 \pm 0.021$ ,  $n=34$ ; Mann-Whitney:  $p=0.0962$ ) (Figure 22A). This could confirm the previous finding of a smaller FSL jitter in KO animals and could indicate a generally increased acuity throughout sustained excitation. To additionally assess the question of temporal resolvability, VS was calculated for higher repetition rates of the presented clicks. Larger, but also insignificant VS

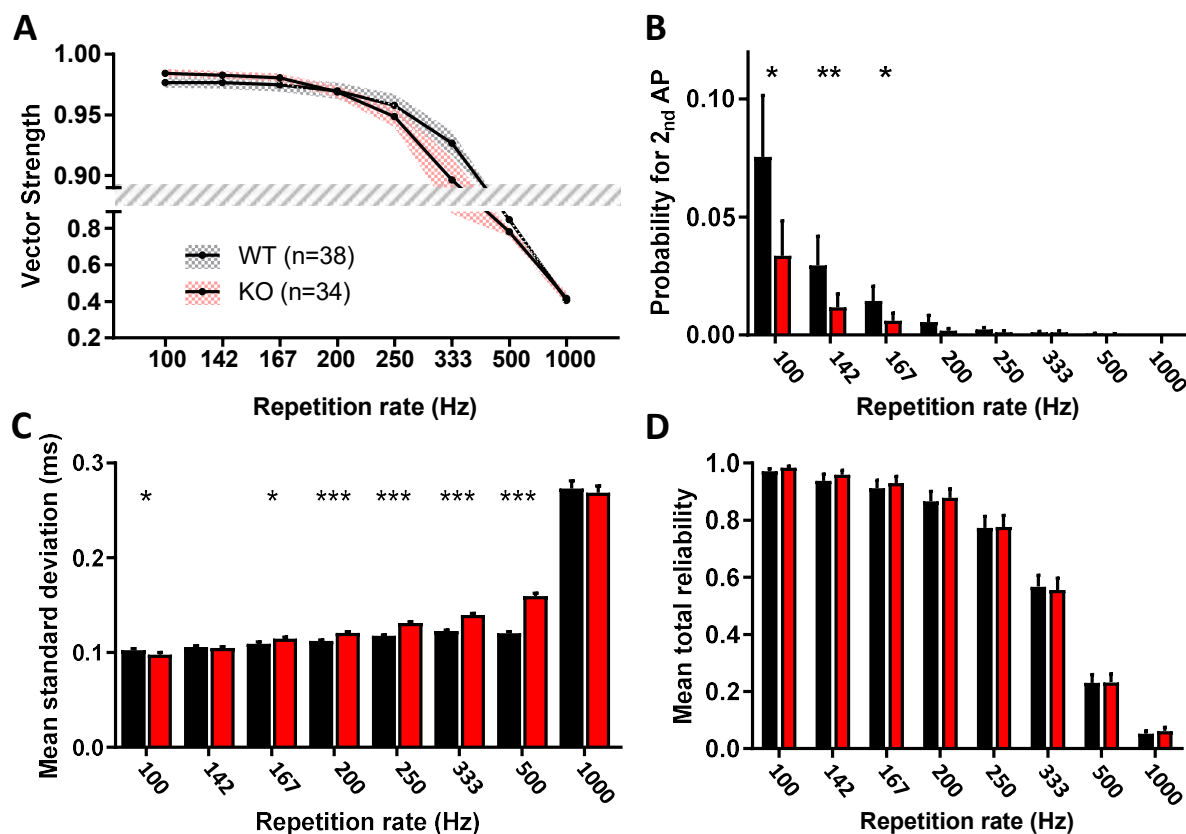


**Figure 22: A:** Temporal processing of repetitive stimulation is traditionally quantified by calculation of vector strength. This conventional approach shows to be biased for the response to clicks of onset firing neurons, likewise giving insignificant results. **B:** Biased results of vector strength calculation are attributed to the increased chance of multiple spiking. Probability for more than one action potential following click stimulation is substantially increased for WT animals. **C:** Analysis of single click responses reveals a reduced standard deviation for the slowest tested repetition rate of 100 Hz in *Fmr1* KO animals. A gradual increase of jitter is observed for rising stimulation frequencies in comparison to WT littermates. This indicates an altered temporal processing in KO mice, including impairments in the computation of rapid stimulation. **D:** General reliability to respond on repetitive click stimulation is not affected by a lack of FMRP at the level of the LSO. Bar graphs depict mean  $\pm$  S.E.M. and  $*p < 0.05$  was considered statistically significant.

values in KO animals were calculated for repetition rates of 142 Hz and 166 Hz (142 Hz: WT:  $0.977 \pm 0.033$ ,  $n=38$  vs. KO:  $0.983 \pm 0.020$ ,  $n=34$ ; Mann-Whitney:  $p=0.2430$ ; 166 Hz: WT:  $0.975 \pm 0.036$ ,  $n=38$  vs. KO:  $0.980 \pm 0.021$ ,  $n=34$ ; Mann-Whitney:  $p=0.3292$ ), likewise suggesting smaller general jitter in KO animals. Conversely, for all higher repetition rates tested, a trend to larger VS values for WT units was observed. These observations could suggest that neurons of *Fmr1* KO animals respond generally more precise when stimulated with single or slowly iterated clicks. However, using VS as a measure for a unit's precision is only suitable for neurons with sustained or strict onset firing pattern (i.e. exclusively one spike per stimulation). If a cell responds with more than one spike, VS decreases significantly (see methods). As previously shown, LSO neurons occasionally elicit two or more action potentials. In case of FXS, sensory hyperexcitability could be a result of increased firing. Yet, the general probability to elicit more than one spike after a single

click was reduced in FXS KO animals (WT:  $0.120 \pm 0.049$  vs. KO:  $0.052 \pm 0.021$ ). For repetitive clicks, analysis of the spike numbers following each click at different stimulation frequencies revealed the same correlation. The probability for the release of more than one spike was more than twice as high in WT mice at slow repetition rates (100 Hz: WT:  $0.0756 \pm 0.0260$  vs. KO:  $0.0335 \pm 0.0147$ ; Mann-Whitney:  $p=0.0102$ ) (Figure 22B). This observation persists also for higher repetition rates, as a significant difference was analyzed for the three slowest stimulation frequencies. As previously described (see methods), more second spikes explain a lower VS in WT animals for slow repetition rates. On the other hand, if VS and thus temporal precision of WT animals was effectively higher in WT animals, this would be inconsistent with the smaller jitter of FSLs for clicks in KO animals. To resolve this dilemma, the standard deviation of each response to every single click was calculated and averaged (Figure 22C). For the slowest tested repetition rate of 100 Hz, a significantly smaller standard deviation was shown across the entire stimulation period (WT:  $0.103 \pm 0.0016$  ms vs. KO:  $0.098 \pm 0.0021$  ms;  $p=0.0168$ ). This finding is in line with the results for single clicks. For 142 Hz, no difference was apparent, whereas for faster stimulation rates a gradual increase of the SD in KO animals was demonstrated. Only for the highest measured stimulation frequency of 1000 Hz, no apparent difference was detected. Yet, as LSO cells commonly are not able to follow such high repetition rates, the standard deviation for 1000 Hz is of minor relevance and reflects a firing at chance. This implies that LSO neurons of *Fmr1* KO animals respond with higher temporal precision on single or slowly repeating clicks, but lose this accuracy with increasing stimulation rate.

A higher excitability, in combination with synaptic inputs from more cells in *Fmr1* KO animals, gives reason for two different assumptions. Increased firing probability could lead to an enhanced reliability, since thresholds can be reached earlier. In contrast, conflicting synaptic inputs due to a fragmentary refinement could result in a less faithful transmission of neuronal signals. Yet, calculation of the mean total reliability, i.e. the averaged reliability of every single click to elicit an action potential revealed no differences between WT and *Fmr1* KO animals at any of the tested click repetition rates (Figure 22D). This finding demonstrates that FMRP has no influence on firing reliability. Moreover, the shapes of the response functions of elicited number of spikes and the mean latency throughout presentation of click trains with different repetition rates likewise showed no differences between genotypes. Hence, these aspects of temporal processing seemed to be unaffected from the knock-out of *Fmr1*.

### 6.2.5 ILD processing of pure tones is shifted in KO animals

LSO neurons encode interaural level differences (ILDs) by integrating excitatory ipsilateral and inhibitory contralateral inputs. The imbalance of these inputs in FXS mice, as observed *in vitro* (Garcia-Pino et al., 2017), suggests that ILD sensitivity is affected by the loss of FMRP. For both *Fmr1* WT and KO mice, LSO neurons responded maximally when the contralateral stimulus

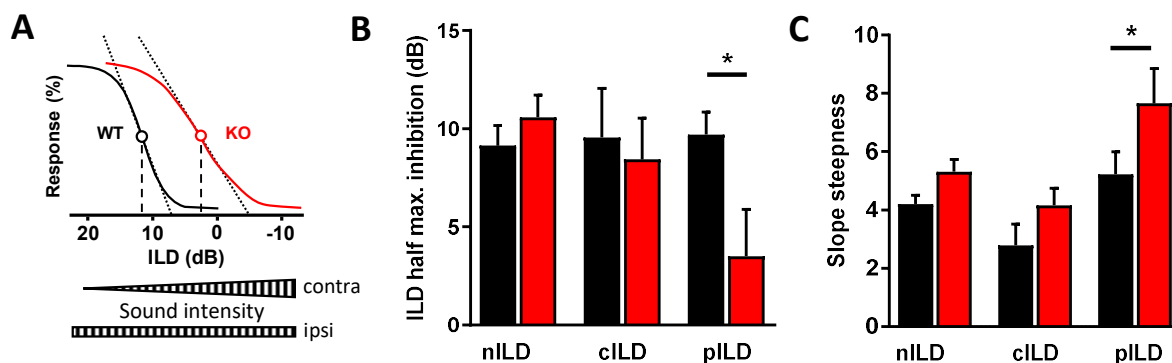


**Figure 23:** Altered ILD processing in FXS KO animals. **A:** Illustration of a fitted ILD function. Points of half-maximal inhibition (hollow dot) quantify the balance of inhibition and excitation. Slopes of function at this point are used to assess efficacy of inhibition. **B:** Half-maximal inhibition as a result of increasing contralateral pure tone stimulation intensity is shifted in favor of ipsilateral excitation in *Fmr1* KO mice. This indicates an altered balance of inhibition and excitation for the processing of binaural pure tone stimuli. Click and noise ILDs are not affected by the loss of FMRP. This is attributed to a decreased impact of lateral inhibition for these broadband acoustic stimuli. **C:** Fitted pure tone ILD functions show a flattened slope, emphasizing a shift in the balance of inhibition and excitation in favor of an enhanced excitability. Unaltered decay functions for click and noise stimuli are likewise suspected to base upon difference in spectral content and thus a reduced lateral inhibition. Bar graphs represent mean  $\pm$  S.E.M. Mann–Whitney test was used to evaluate differences between genotypes. \* $p < 0.05$  was considered statistically significant.

intensity was minimal. Increasing the contralateral intensity gradually inhibited ipsilateral excitation, eventually leading to a total block of firing. This characteristic was observed in animals of either genotype for all three tested acoustic stimuli. However, in agreement with the imbalance of excitation and inhibition in *Fmr1* KO mice, these neurons required louder contralateral sound intensities to reduce spiking activity. To quantify ILD sensitivity of *Fmr1* WT and KO neurons, a Boltzmann function was fitted to the ILD response function and the point of half-maximal inhibition, i.e. the point of inflection of the sigmoidal fit was calculated (Figure 23A). On average, contralateral pure tones had to be 6.2 dB louder in KO animals to obtain half-maximal inhibition, compared with their WT littermates (WT:  $-9.7 \pm 1.15$  dB,  $n=24$  vs. KO:  $-3.5 \pm 2.39$  dB,  $n=16$ ; Unpaired t test with Welch's correction:  $p=0.0295$ ) (Figure 23B). Interestingly, no difference between genotypes were observed for ILD functions from stimulation with either clicks or noise bursts (clicks: WT:  $-9.6 \pm 2.51$  dB,  $n=15$  vs. KO:  $-8.4 \pm 2.11$  dB,  $n=12$ ; Mann-Whitey:  $p=0.5101$ ; noise bursts: WT:  $-9.1 \pm 1.01$  dB,  $n=54$  vs. KO:  $-10.6 \pm 1.13$  dB,  $n=42$ ; Mann-Whitey:  $p=0.2975$ ). For the calculation of these differences in ILD values, we took only biologically relevant ILD values into account. Here, ILD values of larger than  $\pm 20$  dB were considered as being out of the behaviorally and physiologically relevant range and were dismissed. A comparison of both calculations, all recorded cells against units showing only ILDs of the respective range, however produced congruent findings. ILD values for pure tones of all recorded cells, i.e. including ILD values larger than  $\pm 20$  dB, were significantly smaller in FXS KO animals (WT:  $-11.8 \pm 1.60$  dB,  $n=27$  vs. KO:  $-2.8 \pm 3.51$  dB,  $n=24$ ; Unpaired t test with Welch's correction:  $p=0.0258$ ). Interestingly, ILDs of both noise and click stimuli did not show statistically

significant differences (clicks: WT:  $-13.1 \pm 2.20$  dB,  $n=21$  vs. KO:  $-18.5 \pm 2.29$  dB,  $n=25$ ; Mann-Whitey:  $p=0.0854$ ; noise bursts: WT:  $-12.3 \pm 1.11$  dB,  $n=68$  vs. KO:  $-13.5 \pm 1.33$  dB,  $n=57$ ; Unpaired t test:  $p=0.4902$ ).

To quantify the decline in firing with increasing contralateral sound stimulation, the slope of the fitted function was calculated. The Boltzmann slope factor describes the steepness of the curve, such that larger values correspond to a less steep curve. The slope of WT animals was significantly steeper when stimulating with pure tones, illustrating a faster decline of firing compared to KO animals (WT:  $5.2 \pm 0.77$ ,  $n=22$  vs. KO:  $7.7 \pm 1.19$ ,  $n=16$ ; Mann-Whitey:  $p=0.0345$ ) (Figure 23C). In line with the similar ILD values for clicks and noise bursts, slopes of ILD functions likewise did not differ between genotypes for these two acoustic stimuli (clicks: WT:  $2.8 \pm 0.73$ ,  $n=15$  vs. KO:  $4.2 \pm 0.58$ ,  $n=12$ ; Mann-Whitey:  $p=0.0539$ ; noise bursts: WT:  $4.2 \pm 0.30$ ,  $n=23$  vs. KO:  $5.3 \pm 0.43$ ,  $n=29$ ; Mann-Whitey:  $p=0.1670$ ).

## 6.2.6 A loss of FMRP does not change the response following excessive stimulation

One aim of this study was to test for an effect of the loss of FMRP on the ability to adapt to a stimulus already at the level of the auditory brainstem, as adaptation and habituation were reported to be reduced in FXS (Miller et al., 1999b; Castrén et al., 2003b; He et al., 2017). Additionally, FMRP was shown to interact with the potassium channels Slack and BK, which contribute to fast repolarization of the membrane and short-term plasticity (Brown et al., 2010; Deng et al., 2013). A lack of FMRP was thus suspected to affect the precise processing of high frequency stimulation and the ability to adapt to such stimulation. We previously demonstrated a negligible effect of adaptation at the level of the LSO in native conditions, i.e. when acoustic signals reach both ears. However, an effect can be measured for an artificial condition. We applied a binaural adaptation paradigm, where the response to a pure tone following a click train at high stimulation rate was recorded. This click train was presented either mon- or binaurally. On the one hand, it was possible to induce a measurable effect of adaptation with this paradigm and compare it between genotypes. On the other hand we could also test for the impact of intrinsic cellular mechanisms on adaptation, i.e. how much the activation of the cell itself is responsible for this effect of adaptation. In the monaural condition, the click train caused the cell to excessively fire throughout the entire stimulation period. Yet, this represents an artificial situation for the auditory system, as acoustic signals commonly reach both ears. In the binaural condition, the contralateral intensity of the click train was set to a value, which almost entirely suppressed the ipsilateral excitation (Figure 24A). In this condition, the cell thus still received strong excitatory inputs; however, contralateral inhibition prevented the cell from firing. Any observable effect of adaptation in this condition would thus be not a result of somatic activation of the cell itself, but of presynaptic origin. A comparison of the normalized response to the test pure tone showed a significant decrease of the response strength between mon- and binaural conditions

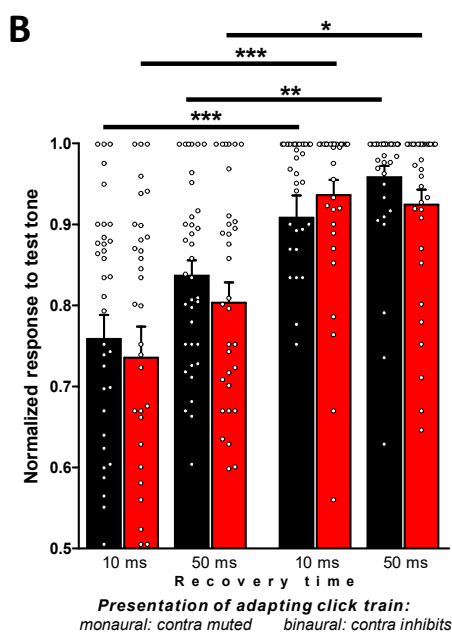
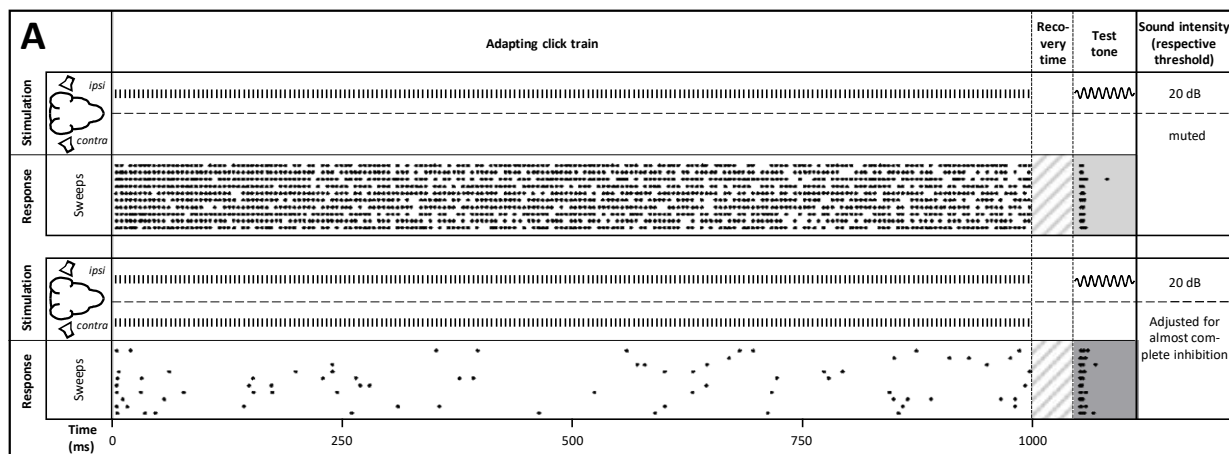


Figure 24: Adaptation is not affected in *Fmr1* KO mice. **A:** Stimulation paradigm with exemplary response pattern. Cells are excessively stimulated by a 200 Hz click train. Binaural stimulation inhibits most of the neuronal response. Subsequent response to an ipsilateral pure tone at the unit's CF (shaded) is modulated by the preceding click train. Normalized response to pure tone is compared. **B:** Response to a pure tone after click train is similarly reduced in both genotypes after excessive somatic activity from only ipsilateral stimulation. Further, it indicates that this aspect of adaptation emerges from intrinsic properties of the LSO cell itself, as adaptation is pronounced after strong firing. No differences between WT and *Fmr1* KO animals for each condition demonstrate that adaptation and channel kinetics at LSO cells are not affected by a lack of FMRP. Bar graphs represent mean  $\pm$  S.E.M. Kruskal-Wallis test with Dunn's post-hoc test was used to evaluate differences between genotypes. \* $p < 0.05$  was considered statistically significant.

for both genotypes (Kruskal-Wallis with Dunn's post-hoc test: WT: 10 ms mon- vs. binaural:  $p=0.0002$ ; 50 ms:  $p=0.0014$ ;  $n=29$ . KO: 10 ms mon- vs. binaural:  $p<0.0001$ ; 50 ms:  $p=0.0127$ ;  $n=33$ )(Figure 24B). This demonstrates an effect of adaptation following strong somatic activation. This is supported by a gradual, yet not statistically significant recovery of the response strength between short (10 ms) and long (50 ms) recovery time. However, no differences between WT and *Fmr1* KO animals were observed for any of the tested conditions. Consequently, the hypothesis of an impact of the loss of FMRP on the ability to adapt to high frequency stimulation has to be rejected. Additionally, the conclusion can be drawn that this adaptation is a result from the strong somatic activation, i.e. it occurs after excessive firing of the cell itself. This demonstrates that intrinsic mechanisms, e.g. ion channel kinetics account for this effect of adaptation. However, no differences between genotypes were found. Thus, lack of FMRP does not significantly affect these intrinsic mechanisms and the hypothesis of altered channel kinetics likewise has to be rejected. Together, these results are in contrast to what has been reported from higher stages of the auditory path, a

primary incentive for this study. Thus, it may be assumed that impairments of adaptation in FXS are not based at low levels of sensory processing, but occur at subsequent centers.

---

## 7 Discussion

In this study, we aimed to elucidate the origins for altered processing of sensory information in the central nervous system in case of the fragile X syndrome (Castrén et al., 2003b; Knoth and Lippe, 2012; Ethridge et al., 2016; Sinclair et al., 2017). We used the LSO of *Fmr1* KO mice as a model circuit to investigate the fundamental changes in sensory processing at an early neuronal stage of the auditory pathway. Here we could show a number of alterations in the processing of neuronal signals already at the level of the auditory brainstem. However, some other aspects of sensory processing in the central nervous system, which were reported to be changed in FXS, did not show differences at this early stage of the auditory path in WT and *Fmr1* KO animals.

As expected, the LSO of mice showed the same functionality as in other species and processed differences in sound level between both ears. However, the observed firing pattern was in contrast to other animals, as most cells exhibited an exclusive onset response. The comparison of WT and *Fmr1* KO mice revealed subtle differences regarding these measurements. Cells of KO animals tended to show a mildly enhanced response upon acoustic stimulation. Tonotopic distribution of the neurons characteristic frequencies was less pronounced as expected, albeit featuring the predicted spatial distribution with no differences between genotypes. The responsive spectrum of frequencies was found within the hearing range of mice, however limited to only about four octaves. In *Fmr1* KO animals, the spectral resolution in terms of tuning bandwidth was broadened, suggesting an enhanced excitatory trafficking and a reduced tonotopic refinement. Temporal processing, especially with focus on accuracy and reliability generally showed to be of high fidelity. For most tested conditions, no significant differences for these parameters were observed between WT and KO mice. In close relation to the temporal processing, LSO cells commonly showed no or only negligible effects of adaptation. The reported differences for both genetic backgrounds could thus only be verified for repetitive click trains with rising stimulation frequencies. Interestingly, a contradictory effect was recorded for the jitter of low repetition rates or single clicks. All tested cells showed clear sensitivity upon ILDs, regardless of the stimulus type. Here, neurons of *Fmr1* KO mice showed a significant shift in half-maximal inhibition and slopes of the ILD function, supporting the idea of an enhanced excitability and a shift in the balance of inhibition and excitation.

### 7.1 General firing patterns of mouse LSO cells show differences to other mammals

Most recorded LSO neurons responded reliably to ipsilateral stimulation with pure tones at the unit's characteristic frequency (CF). Stimulation with other sound signals such as white noise or clicks likewise evoked a robust neuronal response. A gradually increased contralateral stimulation,

however, suppressed the neuronal activity, regardless if this was spontaneous firing or evoked response. Generally, this is in accordance to what is known from other mammals (Boudreau and Tsuchitani, 1968; Harnischfeger et al., 1985; Sanes and Rubel, 1988; Tsuchitani, 1988).

The strong onset firing, especially for pure tones, corresponds to the only existing study in mice, where similar characteristics are shown (Karcz et al., 2011). However, the response pattern differed markedly in comparison to other species to date. In cats, guinea pigs, bats and gerbils, stimulation of either one or both ears with pure tones at the units preferred frequency likewise resulted in a strong onset response, but was followed by a plateau of sustained activity throughout the entire stimulation period (Guinan et al., 1972; Caird and Klinke, 1983; Covey et al., 1991; Pedemonte et al., 1994; Spitzer and Semple, 1995). Similarly, but with more emphasize on the temporal domain of the stimulus, LSO units in rats and chinchillas exhibited a more phase-locked, chopper-like response to pure tone stimulation at CF (Finlayson and Caspary, 1991; Adam et al., 1999). This type of response is commonly referred to as primary-like, as it corresponds to the firing pattern of auditory nerve fibers (ANFs) or hair cells, respectively (Westerman and Smith, 1984). To date, only few ANF studies in mice give insight into the firing pattern *in vivo*. The reported response properties of mouse ANFs are closely related to what has been published from cats and gerbils, i.e. strong onset firing with decreasing sustained activity throughout the entire stimulation period (Taberner and Liberman, 2005; Buran et al., 2010). Consequently, the observed firing pattern in LSO cells is presumably a result of signal transformation in the cochlear nucleus or LSO neurons itself.

## 7.2 Characteristic frequencies are spatially organized with spectral limitations

### 7.2.1 Distribution of CFs covers only a part of the perceptible frequencies

Measured CFs of LSO neurons ranged from 3.4 to 40 kHz. This spectrum covers only a part of the reported hearing range of mice, typically spanning around 2 – 90 kHz (Heffner and Heffner, 2007). Moreover, the dispersion across the measured spectrum appeared to be normally distributed. When plotted as a histogram, the numbers of recorded cells showed a Gaussian curve. This distribution could reflect the essential hearing range, covering most frequencies used for communication. This would be a relevant explanation, if ILD detection was primarily used for localizing mating partners or offspring. However, earlier studies reported mating vocalizations to cover frequencies from 30 to 110 kHz (Sewell, 1972; Holy and Guo, 2005) and pup isolation calls from 50 kHz to 80 kHz (Haack et al., 1983; Hofer et al., 2002), consequently disregarding this interpretation. A plausible explanation for the finding of a Gaussian distribution might be for technical reasons. Recording sessions typically started at the most promising location for successful recording, i.e. in the center of the nucleus, approximated from averaged previous recording coordinates. LSO neurons tend to be tonotopically

---

distributed, with the edges of the CF spectrum located at the periphery of the nucleus. Accordingly, neurons with CF of the central spectrum were encountered with a higher statistical probability.

However, the proportionate overrepresentation of frequencies around 15-25 kHz is in agreement to audiograms (Ehret, 1974) and neurophysiological recordings in the auditory nerve (Taberner and Liberman, 2005), the cochlear nucleus (Ehret and Moffat, 1984), the inferior colliculus (Stiebler and Ehret, 1985) and the auditory cortex (Stiebler et al., 1997) of mice, where a peak in sensitivity is shown for this frequency range. Despite overlapping only partially with the communication spectrum, this frequency band seems to be of major behavioral relevance.

### 7.2.2 Tonotopic arrangement is less pronounced in comparison to other mammals

It is commonly approved for almost all areas of the auditory path that neurons are spatially arranged according to their CF (Pickles, 2008). Likewise in case of the LSO, a tonotopic distribution has been shown for various mammalian species (Tsuchitani and Boudreau, 1966; Müller, 1990; Covey et al., 1991; Friauf, 1992). However, this was not demonstrated for mice to date. In the present study, we investigated the neuronal response of LSO cells and recorded their CF and their position within the nucleus. Here, a tendency towards a distribution in correlation to the units CFs is observable. Calculation of a linear regression showed persuasive  $r^2$  values in the mediolateral and rostrocaudal dimension. However, no correlation was found in the dorsoventral extent. Thus, cells with a comparably low CF tended to be located in the lateral and caudal division of the LSO, whereas higher frequencies were more often represented in the medial and rostral parts. At least for the mediolateral dimension, this is in line with what has been shown in other species. However, spatial segregation of CFs showed to be less pronounced compared to other species, e.g. several high frequency neurons were also found in the lateral division of the LSO. Generally, CFs seemed to be more intermingled compared to what is known from other animals (Sanes et al., 1990; Covey et al., 1991; Tabor et al., 2012).

### 7.3 A differential examination of the temporal fidelity of neuronal responses

The precise timing of action potentials is an essential feature of neurons in the auditory brainstem. Not only relative and absolute timing differences, also the precision of both, initial spikes and the progress of successive action potentials are critical parameters for the faithful conduction of auditory signals. As a first attempt, the variability in timing of the first spikes upon each type of stimulus was analyzed.

### 7.3.1 Small jitter portrays a temporally precise nucleus with promoted click processing in FXS

The observed values of jitter are intriguingly small, but in a comparable range of what has been shown from brainstem nuclei like CN or MNTB, which project to the LSO (e.g. Kopp-Scheinflug et al., 2003; Lorteije et al., 2009). In comparison with *Fmr1* KO animals, however, no differences in jitter of the FSL were observed for noise or pure tone stimuli. Intriguingly, jitter for stimulation with clicks showed to be significantly smaller in cells of KO mice. This correlation might be attributed to the particular rise times of the stimuli. An enhanced excitatory response as a result from more synaptic inputs could thus contribute to a more precise transduction of the neuronal signal in case of an abrupt signal onset, whereas for more slowly increasing stimulus intensities this effect is abolished. With either brain slice recordings and antibody labeling, stronger excitatory inputs were shown for the LSO of *Fmr1* KO mice (Garcia-Pino et al., 2017). This would be in line with studies, where temporal jitter was shown to be most precise in neurons that receive a large number of convergent inputs within a short temporal integration window, e.g. for the presentation of clicks (Rhode and Smith, 1986; Oertel et al., 2000; Typlt et al., 2012).

### 7.3.2 Repetitive click stimulation reveals recessive temporal accuracy for increasing activation in *Fmr1* KO animals

For a closer examination of the firing behavior, especially within the scope of its progress during fast repetitive stimulation, the jitter of responses on monaural click trains was analyzed. At the slowest tested repetition rate of 100 Hz, cells of KO animals showed to respond with a significantly lower jitter. This corresponds to the comparison of the jitter of FSLs. It likewise emphasizes the augmenting impact of a lack of FMRP on the temporally precise transduction of abrupt acoustic signals at low repetition rates and is in line with *in vitro* recordings (Garcia-Pino et al., 2017). Here, smaller latencies of EPSCs were shown for developing KO animals and could indicate a higher precision of temporal transduction of action potentials. However, for the second lowest repetition rate of 142 Hz, no difference were detected anymore. Moreover, for all higher tested relevant stimulation frequencies, the gradual increase of the mean standard deviation across repetition rates showed to be notably pronounced for *Fmr1* KO animals, i.e. averaged jitter grew faster for this genotype. The initially beneficial effect of a loss of FMRP on the accuracy therefore turns into a worsening with rising stimulation frequency. This phenomenon cannot be exclusively explained with enhanced excitability, as previously discussed for the jitter of the FSL.

On the one hand, the deteriorated temporal processing can be interpreted as a reduction of the synchronicity of inputs. FXS mice were shown to have longer and thinner dendritic spines (Comery et al., 1997; Bagni and Greenough, 2005b; Antar et al., 2006). Moreover, spine density was greater

---

in *Fmr1* KO mice, which may reflect impaired developmental organization of synapse consolidation. In this context, developmental refinement of neural circuits was shown to be affected by a loss of FMRP (Wang et al., 2010; Wondolowski and Dickman, 2013). Activity-dependent synapse formation can thus be impaired in absence of this protein. In the auditory system (Rubel and Fay, 2012) and the LSO in particular (Kandler et al., 2009), a developmental reduction of synaptic inputs and surplus afferents was shown. If this refinement was impaired in FXS also at LSO principal cells, this could lead to a reduced synchronicity of inputs and thus a larger jitter. However, such refinement was shown in most cases for inhibitory projections, the development of excitatory inputs remains speculative.

On the other hand, several ion channel complexes were shown to interact with FMRP. A lack of FMRP was associated with a reduced activity of the sodium-activated potassium channel Slack (Brown et al., 2010) and a decreased activation of the calcium activated potassium channel BK (Deng et al., 2013). Present in cells of the mouse LSO (Sausbier et al., 2006; Rizzi et al., 2016), both channels contribute to the fast repolarization of the membrane and thus to the temporally precise processing of high frequency stimulation. This can explain the higher jitter on *Fmr1* KO mice for the high stimulation rates. Additionally, it is not contradictory to the smaller jitter for click FSLs or the 100 Hz repetition rate, as fast repolarization is only crucial for high frequency stimulation.

### 7.3.3 Elevated responses of *Fmr1* KO animals are contrasted by fewer multiple spikes

The recorded number of elicited spikes per click similarly appeared to be closely related to the stimulation rate. Mean spike numbers for the slowest repetition rate tended to fluctuate around or above 1, indicating that a considerable number of cells still responded with more than one spike per click. In general, many LSO cells elicit more than one action potential following the first click. For subsequent clicks, however, the chance for more than one spike and the total number of action potentials remarkably diminishes with rising repetition rates. Related to the progress of mean spike numbers of the 100 Hz condition, this finding suggests that this repetition rate is slow enough for the majority of cells to fully recover. All other, faster stimulation rates already show a drop below 1 in the course of stimulation. It can thus be assumed that neuronal transmission at the level of the LSO is almost completely restored to resting state after as little as 10 ms.

Related to FXS, however, the probability to elicit more than one action potential following a click was suspected to be augmented, as LSO cells of *Fmr1* KO mice generally tended to respond with more spikes. Surprisingly, this probability showed to be significantly reduced in *Fmr1* KO mice. The chance to respond with more than one action potential was less than 50 % for most tested repetition rates, compared to their WT littermates, even though they have the same overall reliability to respond

to clicks. This shows that a lack of FMRP does not affect the general probability to respond to successive clicks, but the chance for more than one spike is reduced. The underlying mechanism for this discrepancy can again be found in the activating effect of FMRP on potassium channels. A reduced activity of BK channels in *Fmr1* KO mice was associated with a reduced influx of potassium and thus a prolonged action potential duration (Deng et al., 2013). This can lead to fewer multiple spiking. Yet, these mechanisms were only shown for hippocampal and cortical neurons. A similar impact on auditory brainstem neurons remains speculative.

Generally, LSO cells of mice showed to process neuronal signals with high temporal fidelity, both for the ability to respond to high stimulation rates as well as for exact timing with small jitter. This is consistent with data from slice recordings, where strong synaptic reliability due to increased quantal content and faster vesicle replenishment in auditory brainstem nuclei including the LSO was shown in comparison to other brain areas (Krächan et al., 2017).

## 7.4 Frequency tuning is broadened in FXS mice

In the auditory system of mammals, single neurons are commonly tuned to a certain frequency range, i.e. they are only responsive to a limited bandwidth (Fay, 2012). This restriction is mainly a result of the physical properties of the basilar membrane and its mechanism of translating pressure changes into neuronal signals. Additionally, lateral inhibition of adjacent hair cells and their neuronal correlates in subsequent auditory nuclei further sharpens this frequency tuning (Eatock and Fay, 2006; Fukui et al., 2010). Moreover, frequency tuning of cochlear projections is refined during development (Saunders et al., 1980; Brugge et al., 1981; Kandler et al., 2009). Neurons in the auditory system of young animals show responses to a broad range of frequencies, which narrow during development. The bandwidth of this tuning can be described and quantified using the Q value of measured tuning curves, or frequency response areas, respectively. Here we could show a significant broadening of the frequency tuning of principal cells in the LSO of FXS mice, represented in smaller Q values. This observation can be interpreted using two different approaches.

### 7.4.1 Balance of excitation and inhibition could be disturbed

Amongst others, the tuning bandwidth of an auditory neuron is a result of excitatory and inhibitory inputs. Here, especially lateral inhibition and inhibitory feedforward and feedback loops shape a neurons response to stimulation with pure tones already at the level of the cochlea (Nobili et al., 1998). Likewise, a similar form of enhancement was proven to occur at higher stages of the auditory system. Cells of auditory nuclei project inhibitory connections to tonotopically proximate cells of the same, but also of downstream nuclei (Suga et al., 1997; Hall, 1999; LeBeau et al., 2001; Wu et al.,

---

2008). This comparable mechanism further increases the spectral contrast and is based on the interplay of excitatory and inhibitory inputs.

This balance of excitation and inhibition seems to be altered in FXS mice. Cortical neurons of FXS mice showed weakened inhibitory interneuron activity and more excitable pyramidal neurons (Gibson et al., 2008; Hays et al., 2011; Paluszkiwicz et al., 2011). Somatosensory neurons of *Fmr1* KO mice are also hyperexcitable, as characterized by longer, less synchronous UP states (Gibson et al., 2008; Hays et al., 2011). Additional evidence for an imbalance of GABAergic and glutamatergic signaling was found in KO mice. mRNAs of GABA-receptor subunits are downregulated in the brainstem of FXS mice (El Idrissi et al., 2005), while immunolabeled area of excitatory inputs of LSO neurons with glutamate transporter proteins is elevated (Garcia-Pino et al., 2017). *In vitro* recordings of this study also showed larger evoked maximal EPSC amplitudes and a higher spontaneous release of excitatory transmitter in *Fmr1* KO mice. These findings, together with data from the present study about a shift in the ILD processing point toward an altered balance of inhibition and excitation in the processing of acoustic signals. This would be especially relevant in edge cases, i.e. at perception thresholds of frequency or intensity, where excitation and inhibition are just in balance. As a tuning curve simply represents the borderline between no or suppressed and effective excitation, this excessive excitability could consequently lead to a broadening of a neurons tuning curve.

#### 7.4.2 Impaired tonotopic refinement during ontogeny could reduce spectral resolution

In the fetal and postnatal development of neural circuits, neuronal projections undergo several alterations. Early in ontogeny, axonal projections spread in the direction of their target nuclei, eventually connecting numerous cells within this nucleus (Ehret and Romand, 1997; Rubel and Fritsch, 2002). Important connections are strengthened, whereas misguided projections degenerate. Amongst others, this process is regulated by neuronal activity (Bi and Poo, 2001; Hebb, 2002; Butts et al., 2007). Considering an increased excitability by a lack of FMRP already in the course of neuronal development and synaptic consolidation, an enhanced excitatory activity could thus lead to an inordinate strengthening of correctly wired connections. More importantly, initially misguided projections would not degenerate completely or less effectively. In case of auditory connectivity, this could have an impact on the development of the tonotopic refinement. Amongst others, frequency tuning is a result of synaptic refinement in the development of auditory circuits (Kandler and Friauf, 1993; Gabriele et al., 2000; Kandler et al., 2009). An enhanced excitatory drive could thus lead to an impaired developmental frequency tuning, finally resulting in broadened tuning curves. In case of the LSO, however, an experience-dependent refinement has only been shown for inhibitory projections from the MNTB (Sanes and Siverls, 1991; Sanes and Takács, 1993). Much less is known

about the refinement of excitatory projections from the CN to the LSO. Yet, anatomical and physiological studies suggest that inhibitory and excitatory connections to the LSO develop simultaneously (Sanes and Rubel, 1988; Kandler and Friauf, 1993; Sanes, 1993; Kandler and Friauf, 1995). Developmental elimination of synapses occur in the CN of chicks (Lu and Trussell, 2007) and a narrowing of tonotopic maps was shown in the CN of cats (Leake et al., 2002). As frequency responses were measured with exclusively monaural stimulation, larger tuning bandwidths could thus already be broadened at the CN and propagated to the LSO. However, this theory is speculative and is not provable with our data.

### 7.4.3 Tuning bandwidths of other auditory nuclei show contradictory Q values

Two recent studies similarly reported changes in the tuning bandwidth in *Fmr1* KO mice of neurons at higher stages of the auditory pathway. Recordings from cells of the inferior colliculus (IC), the primary relay station and integrative plexus of the auditory midbrain, and the auditory cortex (AC), the final brain area of the auditory pathway, show comparable but also controversial findings (Rotschafer and Razak, 2013b; Mott and Wei, 2014).

**Table 1:** Comparison of Q values with neurons of higher stages in the auditory path.

	LSO		IC		AC	
	Q10	Q30	Q10	Q30	Q10	Q30
<b>WT</b>	8.8	3.7	2.9	1.6	4.4	1.5
<b>KO</b>	6.2	2.9	2.1	1.2	3.3	1.2
<b>WT/KO</b>	1.42	1.28	1.38	1.39	1.33	1.21

All three studies describe a similar relationship of Q values in WT and *Fmr1* KO mice. At all levels, frequency tuning was broadened in KO animals. The ratio of the observed differences likewise is of comparable range. Interestingly, no linear relationship of refinement can be observed. Our suggestion proposed a gradual decrease of tuning bandwidth along the auditory path as a result of successive filtering. In fact, LSO cells showed the narrowest tuning curves, as reflected in the largest Q values. At the level of the IC, frequency tuning broadened to its largest extent, whereas in neurons of the AC intermediate bandwidths of tuning curves are reported. Yet, IC recordings were performed with electrode arrays and multi-unit responses were recorded. Single unit recordings from IC neurons in mice showed a number of different cell types with large variations in tuning bandwidth, with Q10 values ranging from 2-13 and Q30 values from 1-6 (Xu and Jen, 2001; Jen and Xu, 2002; Yan et al., 2005). Consequently, a direct comparison of the tuning bandwidth in the ascending auditory centers

---

of FXS mice as stated in table 1 is not suitable and does not allow for the conclusion of a gradual decrease of tuning bandwidths.

## 7.5 A lack of FMRP causes a shift in the processing of interaural level differences

The LSO of mice is an attractive circuit model to study the balance of excitation and inhibition. The processing of sound level differences between both ears is a result of the interplay between excitatory ipsilateral inputs and inhibitory contralateral projections. To date, mice are the preferred species to induce genetic disorders such as FXS. A number of symptoms of this disorder like hypersensitivity to acoustic stimuli and audiogenic seizures are supposed to result from an imbalance between excitation and inhibition (Consortium et al., 1994; Ethridge et al., 2017; Sinclair et al., 2017). Thus, the LSO of genetically engineered mice provides the possibility to investigate changes in this balance *in vivo*. However, the function and physiological properties of LSO neurons in living mice are not well described yet. Our data confirms the general functionality, as LSO principal cells reliably and consistently responded with a decrease in firing upon rising contralateral sound intensities. Additionally, this characteristic mechanism was equally observed for any of the applied stimuli. The comparison of WT and *Fmr1* KO animals, however, revealed an altered processing of interaural level differences (ILDs), indicating a shift in the balance of inhibition and excitation.

### 7.5.1 Smaller ILD values for pure tones could reflect enhanced excitability in *Fmr1* KO animals

In fact, significantly smaller ILD values for *Fmr1* KO animals were shown when stimulated with pure tones. Positive ILD values illustrate a half-maximal inhibition, when the ipsilateral sound intensity still exceeds the contralateral intensity and correspond to a simulated location of the sound source on the ipsilateral side of the head. Hence, smaller or even negative ILD values indicate that a higher contralateral sound intensity is necessary to achieve the same level of suppression of the ipsilateral excitation. This result can thus be interpreted as either reduced inhibition or increased excitation. As inhibitory inputs showed to be unaltered in slice recordings (Garcia-Pino et al., 2017) and an enhanced excitability was demonstrated for other brainstem nuclei (Rotschafer et al., 2015b), this finding matches with the hypothesis of a shift in the balance of excitation and inhibition as a result of enhanced excitability in *Fmr1* KO mice.

However, this effect could not be confirmed for the stimulation with noise bursts and clicks. This discrepancy could be explained by the nature of these acoustic stimuli and the processing of this information along the auditory pathway. Both, white noise and clicks theoretically incorporate frequencies of the entire audible spectrum with identical intensities. Consequently, when stimulated

with such sounds, the basilar membrane will be equally dislocated across its full extent and large subdivisions of the auditory nerve and subsequent nuclei will respond. For pure tones in turn, only the segment of the membrane with corresponding resonant properties will be effectively deflected and only fewer subdivisions of the auditory path will be excited. In this context, the mechanism of lateral inhibition has been shown to shape the response of auditory neurons for enhanced contrast (Kral and Majernik, 1996). Studies from auditory nerve fibers and cochlear nucleus neurons have shown smaller effects of lateral inhibition for stimulation with pure tones in comparison to broadband signals (Schalk and Sachs, 1980; Martin and Dickson, 1983; Rhode and Greenberg, 1994). A computational model proposes a decreased response of inhibitory interneurons in the cochlear nucleus for pure tone stimuli and thus a decreased lateral inhibition (Hancock et al., 1997). Moreover, a loss of FMRP was shown to downregulate GABA-receptor subunits in the brainstem of FXS mice (El Idrissi et al., 2005). This could likewise affect lateral inhibition in the CN. However, lateral inhibition was not investigated in cells of the LSO to date. Yet, the excitatory inputs arise from bushy cells in the ventral cochlear nucleus (Kuwabara et al., 1991; Pickles, 2008), where effective lateral inhibition was shown. Hence, a difference in the processing of pure tones and broadband stimuli could already happen at the level of the cochlear nucleus, in turn being propagated to cells of the LSO. To confirm such a theory, recordings from bushy cells in the CN of *Fmr1* KO mice would be necessary.

### 7.5.2 Suppression efficacy is reduced in FXS

A significant measure in the context of ILD processing is not only the relative point where inhibition successfully suppresses excitation, but also how fast this process is taking place. This question was addressed with calculating the slope of the sigmoid approximation of the ILD function at the point of inflection. Following this procedure, a significant but readily explainable difference between the three applied sound stimuli was observed. In wildtype mice, the slopes of both pure tone and noise ILD functions showed equivalent mean values, which is in accordance with what was reported from the LSO of cats (Greene et al., 2010). Slopes for click ILDs, however, were strikingly smaller. Smaller slope values reflect a steeper decay of the function, i.e. excitation is faster and more efficiently suppressed. Most cells responded to clicks with typically just one action potential, to pure tones and noise, however, with few more spikes. Thus, a gradual increase of inhibition results much faster in a total suppression in case of just one spike, explaining the discrepancy between these stimuli.

Moreover, this incident could possibly explain the flattened slopes in *Fmr1* KO animals. Here, at least for the pure tone condition, a statistically significant difference was observed. As shown, LSO cells of *Fmr1* KO mice tend to respond with more and prolonged firing of action potentials. In KO

---

animals, a gradual reduction of fired action potentials was observed with rising contralateral sound intensity and thus increasing inhibition. It can thus be speculated that more or stronger inhibition is necessary to completely suppress the ipsilateral excitation, eventually resulting in a shallower slope. However, the functional consequences and behavioral implications of such shifted ILD functions and broadened shapes, e.g. impaired sound localization abilities, remain elusive and would have to be addressed in behavioral experiments.

### 7.5.3 ILD values are scattered across the behaviorally relevant range

An additional characteristic comes to mind when we look at the dispersion of the individual data points for half-maximal ILD values. These values are scattered over a broad extent, ranging from -13 to +37 dB. Other studies of ILD processing in different animals with comparable physiological and ecological conditions showed almost exactly the same dispersion of ILD values as observed in this study (Park et al., 1996; Sanes and Rubel, 1988). Here, for bats and gerbils, ILD values ranged from -20 to +50 dB. The only existing work in mice reported a range from -20 dB to +27 dB (Karcz et al., 2011). This makes sense when considering the functional aspect of ILD computation. The auditory system needs to cover the whole range of behaviorally relevant ILDs to faithfully decipher the location of a sound source in the azimuthal plane. Depending on the slope of the ILD function, the dynamic range of a single cell is limited and is thus only capable to account for a certain sector of the entire azimuth. Hence, to provide for the whole extent of the acoustic horizon, cells sensitive to different half-maximal ILD values are essential. Moreover, this can be explained with the persisting model of ILD processing. As shown by Park et al., 1996, ILD sensitivity is supposed to be result of differentially timed inputs of excitation and inhibition. As likewise evident from data of the present study, the latency of an auditory signal is dependent on the intensity of the acoustic stimulus. Here this is shown for excitatory inputs, but suspected to be congruent for inhibitory neuronal transmission as well. Considering this mechanism, the model of so called delay lines (Jeffress, 1948; Irvine et al., 2001; Fontaine and Peremans, 2007) becomes clearly comprehensible: At a fixed ipsilateral stimulus intensity, excitatory inputs show a constant delay of the first spike latency. The same process can be contemplated for inhibitory inputs, however at low contralateral stimulus intensities, the inhibitory delay is considerably longer than the excitatory. Similar effects have already been reported for the coding of sound amplitudes in the IC of mice (Tang et al., 2008). This delay results in an effective neuronal response. When contralateral intensity increases, whereas ipsilateral sound levels remain constant, as it is the case for ILD function measurements, the delay of the inhibitory inputs is gradually reduced and eventually overlaps the excitatory inputs. This mechanism requires an effectively delayed inhibition, which can be realized with e.g. longer transmission distances or additionally intercalated synapses. In case of the LSO, both suppositions are known to be true (Smith et al., 1991; Warr et al., 1997). In connection with the fact of dispersed

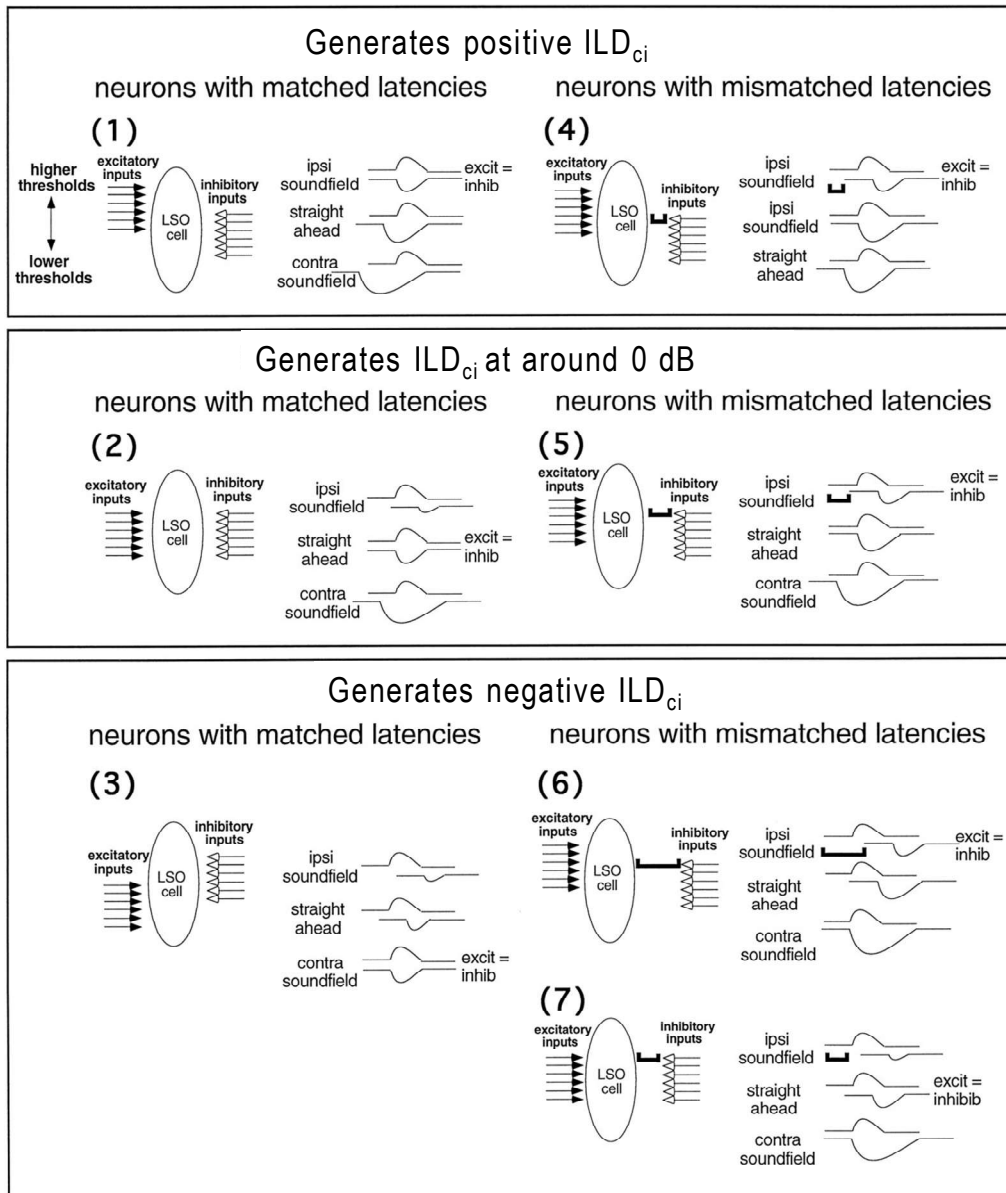


**Figure 25:** Schematic models showing how the matching of thresholds and latencies from the two ears could create the variety of ILDs of complete inhibition ( $ILD_{ci}$ ) in neurons with matched latencies (*panels 1–3*) and in neurons with mismatched latencies (*panels 4–7*). Each LSO cell is innervated by several fibers (*arrows*) from the ipsilateral (excitatory) ear and several fibers from the contralateral (inhibitory) ear. The threshold of each fiber is indicated by its position relative to the target LSO cell: fibers with high thresholds are at the *top*, and fibers with progressively lower thresholds are at the *bottom*. The latency of the input is indicated by the distance of each fiber from the target LSO cell. For neurons with mismatched latencies, the difference between the latencies of the excitatory and inhibitory inputs is indicated by a *bar* that separates the LSO cell from the inputs. Shown next to each LSO cell are three hypothetical records. Each record shows the relative strength and timing of excitation (*top*) and inhibition (*bottom*) that would be generated in the LSO cell by a sound at a particular location in the frontal sound field. The *top records* show the excitation and inhibition resulting from a sound in the ipsilateral field that would generate an ILD that favors the excitatory ear, the *middle records* for a sound directly in front, and the *bottom record* for a sound in the contralateral sound field. The location that would result in equally strong excitation and inhibition is indicated on the *right* of one of the three records. Adapted from Park et al., 1996.

---

ILD values, delay lines of different “lengths” could account for a scattered distribution of ILD sensitivities. This model is illustrated in figure 25, adapted from Park et al., 1996.

#### 7.5.4 ILD values depend on spectral content

Yet, an additional aspects needs to be addressed in the context of biologically relevant ILDs. As previously introduced, the range of behaviorally meaningful ILD values is not only restricted to the distance of both ears and the size of the head, which accounts responsible for the resultant sound shadow at the opposing ear, but is notably dependent on the enclosed frequencies. On the one hand, this correlation is directly linked for physical reasons. Travelling sound waves become attenuated when they encounter an obstacle of at least the size of the wavelength of the carrying frequency. For example, a 1000 Hz sound shows a wavelength of approximately 34 cm. Accordingly, it will not be significantly attenuated by an obstacle of the size of a human head with a mean diameter of 16 cm, hence resulting in a negligible ILD. A sound of 10 kHz with a wavelength of 3.4 cm, however, will be reasonably attenuated, thus producing a relevant ILD. Moreover, 20 kHz with 1.7 cm wavelength will result in an even larger ILD.

Additionally, also the dampening effect of air plays a substantial role for ILD generation. It increases drastically for rising frequencies, especially in the ultrasonic range. In summary, ILDs strongly depend on the engaged frequency. This relationship has already been observed and proven decades ago, especially in the context of auditory research for humans (Mills, 1960) and animals (Wakeford and Robinson, 1974; Keating et al., 2014). Concomitantly, it would be strongly expected that the observed dispersion of ILD values is correlated with the characteristic frequency of the respective auditory neuron. However, analysis of the measured ILD values with regard to the corresponding CF revealed no correlation, neither for wildtype mice nor for *Fmr1* KO animals. Yet, this finding is in accordance to a number of studies about ILD coding (Caird and Klinke, 1983; Sanes and Rubel, 1988; Siveke et al., 2006; Jones et al., 2015). Here it was shown that psychophysical sensitivity to ILD is virtually invariant across frequencies. Likewise, in various species ILD-coding neurons were found spanning the entire tonotopic axis, regardless of the fact that ILD processing was irrelevant for the lower end of this spectrum. Here, these findings are explained with additional mechanisms of ILD generation. Beside sound shadows and air dampening, also large low-frequency ILDs can occur in multisource, reverberant environments (Gourévitch and Brette, 2012; Młynarski and Jost, 2014) or as a result of distance-dependent sound dispersion (Brungart et al., 1999; Kim et al., 2010). However, in this context, a fairly broad distribution of observed ILD values becomes more intelligible.

## 7.6 Processing of pure tones after repetitive stimulation is not affected in FXS

We were interested in how LSO cells process single pure tones following strong stimulation at high repetition rates. Two main objectives were addressed:

A prevailing symptom of FXS is hyperresponsiveness to sensory stimuli. In this context, deficits to adapt to repetitive stimulation in *Fmr1* KO mice were shown (He et al., 2017). Closely related are reports from reduced habituation to repetitive sensory stimuli (Castrén et al., 2003b; Ethridge et al., 2016; McDiarmid et al., 2017; Miller et al., 1999b; Sinclair et al., 2017). Although qualitatively referring to similar processes, i.e. a reduced response following repetitive stimulation, many different mechanisms are involved in adaptation and habituation (Kandel, 1976). Nonetheless, the most basic feature of adaptation and habituation is the processing of periodic stimuli and a gradual decay of its response. In the context of hyperresponsiveness to sensory stimuli, we tested if such a reduction is affected in FXS.

Additionally, the circuitry of the LSO allows for a unique approach of intrinsic properties *in vivo*. FMRP interacts with a number of ion channel complexes and two of which were shown to be expressed at LSO cells (Rizzi et al., 2016; Sausbier et al., 2006). A lack of FMRP was associated with a reduced activity of the sodium-activated potassium channel Slack (Brown et al., 2010) and a decreased activation of the calcium-activated potassium channel BK (Deng et al., 2013). As a functional consequence, synaptic short-term plasticity and the precise temporal processing of action potentials is affected in *Fmr1* KO mice. Our hypothesis was that a reduced activation of these potassium channels is reflected in the processing of auditory stimuli. The applied paradigm allowed conclusions about the impact of a loss of FMRP on these ion channels directly at LSO cells, i.e. disregarding propagated effects from lower stages of the auditory path.

### 7.6.1 Artificial adaptation results from strong activation of LSO cells

Adaptation is commonly observed as a gradual decline of neuronal activity upon ongoing stimulation (Givois and Pollack, 2000; Mutschler et al., 2010). Many cells of nuclei within the auditory system show neuronal activity on stimulation with sounds throughout the entire stimulation period, often with a pronounced onset and/or offset response (Ulanovsky et al., 2004; Pérez-González and Malmierca, 2014). Here, adaptation can be observed as a gradual decline in the firing rate during the time course of the stimulation signal. Respectively, repetitive stimulation likewise can result in adaptive behavior, as the neuronal response progressively decreases with the number of stimulus iterations. In case of the LSO of mice, most principal cells showed a strong and exclusive onset firing pattern, regardless of the stimulus duration. Consequently, no adaptation was observed with single

---

long-duration sounds. Likewise, the adaptation paradigm with preceding click train resulted only in a reduced firing for the monaural condition. With this finding, however, the reduced response can be clearly attributed to a somatic, i.e. postsynaptic and thus intrinsic origin of the LSO cell itself. If the response to the pure tone would have been similarly reduced with and without preceding firing, this would have indicated a presynaptic effect. Various parameters of signal transduction, such as a shift in the concentration of the intra- and extracellular ionic composition or channel adaptation can account for this effect (Sah and Faber, 2002; Bhattacharjee and Kaczmarek, 2005; Schmid et al., 2010; Typlt et al., 2013). The underlying mechanism, however, is not provable with our experiments, but was also not subject of this study.

Additionally, the apparent increase of response strength to the pure tone between short and long recovery conditions indicates the transient adapting impact of the click train. The tested delays between click train and pure tone of 10 and 50 ms and the resulting recovery are in accordance to studies in guinea pigs, gerbils and rats, where recovery times from adaptation in ANFs and the SOC between 25 and 100 ms were demonstrated (Westerman and Smith, 1984; Yates et al., 1985; Finlayson and Adam, 1997). At higher stages, such as the IC, recovery durations of already 225 ms were measured (Ingham and McAlpine, 2004). Still, it has to be considered that these effects of adaptation are only measurable after exclusively monaural stimulation. This represents an artificial situation that will hardly occur in natural environments, where sounds commonly reach both ears. In most cases of binaural stimulation, a significant reduction due to contralateral inhibition was already measurable. Consequently, adaptation will presumably not occur in native conditions or is of small relevance. This is in line with suggestions that adaptation at such early stages of auditory processing needs to be of minor impact to allow for the processing of basic acoustic features in the brainstem nuclei, such as sound location (Sumner and Palmer, 2012). However, it demonstrates a measurable adaptation of LSO cells and served as control condition for the subsequent comparison with *Fmr1* KO animals.

### 7.6.2 Altered cortical adaptation in FXS is not reflected at the level of the LSO

Comparisons between WT and FXS animals likewise did not reveal measurable differences. This is reflected by no significant changes in the total reliability on increasing stimulation rates between WT and *Fmr1* KO animals. Additionally, the shape of the response function throughout presentation of click trains with different repetition rates should have been affected, if adaptation was altered in *Fmr1* KO. However, no significant changes were observed also in this case, once more suggesting a negligible impact of adaptation on principal cells of the LSO and in comparison between *Fmr1* KO and WT mice. Further information was expected from the adapting effect of a click train on the response to a subsequent pure tone, especially in the scope of the discussed origin of this adaptation.

In this scenario, an artificial adaptation for only monaural conditions was observed, yet again no differences between genotypes were measured. This leads to the main conclusion that the reported impairments of acoustic habituation and adaptation in FXS are not reflected in such an early stage of auditory processing and thus have to be generated at higher brain areas.

These results and the discrepancy to the reported effects of habituation and adaptation in FXS can be interpreted, as habituation and adaptation to auditory stimuli is often described as a multi-modal phenomenon, especially at processing stages like the midbrain or the cortex (Ulanovsky et al., 2004; Skoe and Kraus, 2010; Costa-Faidella et al., 2011). With complex habituation paradigms, the presence of different types of habituation were proposed. Here, effects of habituation over several time ranges are shown, supporting the idea of a hierarchically organized system of habituation, but still based on sensory adaptation (Grimm et al., 2011; Grimm and Escera, 2012). Potential cortical mechanisms for these effects were discussed as for example synaptic depression (Wehr and Zador, 2005), increased inhibition (Zhang et al., 2003), decreased excitation or lateral inhibition (Qin and Sato, 2004) or an imbalanced interplay of excitation and inhibition (De Ribaupierre et al., 1972; Volkov and Galazjuk, 1991; Ojima and Murakami, 2002; Oswald et al., 2006). More complex habituation mechanisms, which are addressable with paradigms aiming for mismatch negativity (MMN) or stimulus-specific adaptation (SSA) were formerly suspected to occur only at cortical stages (Ulanovsky et al., 2003; Nelken and Ulanovsky, 2007). In recent studies, however, it was demonstrated that phenomena like SSA occur also subcortically, e.g. in the MGB or the IC (Anderson et al., 2009; Yu et al., 2009; Antunes et al., 2010; Bäuerle et al., 2011; Ayala et al., 2012; Duque and Malmierca, 2014). Yet, no evidence was found for such effects already at the auditory brainstem. Accordingly, the reported impairments of acoustic habituation of FXS patients could thus be assumed to be dependent from alterations in these higher centers of sensory processing. In this context, no changes in this basic form of artificial adaptation are not necessarily in contrast to the reported impairments, but more likely outline the robustness and reliability of a basic nucleus like the LSO.

### 7.6.3 Ion channel interactions of FMRP have no effect on response strength

The lack of FMRP was suspected to result in a reduced activation of the potassium channels Slack and BK. *Fmr1* KO mice showed impaired short-term plasticity and a reduced temporal precision of action potentials (Brown et al., 2010; Deng et al., 2013). As a functional consequence, the ability to respond to high frequent stimulation trains was predicted to be impaired. Finally, this was supposed to result in a less effective adaptation and thus in a stronger response to the test tone. However, no significant changes in the response strength after strong firing of LSO cells were observed. In line with these results are *in vivo* recordings from MNTB neurons in *Fmr1* KO mice where no significant effects from a lack of FMRP on synaptic strength or short-term potentiation were found (Wang et

---

al., 2015). One suggestion was the direct interaction of FMRP with N-type calcium channels (Ferron et al., 2014), which are absent in the adult MNTB presynapse (Iwasaki et al., 2000). Yet, this could account only for effects in the MNTB. Another explanation could be a smaller general effect of both mentioned channels on the effective processing of high frequency stimulation. One indication for such a minor impact is the fact that cells of KO animals were still able to follow high stimulation rates with similar reliability. If potassium channels were severely affected, LSO cells lacking FMRP would not be able to follow high stimulation rates, as Johnston et al. (2010) suggested for the role of potassium channels in the auditory system. Further, if repolarization was effectively slowed down by a reduced activity of both channels, we would expect elongated action potentials in the LSO of *Fmr1* KO mice. In fact, slice recordings showed similar action potential half-widths in WT and *Fmr1* KO mice (Garcia-Pino et al., 2017), again pointing towards a minor impact of FMRP on potassium channel kinetics. Additionally, other potassium channels could rescue or alleviate a reduced activity of Slack and BK channels. Kv1.1 channels were also shown to contribute to precise timing of action potentials in the MNTB (Kopp-Scheinflug et al., 2003) and are expressed in the LSO of rodents (Barnes-Davies et al., 2004; Karcz et al., 2011). Similarly, channels of the Kv7/KCNQ family are supposed to modulate neuronal excitability in auditory nuclei (Navarro-López et al., 2009) and are present in the LSO of rats (Caminos et al., 2007). Yet, immunoreactivity for BK channels in LSO is relatively low in comparison to other brain areas like the cortex or the hippocampus (Sausbier et al., 2006). This could indicate a minor impact of this channel on the processing of high frequency stimulation. However, the results once more illustrate the temporal robustness of a basic nucleus like the LSO.

## 7.7 Concluding remarks

The LSO of mice has shown to comprise an attractive circuit model to address the question of basic auditory processing. Especially for the assessment of the interplay of excitation and inhibition, this nucleus represents a valuable tool to study physiological properties *in vivo*. Our results provide supplemental evidence for an enhanced excitability in case of FXS as a consequence from the lack of FMRP. The role of FMRP in the variety of symptoms in FXS, however, might be further addressed with developmental studies. A number of symptoms are suggested to manifest in the course of maturation. The influence of FMRP on a developing organism could thus be subject of future research with still many open questions.

## 8 References

- Adam, T.J., Schwarz, D.W., Finlayson, P.G., 1999. Firing properties of chopper and delay neurons in the lateral superior olive of the rat. *Exp. Brain Res.* 124, 489–502.
- Amano, K., Goda, N., Nishida, S., Ejima, Y., Takeda, T., Ohtani, Y., 2006. Estimation of the Timing of Human Visual Perception from Magnetoencephalography. *J. Neurosci.* 26, 3981–3991. <https://doi.org/10.1523/JNEUROSCI.4343-05.2006>
- Anderson, L.A., Christianson, G.B., Linden, J.F., 2009. Stimulus-specific adaptation occurs in the auditory thalamus. *J. Neurosci. Off. J. Soc. Neurosci.* 29, 7359–7363. <https://doi.org/10.1523/JNEUROSCI.0793-09.2009>
- Antar, L.N., Li, C., Zhang, H., Carroll, R.C., Bassell, G.J., 2006. Local functions for FMRP in axon growth cone motility and activity-dependent regulation of filopodia and spine synapses. *Mol. Cell. Neurosci.* 32, 37–48. <https://doi.org/10.1016/j.mcn.2006.02.001>
- Antunes, F.M., Nelken, I., Covey, E., Malmierca, M.S., 2010. Stimulus-Specific Adaptation in the Auditory Thalamus of the Anesthetized Rat. *PLoS ONE* 5. <https://doi.org/10.1371/journal.pone.0014071>
- Arinami, T., Sato, M., Nakajima, S., Kondo, I., 1988a. Auditory brain-stem responses in the fragile X syndrome. *Am. J. Hum. Genet.* 43, 46–51.
- Arinami, T., Sato, M., Nakajima, S., Kondo, I., 1988b. Auditory brain-stem responses in the fragile X syndrome. *Am. J. Hum. Genet.* 43, 46–51.
- Attenborough, D., 1995. *The Private Life of Plants*, 1st edition. ed. Princeton University Press, Princeton, NJ.
- Ayala, Y.A., Pérez-González, D., Duque, D., Nelken, I., Malmierca, M.S., 2012. Frequency discrimination and stimulus deviance in the inferior colliculus and cochlear nucleus. *Front. Neural Circuits* 6, 119. <https://doi.org/10.3389/fncir.2012.00119>
- Bagni, C., Greenough, W.T., 2005a. From mRNP trafficking to spine dysmorphogenesis: the roots of fragile X syndrome. *Nat. Rev. Neurosci.* 6, 376–387. <https://doi.org/10.1038/nrn1667>
- Bagni, C., Greenough, W.T., 2005b. From mRNP trafficking to spine dysmorphogenesis: the roots of fragile X syndrome. *Nat. Rev. Neurosci.* 6, 376–387. <https://doi.org/10.1038/nrn1667>
- Barnes, E., Roberts, J., Long, S.H., Martin, G.E., Berni, M.C., Mandulak, K.C., Sideris, J., 2009. Phonological Accuracy and Intelligibility in Connected Speech of Boys With Fragile X Syndrome or Down Syndrome. *J. Speech Lang. Hear. Res.* 52, 1048–1061. [https://doi.org/10.1044/1092-4388\(2009/08-0001\)](https://doi.org/10.1044/1092-4388(2009/08-0001))
- Barnes-Davies, M., Barker, M.C., Osmani, F., Forsythe, I.D., 2004. Kv1 currents mediate a gradient of principal neuron excitability across the tonotopic axis in the rat lateral superior olive. *Eur. J. Neurosci.* 19, 325–333. <https://doi.org/10.1111/j.0953-816X.2003.03133.x>
- Bäuerle, P., von der Behrens, W., Kössl, M., Gaese, B.H., 2011. Stimulus-specific adaptation in the gerbil primary auditory thalamus is the result of a fast frequency-specific habituation and is regulated by the corticofugal system. *J. Neurosci. Off. J. Soc. Neurosci.* 31, 9708–9722. <https://doi.org/10.1523/JNEUROSCI.5814-10.2011>
- Bear, M.F., Connors, B.W., Paradiso, M.A., 2015. *Neuroscience: Exploring the Brain*, 00004 ed. Wolters Kluwer Health, Philadelphia.
- Bear, M.F., Huber, K.M., Warren, S.T., 2004. The mGluR theory of fragile X mental retardation. *Trends Neurosci.* 27, 370–377. <https://doi.org/10.1016/j.tins.2004.04.009>
- Békésy, G.V., 1967. *Sensory inhibition*. Princeton University Press.
- Berry-Kravis, E., Abrams, L., Coffey, S.M., Hall, D.A., Greco, C., Gane, L.W., Grigsby, J., Bourgeois, J.A., Finucane, B., Jacquemont, S., Brunberg, J.A., Zhang, L., Lin, J., Tassone, F., Hagerman, P.J., Hagerman, R.J., Leehey, M.A., 2007. Fragile X-associated tremor/ataxia syndrome: Clinical features, genetics, and testing guidelines. *Mov. Disord.* 22, 2018–2030. <https://doi.org/10.1002/mds.21493>
- Bhattacharjee, A., Kaczmarek, L.K., 2005. For K<sup>+</sup> channels, Na<sup>+</sup> is the new Ca<sup>2+</sup>. *Trends Neurosci.* 28, 422–428. <https://doi.org/10.1016/j.tins.2005.06.003>

- Bi, G., Poo, M., 2001. Synaptic modification by correlated activity: Hebb's postulate revisited. *Annu. Rev. Neurosci.* 24, 139–166. <https://doi.org/10.1146/annurev.neuro.24.1.139>
- Blauert, J., 1996. *Spatial Hearing: Psychophysics of Human Sound Localization*, Rev ed. ed. MIT University Press Group Ltd, Cambridge, Mass.
- Blauert, J., Xiang, N., 2009. *Acoustics for Engineers: Troy Lectures*. Springer Science & Business Media.
- Boudreau, J.C., Tsuchitani, C., 1968. Binaural interaction in the cat superior olive S segment. *J. Neurophysiol.* 31, 442–454.
- Brody, S.A., Conquet, F., Geyer, M.A., 2003. Disruption of prepulse inhibition in mice lacking mGluR1. *Eur. J. Neurosci.* 18, 3361–3366.
- Brown, M.R., Kronengold, J., Gazula, V.-R., Chen, Y., Strumbos, J.G., Sigworth, F.J., Navaratnam, D., Kaczmarek, L.K., 2010. Fragile X mental retardation protein controls gating of the sodium-activated potassium channel Slack. *Nat. Neurosci.* 13, 819–821. <https://doi.org/10.1038/nn.2563>
- Brownell, W.E., Manis, P.B., Ritz, L.A., 1979. Ipsilateral inhibitory responses in the cat lateral superior olive. *Brain Res.* 177, 189–193.
- Brugge, J.F., Kitzes, L.M., Javel, E., 1981. Postnatal development of frequency and intensity sensitivity of neurons in the anteroventral cochlear nucleus of kittens. *Hear. Res.* 5, 217–229.
- Brungart, D.S., Durlach, N.I., Rabinowitz, W.M., 1999. Auditory localization of nearby sources. II. Localization of a broadband source. *J. Acoust. Soc. Am.* 106, 1956–1968.
- Buran, B.N., Strenzke, N., Neef, A., Gundelfinger, E.D., Moser, T., Liberman, M.C., 2010. Onset coding is degraded in auditory nerve fibers from mutant mice lacking synaptic ribbons. *J. Neurosci. Off. J. Soc. Neurosci.* 30, 7587–7597. <https://doi.org/10.1523/JNEUROSCI.0389-10.2010>
- Butts, D.A., Kanold, P.O., Shatz, C.J., 2007. A burst-based “Hebbian” learning rule at retinogeniculate synapses links retinal waves to activity-dependent refinement. *PLoS Biol.* 5, e61. <https://doi.org/10.1371/journal.pbio.0050061>
- Caird, D., Klinke, R., 1983. Processing of binaural stimuli by cat superior olivary complex neurons. *Exp. Brain Res.* 52, 385–399.
- Caminos, E., Garcia-Pino, E., Martinez-Galan, J.R., Juiz, J.M., 2007. The potassium channel KCNQ5/Kv7.5 is localized in synaptic endings of auditory brainstem nuclei of the rat. *J. Comp. Neurol.* 505, 363–378. <https://doi.org/10.1002/cne.21497>
- Campbell, J.P., Henson, M.M., 1988. Olivocochlear neurons in the brainstem of the mouse. *Hear. Res.* 35, 271–274.
- Capsius, B., Leppelsack, H.J., 1996. Influence of urethane anesthesia on neural processing in the auditory cortex analogue of a songbird. *Hear. Res.* 96, 59–70.
- Case, D.T., Zhao, X., Gillespie, D.C., 2011. Functional Refinement in the Projection from Ventral Cochlear Nucleus to Lateral Superior Olive Precedes Hearing Onset in Rat. *PLoS ONE* 6. <https://doi.org/10.1371/journal.pone.0020756>
- Caspary, D.M., Faingold, C.L., 1989. Non-N-methyl-d-aspartate receptors may mediate ipsilateral excitation at lateral superior olivary synapses. *Brain Res.* 503, 83–90. [https://doi.org/10.1016/0006-8993\(89\)91707-1](https://doi.org/10.1016/0006-8993(89)91707-1)
- Castellucci, V.F., Kandel, E.R., 1974. A Quantal Analysis of the Synaptic Depression Underlying Habituation of the Gill-Withdrawal Reflex in Aplysia. *Proc. Natl. Acad. Sci.* 71, 5004–5008.
- Castrén, M., Pääkkönen, A., Tarkka, I.M., Ryyänen, M., Partanen, J., 2003a. Augmentation of auditory N1 in children with fragile X syndrome. *Brain Topogr.* 15, 165–171.
- Castrén, M., Pääkkönen, A., Tarkka, I.M., Ryyänen, M., Partanen, J., 2003b. Augmentation of Auditory N1 in Children with Fragile X Syndrome. *Brain Topogr.* 15, 165–171. <https://doi.org/10.1023/A:1022606200636>
- Chapman, A.G., Nanan, K., Williams, M., Meldrum, B.S., 2000. Anticonvulsant activity of two metabotropic glutamate Group I antagonists selective for the mGlu5 receptor: 2-methyl-6-

- (phenylethynyl)-pyridine (MPEP), and (E)-6-methyl-2-styryl-pyridine (SIB 1893). *Neuropharmacology* 39, 1567–1574. [https://doi.org/10.1016/S0028-3908\(99\)00242-7](https://doi.org/10.1016/S0028-3908(99)00242-7)
- Chen, L., Toth, M., 2001a. Fragile X mice develop sensory hyperreactivity to auditory stimuli. *Neuroscience* 103, 1043–1050. [https://doi.org/10.1016/S0306-4522\(01\)00036-7](https://doi.org/10.1016/S0306-4522(01)00036-7)
- Chen, L., Toth, M., 2001b. Fragile X mice develop sensory hyperreactivity to auditory stimuli. *Neuroscience* 103, 1043–1050. [https://doi.org/10.1016/S0306-4522\(01\)00036-7](https://doi.org/10.1016/S0306-4522(01)00036-7)
- Chinwalla, A.T., Cook, L.L., Delehaunty, K.D., Fewell, G.A., Fulton, L.A., Fulton, R.S., Graves, T.A., Hillier, L.W., Mardis, E.R., McPherson, J.D., Miner, T.L., Nash, W.E., Nelson, J.O., Nhan, M.N., Pepin, K.H., Pohl, C.S., Ponce, T.C., Schultz, B., Thompson, J., Trevaskis, E., Waterston, R.H., Wendl, M.C., Wilson, R.K., Yang, S.-P., An, P., Berry, E., Birren, B., Bloom, T., Brown, D.G., Butler, J., Daly, M., David, R., Deri, J., Dodge, S., Foley, K., Gage, D., Gnerre, S., Holzer, T., Jaffe, D.B., Kamal, M., Karlsson, E.K., Kells, C., Kirby, A., Kulbokas, E.J., Lander, E.S., Landers, T., Leger, J.P., Levine, R., Lindblad-Toh, K., Mauceli, E., Mayer, J.H., McCarthy, M., Meldrim, J., Mesirov, J.P., Nicol, R., Nusbaum, C., Seaman, S., Sharpe, T., Sheridan, A., Singer, J.B., Santos, R., Spencer, B., Stange-Thomann, N., Vinson, J.P., Wade, C.M., Wierzbowski, J., Wyman, D., Zody, M.C., Birney, E., Goldman, N., Kasprzyk, A., Mongin, E., Rust, A.G., Slater, G., Stabenau, A., Ureta-Vidal, A., Whelan, S., Ainscough, R., Attwood, J., Bailey, J., Barlow, K., Beck, S., Burton, J., Clamp, M., Clee, C., Coulson, A., Cuff, J., Curwen, V., Cutts, T., Davies, J., Eyraes, E., Grafham, D., Gregory, S., Hubbard, T., Hunt, A., Jones, M., Joy, A., Leonard, S., Lloyd, C., Matthews, L., McLaren, S., McLay, K., Meredith, B., Mullikin, J.C., Ning, Z., Oliver, K., Overton-Larty, E., Plumb, R., Potter, S., Quail, M., Rogers, J., Scott, C., Searle, S., Shownkeen, R., Sims, S., Wall, M., West, A.P., Willey, D., Williams, S., Abril, J.F., Guigó, R., Parra, G., Agarwal, P., Agarwala, R., Church, D.M., Hlavina, W., Maglott, D.R., Sapojnikov, V., Alexandersson, M., Pachter, L., Antonarakis, S.E., Dermitzakis, E.T., Reymond, A., Ucla, C., Baertsch, R., Diekhans, M., Furey, T.S., Hinrichs, A., Hsu, F., Karolchik, D., Kent, W.J., Roskin, K.M., Schwartz, M.S., Sugnet, C., Weber, R.J., Bork, P., Letunic, I., Suyama, M., Torrents, D., Zdobnov, E.M., Botcherby, M., Brown, S.D., Campbell, R.D., Jackson, I., Bray, N., Couronne, O., Dubchak, I., Poliakov, A., Rubin, E.M., Brent, M.R., Flicek, P., Keibler, E., Korf, I., Batalov, S., Bult, C., Frankel, W.N., Carninci, P., Hayashizaki, Y., Kawai, J., Okazaki, Y., Cawley, S., Kulp, D., Wheeler, R., Chiaromonte, F., Collins, F.S., Felsenfeld, A., Guyer, M., Peterson, J., Wetterstrand, K., Copley, R.R., Mott, R., Dewey, C., Dickens, N.J., Emes, R.D., Goodstadt, L., Ponting, C.P., Winter, E., Dunn, D.M., Niederhausern, A.C. von, Weiss, R.B., Eddy, S.R., Johnson, L.S., Jones, T.A., Elnitski, L., Kolbe, D.L., Eswara, P., Miller, W., O'Connor, M.J., Schwartz, S., Gibbs, R.A., Muzny, D.M., Glusman, G., Smit, A., Green, E.D., Hardison, R.C., Yang, S., Haussler, D., Hua, A., Roe, B.A., Kucherlapati, R.S., Montgomery, K.T., Li, J., Li, M., Lucas, S., Ma, B., McCombie, W.R., Morgan, M., Pevzner, P., Tesler, G., Schultz, J., Smith, D.R., Tromp, J., Worley, K.C., Green, E.D., 2002. Initial sequencing and comparative analysis of the mouse genome. *Nature* 420, 520–562. <https://doi.org/10.1038/nature01262>
- Comery, T.A., Harris, J.B., Willems, P.J., Oostra, B.A., Irwin, S.A., Weiler, I.J., Greenough, W.T., 1997. Abnormal dendritic spines in fragile X knockout mice: maturation and pruning deficits. *Proc. Natl. Acad. Sci. U. S. A.* 94, 5401–5404.
- Consortium, T.D.-B.F.X., Bakker, C.E., Verheij, C., Willemsen, R., van der Helm, R., Oerlemans, F., Vermey, M., Bygrave, A., Hoogetveen, A., Oostra, B.A., Reyniers, E., De Boule, K., D'Hooge, R., Cras, P., van Velzen, D., Nagels, G., Martin, J.-J., De Deyn, P.P., Darby, J.K., Willems, P.J., 1994. *Fmr1* knockout mice: A model to study fragile X mental retardation. *Cell* 78, 23–33. [https://doi.org/10.1016/0092-8674\(94\)90569-X](https://doi.org/10.1016/0092-8674(94)90569-X)
- Costa-Faidella, J., Baldeweg, T., Grimm, S., Escera, C., 2011. Interactions between “what” and “when” in the auditory system: temporal predictability enhances repetition suppression. *J. Neurosci. Off. J. Soc. Neurosci.* 31, 18590–18597. <https://doi.org/10.1523/JNEUROSCI.2599-11.2011>

- Covey, E., Vater, M., Casseday, J.H., 1991. Binaural properties of single units in the superior olivary complex of the mustached bat. *J. Neurophysiol.* 66, 1080–1094.
- De Ribaupierre, F., Goldstein, M.H., Yeni-Komshian, G., 1972. Intracellular study of the cat's primary auditory cortex. *Brain Res.* 48, 185–204.
- Deng, P.-Y., Rotman, Z., Blundon, J.A., Cho, Y., Cui, J., Cavalli, V., Zakharenko, S.S., Klyachko, V.A., 2013. FMRP regulates neurotransmitter release and synaptic information transmission by modulating action potential duration via BK channels. *Neuron* 77, 696–711. <https://doi.org/10.1016/j.neuron.2012.12.018>
- Duque, D., Malmierca, M.S., 2014. Stimulus-specific adaptation in the inferior colliculus of the mouse: anesthesia and spontaneous activity effects. *Brain Struct. Funct.* 220, 3385–3398. <https://doi.org/10.1007/s00429-014-0862-1>
- Eatock, R., Fay, R.R., 2006. *Vertebrate Hair Cells*. Springer Science & Business Media.
- Ehret, G., 1976. Development of absolute auditory thresholds in the house mouse (*Mus musculus*). *J. Am. Audiol. Soc.* 1, 179–184.
- Ehret, G., 1974. Age-dependent hearing loss in normal hearing mice. *Naturwissenschaften* 61, 506–507.
- Ehret, G., Moffat, A.J.M., 1984. Noise masking of tone responses and critical ratios in single units of the mouse cochlear nerve and cochlear nucleus. *Hear. Res.* 14, 45–57. [https://doi.org/10.1016/0378-5955\(84\)90068-6](https://doi.org/10.1016/0378-5955(84)90068-6)
- Ehret, G., Romand, R., 1997. *The Central Auditory System*. Oxford University Press.
- El Idrissi, A., Ding, X.-H., Scalia, J., Trenkner, E., Brown, W.T., Dobkin, C., 2005. Decreased GABA(A) receptor expression in the seizure-prone fragile X mouse. *Neurosci. Lett.* 377, 141–146. <https://doi.org/10.1016/j.neulet.2004.11.087>
- Ethridge, L.E., White, S.P., Mosconi, M.W., Wang, J., Byerly, M.J., Sweeney, J.A., 2016. Reduced habituation of auditory evoked potentials indicate cortical hyper-excitability in Fragile X Syndrome. *Transl. Psychiatry* 6, e787. <https://doi.org/10.1038/tp.2016.48>
- Ethridge, L.E., White, S.P., Mosconi, M.W., Wang, J., Pedapati, E.V., Erickson, C.A., Byerly, M.J., Sweeney, J.A., 2017. Neural synchronization deficits linked to cortical hyper-excitability and auditory hypersensitivity in fragile X syndrome. *Mol. Autism* 8. <https://doi.org/10.1186/s13229-017-0140-1>
- Evans, E.F., Nelson, P.G., 1973. The responses of single neurones in the cochlear nucleus of the cat as a function of their location and the anaesthetic state. *Exp. Brain Res.* 17, 402–427. <https://doi.org/10.1007/BF00234103>
- Evans, E.F., Ross, H.F., Whitfield, I.C., 1965. The spatial distribution of unit characteristic frequency in the primary auditory cortex of the cat. *J. Physiol.* 179, 238–247.
- Farel, P.B., Thompson, R.F., 1976. Habituation of a monosynaptic response in frog spinal cord: evidence for a presynaptic mechanism. *J. Neurophysiol.* 39, 661–666.
- Fay, R.R., 2012. *Comparative Hearing: Mammals*. Springer Science & Business Media.
- Fay, R.R., 1988. *Hearing in vertebrates : a psychophysics databook*. Winnetka, Ill. : Hill-Fay Associates.
- Fech, T., Calderón-Garcidueñas, L., Kulesza, R.J., 2017. Characterization of the superior olivary complex of *Canis lupus domesticus*. *Hear. Res.* 351, 130–140. <https://doi.org/10.1016/j.heares.2017.06.010>
- Felix, R.A., Vonderschen, K., Berrebi, A.S., Magnusson, A.K., 2013. Development of on-off spiking in superior paraolivary nucleus neurons of the mouse. *J. Neurophysiol.* 109, 2691–2704. <https://doi.org/10.1152/jn.01041.2012>
- Ferri, R., 1989. Brain-stem auditory evoked potentials in the fragile X syndrome. *Am. J. Hum. Genet.* 45, 977–979.
- Ferron, L., Nieto-Rostro, M., Cassidy, J.S., Dolphin, A.C., 2014. Fragile X mental retardation protein controls synaptic vesicle exocytosis by modulating N-type calcium channel density. *Nat. Commun.* 5, 3628. <https://doi.org/10.1038/ncomms4628>
- Finlayson, P.G., Adam, T.J., 1997. Excitatory and inhibitory response adaptation in the superior olive complex affects binaural acoustic processing. *Hear. Res.* 103, 1–18.

- Finlayson, P.G., Caspary, D.M., 1991. Low-frequency neurons in the lateral superior olive exhibit phase-sensitive binaural inhibition. *J. Neurophysiol.* 65, 598–605.
- Fontaine, B., Peremans, H., 2007. Tuning bat LSO neurons to interaural intensity differences through spike-timing dependent plasticity. *Biol. Cybern.* 97, 261–267. <https://doi.org/10.1007/s00422-007-0178-9>
- Friauf, E., 1992. Tonotopic Order in the Adult and Developing Auditory System of the Rat as Shown by c-fos Immunocytochemistry. *Eur. J. Neurosci.* 4, 798–812.
- Fukui, I., Burger, R.M., Ohmori, H., Rubel, E.W., 2010. GABAergic inhibition sharpens the frequency tuning and enhances phase locking in chicken nucleus magnocellularis neurons. *J. Neurosci. Off. J. Soc. Neurosci.* 30, 12075–12083. <https://doi.org/10.1523/JNEUROSCI.1484-10.2010>
- Gabriele, M.L., Brunso-Bechtold, J.K., Henkel, C.K., 2000. Development of afferent patterns in the inferior colliculus of the rat: Projection from the dorsal nucleus of the lateral lemniscus. *J. Comp. Neurol.* 416, 368–382. [https://doi.org/10.1002/\(SICI\)1096-9861\(20000117\)416:3<368::AID-CNE8>3.0.CO;2-C](https://doi.org/10.1002/(SICI)1096-9861(20000117)416:3<368::AID-CNE8>3.0.CO;2-C)
- Galvez, R., Greenough, W.T., 2005. Sequence of abnormal dendritic spine development in primary somatosensory cortex of a mouse model of the fragile X mental retardation syndrome. *Am. J. Med. Genet. A.* 135A, 155–160. <https://doi.org/10.1002/ajmg.a.30709>
- Galvez, R., Smith, R.L., Greenough, W.T., 2005. Olfactory bulb mitral cell dendritic pruning abnormalities in a mouse model of the Fragile-X mental retardation syndrome: Further support for FMRP's involvement in dendritic development. *Dev. Brain Res.* 157, 214–216. <https://doi.org/10.1016/j.devbrainres.2005.03.010>
- Garcia-Lazaro, J.A., Shepard, K.N., Miranda, J.A., Liu, R.C., Lesica, N.A., 2015. An Overrepresentation of High Frequencies in the Mouse Inferior Colliculus Supports the Processing of Ultrasonic Vocalizations. *PloS One* 10, e0133251. <https://doi.org/10.1371/journal.pone.0133251>
- Garcia-Pino, E., Gessele, N., Koch, U., 2017. Enhanced Excitatory Connectivity and Disturbed Sound Processing in the Auditory Brainstem of Fragile X Mice. *J. Neurosci.* 2310–16. <https://doi.org/10.1523/JNEUROSCI.2310-16.2017>
- Gibson, J.R., Bartley, A.F., Hays, S.A., Huber, K.M., 2008. Imbalance of Neocortical Excitation and Inhibition and Altered UP States Reflect Network Hyperexcitability in the Mouse Model of Fragile X Syndrome. *J. Neurophysiol.* 100, 2615–2626. <https://doi.org/10.1152/jn.90752.2008>
- Gillaspy, C.C., 1958. Superior olive in the alligator. *Proc. Soc. Exp. Biol. Med. Soc. Exp. Biol. Med. N. Y.* N 98, 492–494.
- Gillespie, D.C., Kim, G., Kandler, K., 2005. Inhibitory synapses in the developing auditory system are glutamatergic. *Nat. Neurosci.* 8, 332–338. <https://doi.org/10.1038/nn1397>
- Givois, V., Pollack, G.S., 2000. Sensory habituation of auditory receptor neurons: implications for sound localization. *J. Exp. Biol.* 203, 2529–2537.
- Goldberg, J.M., Brown, P.B., 1969. Response of binaural neurons of dog superior olivary complex to dichotic tonal stimuli: some physiological mechanisms of sound localization. *J. Neurophysiol.* 32, 613–636.
- Gourévitch, B., Brette, R., 2012. The impact of early reflections on binaural cues. *J. Acoust. Soc. Am.* 132, 9–27. <https://doi.org/10.1121/1.4726052>
- Greene, N.T., Lomakin, O., Davis, K.A., 2010. Monaural spectral processing differs between the lateral superior olive and the inferior colliculus: physiological evidence for an acoustic chiasm. *Hear. Res.* 269, 134–145. <https://doi.org/10.1016/j.heares.2010.06.018>
- Greenough, W.T., Klintsova, A.Y., Irwin, S.A., Galvez, R., Bates, K.E., Weiler, I.J., 2001. Synaptic regulation of protein synthesis and the fragile X protein. *Proc. Natl. Acad. Sci.* 98, 7101–7106. <https://doi.org/10.1073/pnas.141145998>
- Grimm, S., Escera, C., 2012. Auditory deviance detection revisited: evidence for a hierarchical novelty system. *Int. J. Psychophysiol. Off. J. Int. Organ. Psychophysiol.* 85, 88–92. <https://doi.org/10.1016/j.ijpsycho.2011.05.012>

- Grimm, S., Escera, C., Slabu, L., Costa-Faidella, J., 2011. Electrophysiological evidence for the hierarchical organization of auditory change detection in the human brain. *Psychophysiology* 48, 377–384. <https://doi.org/10.1111/j.1469-8986.2010.01073.x>
- Guinan, J.J., Guinan, S.S., Norris, B.E., 1972. Single Auditory Units in the Superior Olivary Complex: I: Responses to Sounds and Classifications Based on Physiological Properties. *Int. J. Neurosci.* 4, 101–120. <https://doi.org/10.3109/00207457209147165>
- Guinan, J.J., Li, R.Y.-S., 1990. Signal processing in brainstem auditory neurons which receive giant endings (calyces of Held) in the medial nucleus of the trapezoid body of the cat. *Hear. Res.* 49, 321–334. [https://doi.org/10.1016/0378-5955\(90\)90111-2](https://doi.org/10.1016/0378-5955(90)90111-2)
- Gustavson, K.H., Blomquist, H.K., Holmgren, G., 1986. Prevalence of the fragile-X syndrome in mentally retarded boys in a Swedish county. *Am. J. Med. Genet.* 23, 581–587.
- Haack, B., Markl, H., Ehret, G., 1983. Sound communication between parents and offspring. <http://dx.doi.org/10.18725/OPARU-1174>
- Hagerman, R., Hoem, G., Hagerman, P., 2010. Fragile X and autism: Intertwined at the molecular level leading to targeted treatments. *Mol. Autism* 1, 12. <https://doi.org/10.1186/2040-2392-1-12>
- Hagerman, R.J., Berry-Kravis, E., Kaufmann, W.E., Ono, M.Y., Tartaglia, N., Lachiewicz, A., Kronk, R., Delahunty, C., Hessler, D., Visootsak, J., Picker, J., Gane, L., Tranfaglia, M., 2009. Advances in the Treatment of Fragile X Syndrome. *Pediatrics* 123, 378–390. <https://doi.org/10.1542/peds.2008-0317>
- Hagerman, R.J., Jackson, A.W., Levitas, A., Rimland, B., Braden, M., 1986. An analysis of autism in fifty males with the fragile X syndrome. *Am. J. Med. Genet.* 23, 359–374.
- Hall, J.C., 1999. GABAergic inhibition shapes frequency tuning and modifies response properties in the auditory midbrain of the leopard frog. *J. Comp. Physiol. [A]* 185, 479–491.
- Hancock, K.E., Davis, K.A., Voigt, H.F., 1997. Modeling inhibition of type II units in the dorsal cochlear nucleus. *Biol. Cybern.* 76, 419–428. <https://doi.org/10.1007/s004220050355>
- Harnischfeger, G., Neuweiler, G., Schlegel, P., 1985. Interaural time and intensity coding in superior olivary complex and inferior colliculus of the echolocating bat *Molossus ater*. *J. Neurophysiol.* 53, 89–109.
- Harrison, J.M., Irving, R., 1966. Visual and nonvisual auditory systems in mammals. Anatomical evidence indicates two kinds of auditory pathways and suggests two kinds of hearing in mammals. *Science* 154, 738–743.
- Hays, S.A., Huber, K.M., Gibson, J.R., 2011. Altered neocortical rhythmic activity states in *Fmr1* KO mice are due to enhanced mGluR5 signaling and involve changes in excitatory circuitry. *J. Neurosci. Off. J. Soc. Neurosci.* 31, 14223–14234. <https://doi.org/10.1523/JNEUROSCI.3157-11.2011>
- He, C.X., Cantu, D.A., Mantri, S.S., Zeiger, W.A., Goel, A., Portera-Cailliau, C., 2017. Tactile Defensiveness and Impaired Adaptation of Neuronal Activity in the *Fmr1* Knock-Out Mouse Model of Autism. *J. Neurosci. Off. J. Soc. Neurosci.* 37, 6475–6487. <https://doi.org/10.1523/JNEUROSCI.0651-17.2017>
- Hebb, D.O., 2002. *The Organization of Behavior: A Neuropsychological Theory*. Taylor & Francis.
- Heffner, H., Masterton, B., 1980. Hearing in Glires: Domestic rabbit, cotton rat, feral house mouse, and kangaroo rat. *J. Acoust. Soc. Am.* 68, 1584–1599. <https://doi.org/10.1121/1.385213>
- Heffner, H.E., Heffner, R.S., 2007. Hearing ranges of laboratory animals. *J. Am. Assoc. Lab. Anim. Sci. JAALAS* 46, 20–22.
- Helfert, R.H., Schwartz, I.R., 1986. Morphological evidence for the existence of multiple neuronal classes in the cat lateral superior olivary nucleus. *J. Comp. Neurol.* 244, 533–549. <https://doi.org/10.1002/cne.902440409>
- Hines, M., 1921. The Superior Olive in *Ornithorhynchus*. *J. Anat.* 55, 290–291.
- Hirsch, J.A., Oertel, D., 1988. Synaptic connections in the dorsal cochlear nucleus of mice, in vitro. *J. Physiol.* 396, 549–562.

- Hofer, M.A., Shair, H.N., Brunelli, S.A., 2002. Ultrasonic vocalizations in rat and mouse pups. *Curr. Protoc. Neurosci.* Chapter 8, Unit 8.14. <https://doi.org/10.1002/0471142301.ns0814s17>
- Hoffmann, S., Firzlaff, U., Radtke-Schuller, S., Schwellnus, B., Schuller, G., 2008. The auditory cortex of the bat *Phyllostomus discolor*: Localization and organization of basic response properties. *BMC Neurosci.* 9, 65. <https://doi.org/10.1186/1471-2202-9-65>
- Holy, T.E., Guo, Z., 2005. Ultrasonic Songs of Male Mice. *PLOS Biol.* 3, e386. <https://doi.org/10.1371/journal.pbio.0030386>
- Horowitz, S., 2013. *The Universal Sense: How Hearing Shapes the Mind*. Bloomsbury.
- Indig, F.E., Diaz-Gonzalez, F., Ginsberg, M.H., 1997. Analysis of the tetraspanin CD9-integrin alphaIIb beta3 (GPIIb-IIIa) complex in platelet membranes and transfected cells. *Biochem. J.* 327, 291–298.
- Ingham, N.J., McAlpine, D., 2004. Spike-frequency adaptation in the inferior colliculus. *J. Neurophysiol.* 91, 632–645. <https://doi.org/10.1152/jn.00779.2003>
- Irvine, D.R., Park, V.N., McCormick, L., 2001. Mechanisms underlying the sensitivity of neurons in the lateral superior olive to interaural intensity differences. *J. Neurophysiol.* 86, 2647–2666.
- Irvine, D.R., Rajan, R., Aitkin, L.M., 1996. Sensitivity to interaural intensity differences of neurons in primary auditory cortex of the cat. I. types of sensitivity and effects of variations in sound pressure level. *J. Neurophysiol.* 75, 75–96.
- Irwin, S.A., Patel, B., Idupulapati, M., Harris, J.B., Crisostomo, R.A., Larsen, B.P., Kooy, F., Willems, P.J., Cras, P., Kozlowski, P.B., Swain, R.A., Weiler, I.J., Greenough, W.T., 2001. Abnormal dendritic spine characteristics in the temporal and visual cortices of patients with fragile-X syndrome: a quantitative examination. *Am. J. Med. Genet.* 98, 161–167.
- Ito, T., Inoue, K., Takada, M., 2015. Distribution of glutamatergic, GABAergic, and glycinergic neurons in the auditory pathways of macaque monkeys. *Neuroscience* 310, 128–151. <https://doi.org/10.1016/j.neuroscience.2015.09.041>
- Iwasaki, S., Momiyama, A., Uchitel, O.D., Takahashi, T., 2000. Developmental changes in calcium channel types mediating central synaptic transmission. *J. Neurosci. Off. J. Soc. Neurosci.* 20, 59–65.
- Javel, E., 1994. Shapes of cat auditory nerve fiber tuning curves. *Hear. Res.* 81, 167–188.
- Jeffress, L.A., 1948. A place theory of sound localization. *J. Comp. Physiol. Psychol.* 41, 35–39.
- Jen, P.H.-S., Xu, L., 2002. Monaural middle ear destruction in juvenile and adult mice: effects on responses to sound direction in the inferior colliculus ipsilateral to the intact ear. *Hear. Res.* 174, 249–259.
- Johnston, J., Forsythe, I.D., Kopp-Scheinflug, C., 2010. Going native: voltage-gated potassium channels controlling neuronal excitability. *J. Physiol.* 588, 3187–3200. <https://doi.org/10.1113/jphysiol.2010.191973>
- Jones, H.G., Brown, A.D., Koka, K., Thornton, J.L., Tollin, D.J., 2015. Sound frequency-invariant neural coding of a frequency-dependent cue to sound source location. *J. Neurophysiol.* 114, 531–539. <https://doi.org/10.1152/jn.00062.2015>
- Joris, P.X., Smith, P.H., Yin, T.C., 1994. Enhancement of neural synchronization in the anteroventral cochlear nucleus. II. Responses in the tuning curve tail. *J. Neurophysiol.* 71, 1037–1051.
- Kaltenbach, J.A., Saunders, J.C., 1987. Spectral and temporal response patterns of single units in the chinchilla dorsal cochlear nucleus. *Exp. Neurol.* 96, 406–419.
- Kandel, E.R., 1976. *Cellular Basis of Behavior: An Introduction to Behavioral Neurobiology*. W. H. Freeman.
- Kandler, K., Clause, A., Noh, J., 2009. Tonotopic reorganization of developing auditory brainstem circuits. *Nat. Neurosci.* 12, nn.2332. <https://doi.org/10.1038/nn.2332>
- Kandler, K., Friauf, E., 1995. Development of glycinergic and glutamatergic synaptic transmission in the auditory brainstem of perinatal rats. *J. Neurosci. Off. J. Soc. Neurosci.* 15, 6890–6904.

- Kandler, K., Friauf, E., 1993. Pre- and postnatal development of efferent connections of the cochlear nucleus in the rat. *J. Comp. Neurol.* 328, 161–184.  
<https://doi.org/10.1002/cne.903280202>
- Karcz, A., Hennig, M.H., Robbins, C.A., Tempel, B.L., RübSamen, R., Kopp-Scheinflug, C., 2011. Low-voltage activated Kv1.1 subunits are crucial for the processing of sound source location in the lateral superior olive in mice. *J. Physiol.* 589, 1143–1157.  
<https://doi.org/10.1113/jphysiol.2010.203331>
- Keating, P., Nodal, F.R., King, A.J., 2014. Behavioural sensitivity to binaural spatial cues in ferrets: evidence for plasticity in the duplex theory of sound localization. *Eur. J. Neurosci.* 39, 197–206. <https://doi.org/10.1111/ejn.12402>
- Kelly, J.B., Glenn, S.L., Beaver, C.J., 1991. Sound frequency and binaural response properties of single neurons in rat inferior colliculus. *Hear. Res.* 56, 273–280.  
[https://doi.org/10.1016/0378-5955\(91\)90177-B](https://doi.org/10.1016/0378-5955(91)90177-B)
- Kennedy, E., Aubusson, P., Hickman, P., 2009. *Biology in context : the spectrum of life.*
- Kiang, N.Y., Sachs, M.B., Peake, W.T., 1967. Shapes of tuning curves for single auditory-nerve fibers. *J. Acoust. Soc. Am.* 42, 1341–1342.
- Kim, D.O., Bishop, B., Kuwada, S., 2010. Acoustic Cues for Sound Source Distance and Azimuth in Rabbits, a Racquetball and a Rigid Spherical Model. *JARO J. Assoc. Res. Otolaryngol.* 11, 541–557. <https://doi.org/10.1007/s10162-010-0221-8>
- Kim, H., Gibboni, R., Kirkhart, C., Bao, S., 2013. Impaired Critical Period Plasticity in Primary Auditory Cortex of Fragile X Model Mice. *J. Neurosci.* 33, 15686–15692.  
<https://doi.org/10.1523/JNEUROSCI.3246-12.2013>
- Klug, A., Park, T.J., Pollak, G.D., 1995. Glycine and GABA influence binaural processing in the inferior colliculus of the mustache bat. *J. Neurophysiol.* 74, 1701–1713.
- Knoth, I.S., Lippe, S., 2012. Event-related potential alterations in fragile X syndrome. *Front. Hum. Neurosci.* 6. <https://doi.org/10.3389/fnhum.2012.00264>
- Knoth, I.S., Vannasing, P., Major, P., Michaud, J.L., Lippé, S., 2014. Alterations of visual and auditory evoked potentials in fragile X syndrome. *Int. J. Dev. Neurosci.* 36, 90–97.  
<https://doi.org/10.1016/j.ijdevneu.2014.05.003>
- Kopp-Scheinflug, C., Fuchs, K., Lippe, W.R., Tempel, B.L., RübSamen, R., 2003. Decreased Temporal Precision of Auditory Signaling in Kcna1-Null Mice: An Electrophysiological Study In Vivo. *J. Neurosci.* 23, 9199–9207.
- Krächan, E.G., Fischer, A.U., Franke, J., Friauf, E., 2017. Synaptic reliability and temporal precision are achieved via high quantal content and effective replenishment: auditory brainstem versus hippocampus. *J. Physiol.* 595, 839–864. <https://doi.org/10.1113/JP272799>
- Kral, A., Majernik, V., 1996. On lateral inhibition in the auditory system. *Gen. Physiol. Biophys.* 15, 109–127.
- Kulesza Jr., R.J., Lukose, R., Stevens, L.V., 2011. Malformation of the human superior olive in autistic spectrum disorders. *Brain Res.* 1367, 360–371.  
<https://doi.org/10.1016/j.brainres.2010.10.015>
- Kulesza, R.J., Mangunay, K., 2008. Morphological features of the medial superior olive in autism. *Brain Res.* 1200, 132–137. <https://doi.org/10.1016/j.brainres.2008.01.009>
- Kullmann, P.H., Kandler, K., 2001. Glycinergic/GABAergic synapses in the lateral superior olive are excitatory in neonatal C57Bl/6J mice. *Brain Res. Dev. Brain Res.* 131, 143–147.
- Kupfermann, I., Castellucci, V., Pinsker, H., Kandel, E., 1970. Neuronal Correlates of Habituation and Dishabituation of the Gill-Withdrawal Reflex in Aplysia. *Science* 167, 1743–1745.  
<https://doi.org/10.1126/science.167.3926.1743>
- Kuwabara, N., DiCaprio, R.A., Zook, J.M., 1991. Afferents to the medial nucleus of the trapezoid body and their collateral projections. *J. Comp. Neurol.* 314, 684–706.  
<https://doi.org/10.1002/cne.903140405>
- Kuwada, S., Batra, R., Stanford, T.R., 1989. Monaural and binaural response properties of neurons in the inferior colliculus of the rabbit: effects of sodium pentobarbital. *J. Neurophysiol.* 61, 269–282. <https://doi.org/10.1152/jn.1989.61.2.269>

- Laughlin, M.M., Heijden, M. van der, Joris, P.X., 2008. How Secure Is *In Vivo* Synaptic Transmission at the Calyx of Held? *J. Neurosci.* 28, 10206–10219. <https://doi.org/10.1523/JNEUROSCI.2735-08.2008>
- Leake, P.A., Snyder, R.L., Hradek, G.T., 2002. Postnatal Refinement of Auditory Nerve Projections to the Cochlear Nucleus in Cats. *J. Comp. Neurol.* 448, 6–27. <https://doi.org/10.1002/cne.10176>
- LeBeau, F.E., Malmierca, M.S., Rees, A., 2001. Iontophoresis in vivo demonstrates a key role for GABA(A) and glycinergic inhibition in shaping frequency response areas in the inferior colliculus of guinea pig. *J. Neurosci. Off. J. Soc. Neurosci.* 21, 7303–7312.
- Li, Y., Zhao, X., 2014. Fragile X proteins in stem cell maintenance and differentiation. *Stem Cells Dayt. Ohio* 32, 1724–1733. <https://doi.org/10.1002/stem.1698>
- Lorteije, J.A.M., Rusu, S.I., Kushmerick, C., Borst, J.G.G., 2009. Reliability and Precision of the Mouse Calyx of Held Synapse. *J. Neurosci.* 29, 13770–13784. <https://doi.org/10.1523/JNEUROSCI.3285-09.2009>
- Louage, D.H.G., van der Heijden, M., Joris, P.X., 2005. Enhanced temporal response properties of anteroventral cochlear nucleus neurons to broadband noise. *J. Neurosci. Off. J. Soc. Neurosci.* 25, 1560–1570. <https://doi.org/10.1523/JNEUROSCI.4742-04.2005>
- Lu, T., Trussell, L.O., 2007. Development and elimination of endbulb synapses in the chick cochlear nucleus. *J. Neurosci. Off. J. Soc. Neurosci.* 27, 808–817. <https://doi.org/10.1523/JNEUROSCI.4871-06.2007>
- Majorossy, K., Kiss, A., 1990. Types of neurons and synaptic relations in the lateral superior olive of the cat: normal structure and experimental observations. *Acta Morphol. Hung.* 38, 207–215.
- Martin, M.R., Dickson, J.W., 1983. Lateral inhibition in the anteroventral cochlear nucleus of the cat: a microiontophoretic study. *Hear. Res.* 9, 35–41.
- McAlpine, D., 2005. Creating a sense of auditory space. *J. Physiol.* 566, 21–28. <https://doi.org/10.1113/jphysiol.2005.083113>
- McDiarmid, T.A., Bernardos, A.C., Rankin, C.H., 2017. Habituation is altered in neuropsychiatric disorders—A comprehensive review with recommendations for experimental design and analysis. *Neurosci. Biobehav. Rev.* 80, 286–305. <https://doi.org/10.1016/j.neubiorev.2017.05.028>
- Miller, L.J., McIntosh, D.N., McGrath, J., Shyu, V., Lampe, M., Taylor, A.K., Tassone, F., Neitzel, K., Stackhouse, T., Hagerman, R.J., 1999a. Electrodermal responses to sensory stimuli in individuals with fragile X syndrome: a preliminary report. *Am. J. Med. Genet.* 83, 268–279.
- Miller, L.J., McIntosh, D.N., McGrath, J., Shyu, V., Lampe, M., Taylor, A.K., Tassone, F., Neitzel, K., Stackhouse, T., Hagerman, R.J., 1999b. Electrodermal responses to sensory stimuli in individuals with fragile X syndrome: a preliminary report. *Am. J. Med. Genet.* 83, 268–279.
- Mills, A.W., 1960. Lateralization of High-Frequency Tones. *J. Acoust. Soc. Am.* 32, 132–134. <https://doi.org/10.1121/1.1907864>
- Mills, A.W., 1958. On the Minimum Audible Angle. *J. Acoust. Soc. Am.* 30, 237–246. <https://doi.org/10.1121/1.1909553>
- Młynarski, W., Jost, J., 2014. Statistics of Natural Binaural Sounds. *PLoS ONE* 9. <https://doi.org/10.1371/journal.pone.0108968>
- Mott, B., Wei, S., 2014. Firing Property of Inferior Colliculus Neurons Affected by FMR1 Gene Mutation. *J. Otol.* 9, 86–90. [https://doi.org/10.1016/S1672-2930\(14\)50020-7](https://doi.org/10.1016/S1672-2930(14)50020-7)
- Müller, M., 1990. Quantitative comparison of frequency representation in the auditory brainstem nuclei of the gerbil, *Pachyuromys duprasi*. *Exp. Brain Res.* 81, 140–149.
- Musumeci, S.A., Bosco, P., Calabrese, G., Bakker, C., De Sarro, G.B., Elia, M., Ferri, R., Oostra, B.A., 2000. Audiogenic Seizures Susceptibility in Transgenic Mice with Fragile X Syndrome. *Epilepsia* 41, 19–23. <https://doi.org/10.1111/j.1528-1157.2000.tb01499.x>

- Mutschler, I., Wieckhorst, B., Speck, O., Schulze-Bonhage, A., Hennig, J., Seifritz, E., Ball, T., 2010. Time scales of auditory habituation in the amygdala and cerebral cortex. *Cereb. Cortex N. Y. N* 1991 20, 2531–2539. <https://doi.org/10.1093/cercor/bhq001>
- Navarro-López, J., Jiménez-Díaz, L., Géranton, S.M., Ashmore, J.F., 2009. Electrophysiological and molecular analysis of Kv7/KCNQ potassium channels in the inferior colliculus of adult guinea pig. *J. Mol. Neurosci. MN* 37, 263–268. <https://doi.org/10.1007/s12031-008-9130-2>
- Nelken, I., Ulanovsky, N., 2007. Mismatch Negativity and Stimulus-Specific Adaptation in Animal Models. *J. Psychophysiol.* 21, 214–223. <https://doi.org/10.1027/0269-8803.21.34.214>
- Nobili, R., Mammano, F., Ashmore, J., 1998. How well do we understand the cochlea? *Trends Neurosci.* 21, 159–167. [https://doi.org/10.1016/S0166-2236\(97\)01192-2](https://doi.org/10.1016/S0166-2236(97)01192-2)
- O'Donnell, W.T., Warren, S.T., 2002. A decade of molecular studies of fragile X syndrome. *Annu. Rev. Neurosci.* 25, 315–338. <https://doi.org/10.1146/annurev.neuro.25.112701.142909>
- Oertel, D., Bal, R., Gardner, S.M., Smith, P.H., Joris, P.X., 2000. Detection of synchrony in the activity of auditory nerve fibers by octopus cells of the mammalian cochlear nucleus. *Proc. Natl. Acad. Sci.* 97, 11773–11779. <https://doi.org/10.1073/pnas.97.22.11773>
- Ojima, H., Murakami, K., 2002. Intracellular characterization of suppressive responses in supragranular pyramidal neurons of cat primary auditory cortex in vivo. *Cereb. Cortex N. Y. N* 1991 12, 1079–1091.
- Ollo, C., Schwartz, I.R., 1979. The superior olivary complex in C57BL/6 mice. *Am. J. Anat.* 155, 349–373. <https://doi.org/10.1002/aja.1001550306>
- Opdam, R., Kemali, M., Nieuwenhuys, R., 1976. Topological analysis of the brain stem of the frogs *Rana esculenta* and *Rana catesbeiana*. *J. Comp. Neurol.* 165, 307–332. <https://doi.org/10.1002/cne.901650304>
- Oswald, A.-M.M., Schiff, M.L., Reyes, A.D., 2006. Synaptic mechanisms underlying auditory processing. *Curr. Opin. Neurobiol.* 16, 371–376. <https://doi.org/10.1016/j.conb.2006.06.015>
- Paluszkiwicz, S.M., Olmos-Serrano, J.L., Corbin, J.G., Huntsman, M.M., 2011. Impaired inhibitory control of cortical synchronization in fragile X syndrome. *J. Neurophysiol.* 106, 2264–2272. <https://doi.org/10.1152/jn.00421.2011>
- Paolini, A.G., FitzGerald, J.V., Burkitt, A.N., Clark, G.M., 2001. Temporal processing from the auditory nerve to the medial nucleus of the trapezoid body in the rat. *Hear. Res.* 159, 101–116.
- Park, T.J., Grothe, B., Pollak, G.D., Schuller, G., Koch, U., 1996. Neural Delays Shape Selectivity to Interaural Intensity Differences in the Lateral Superior Olive. *J. Neurosci.* 16, 6554–6566.
- Park, T.J., Klug, A., Holinstat, M., Grothe, B., 2004. Interaural Level Difference Processing in the Lateral Superior Olive and the Inferior Colliculus. *J. Neurophysiol.* 92, 289–301. <https://doi.org/10.1152/jn.00961.2003>
- Patel, A.B., Loerwald, K.W., Huber, K.M., Gibson, J.R., 2014. Postsynaptic FMRP Promotes the Pruning of Cell-to-Cell Connections among Pyramidal Neurons in the L5A Neocortical Network. *J. Neurosci.* 34, 3413–3418. <https://doi.org/10.1523/JNEUROSCI.2921-13.2014>
- Paxinos, G., Franklin, K.B.J., 2004. *The Mouse Brain in Stereotaxic Coordinates*. Gulf Professional Publishing.
- Pedemonte, M., Peña, J.L., Morales-Cobas, G., Velluti, R.A., 1994. Effects of sleep on the responses of single cells in the lateral superior olive. *Arch. Ital. Biol.* 132, 165–178.
- Pérez-González, D., Malmierca, M.S., 2014. Adaptation in the auditory system: an overview. *Front. Integr. Neurosci.* 8, 19. <https://doi.org/10.3389/fnint.2014.00019>
- Pfeiffer, B.E., Huber, K.M., 2007. Fragile X Mental Retardation Protein Induces Synapse Loss through Acute Postsynaptic Translational Regulation. *J. Neurosci.* 27, 3120–3130. <https://doi.org/10.1523/JNEUROSCI.0054-07.2007>
- Pickles, J.O., 2008. *An Introduction to the Physiology of Hearing*, Third Edition, 3 edition. ed. Academic Press, London.
- Purves, D., Augustine, G.J., Hall, W.C., LaMantia, A.-S., White, L.E., 2012. *Neuroscience*, 5th ed. 2012. ed. Sinauer, Sunderland, Mass.

- Qin, L., Sato, Y., 2004. Suppression of auditory cortical activities in awake cats by pure tone stimuli. *Neurosci. Lett.* 365, 190–194. <https://doi.org/10.1016/j.neulet.2004.04.092>
- Quiroga, R.Q., Panzeri, S., 2013. *Principles of Neural Coding*. CRC Press.
- Radziwon, K.E., June, K.M., Stolzberg, D.J., Xu-Friedman, M.A., Salvi, R.J., Dent, M.L., 2009. Behaviorally measured audiograms and gap detection thresholds in CBA/CaJ mice. *J. Comp. Physiol. A* 195, 961–969. <https://doi.org/10.1007/s00359-009-0472-1>
- Rasmussen, G.L., 1946. The olivary peduncle and other fiber projections of the superior olivary complex. *J. Comp. Neurol.* 84, 141–219.
- Rhode, W.S., Geisler, C.D., Kennedy, D.T., 1978. Auditory nerve fiber response to wide-band noise and tone combinations. *J. Neurophysiol.* 41, 692–704.
- Rhode, W.S., Greenberg, S., 1994. Lateral suppression and inhibition in the cochlear nucleus of the cat. *J. Neurophysiol.* 71, 493–514.
- Rhode, W.S., Smith, P.H., 1986. Encoding timing and intensity in the ventral cochlear nucleus of the cat. *J. Neurophysiol.* 56, 261–286.
- Rietzel, H.J., Friauf, E., 1998. Neuron types in the rat lateral superior olive and developmental changes in the complexity of their dendritic arbors. *J. Comp. Neurol.* 390, 20–40.
- Risch, D., Corkeron, P.J., Ellison, W.T., Parijs, S.M.V., 2012. Changes in humpback whale song occurrence in response to an acoustic source 200 km away. *PloS One* 7, e29741. <https://doi.org/10.1371/journal.pone.0029741>
- Rizzi, S., Knaus, H., Schwarzer, C., 2016. Differential distribution of the sodium-activated potassium channels *slack* and *slick* in mouse brain. *J. Comp. Neurol.* 524, 2093–2116. <https://doi.org/10.1002/cne.23934>
- Roberts, J., Price, J., Barnes, E., Nelson, L., Burchinal, M., Hennon, E.A., Moskowitz, L., Edwards, A., Malkin, C., Anderson, K., Misenheimer, J., Hooper, S.R., 2007. Receptive Vocabulary, Expressive Vocabulary, and Speech Production of Boys With Fragile X Syndrome in Comparison to Boys With Down Syndrome. *Am. J. Ment. Retard.* 112, 177–193. [https://doi.org/10.1352/0895-8017\(2007\)112\[177:RVEVAS\]2.0.CO;2](https://doi.org/10.1352/0895-8017(2007)112[177:RVEVAS]2.0.CO;2)
- Romand, R., 2012. *Development of Auditory and Vestibular Systems*. Elsevier.
- Rossing, T., 2015. *Springer Handbook of Acoustics*. Springer.
- Rotschafer, S., Razak, K., 2013a. Altered auditory processing in a mouse model of fragile X syndrome. *Brain Res.* 1506, 12–24. <https://doi.org/10.1016/j.brainres.2013.02.038>
- Rotschafer, S., Razak, K., 2013b. Altered auditory processing in a mouse model of fragile X syndrome. *Brain Res.* 1506, 12–24. <https://doi.org/10.1016/j.brainres.2013.02.038>
- Rotschafer, S.E., Marshak, S., Cramer, K.S., 2015a. Deletion of *Fmr1* Alters Function and Synaptic Inputs in the Auditory Brainstem. *PLoS ONE* 10, e0117266. <https://doi.org/10.1371/journal.pone.0117266>
- Rotschafer, S.E., Marshak, S., Cramer, K.S., 2015b. Deletion of *Fmr1* alters function and synaptic inputs in the auditory brainstem. *PloS One* 10, e0117266. <https://doi.org/10.1371/journal.pone.0117266>
- Rotschafer, S.E., Razak, K.A., 2014. Auditory processing in fragile X syndrome. *Front. Cell. Neurosci.* 8, 19. <https://doi.org/10.3389/fncel.2014.00019>
- Rubel, E.W., Fay, R.R., 2012. *Development of the Auditory System*. Springer Science & Business Media.
- Rubel, E.W., Fritsch, B., 2002. Auditory system development: primary auditory neurons and their targets. *Annu. Rev. Neurosci.* 25, 51–101. <https://doi.org/10.1146/annurev.neuro.25.112701.142849>
- Sachs, M.B., Kiang, N.Y.S., 1968. Two-Tone Inhibition in Auditory-Nerve Fibers. *J. Acoust. Soc. Am.* 43, 1120–1128. <https://doi.org/10.1121/1.1910947>
- Sah, P., Faber, E.S.L., 2002. Channels underlying neuronal calcium-activated potassium currents. *Prog. Neurobiol.* 66, 345–353.
- Sanes, D.H., 1993. The development of synaptic function and integration in the central auditory system. *J. Neurosci. Off. J. Soc. Neurosci.* 13, 2627–2637.
- Sanes, D.H., 1990. An in vitro analysis of sound localization mechanisms in the gerbil lateral superior olive. *J. Neurosci. Off. J. Soc. Neurosci.* 10, 3494–3506.

- Sanes, D.H., Friauf, E., 2000. Development and influence of inhibition in the lateral superior olivary nucleus. *Hear. Res.* 147, 46–58.
- Sanes, D.H., Goldstein, N.A., Ostad, M., Hillman, D.E., 1990. Dendritic morphology of central auditory neurons correlates with their tonotopic position. *J. Comp. Neurol.* 294, 443–454. <https://doi.org/10.1002/cne.902940312>
- Sanes, D.H., Merickel, M., Rubel, E.W., 1989. Evidence for an alteration of the tonotopic map in the gerbil cochlea during development. *J. Comp. Neurol.* 279, 436–444. <https://doi.org/10.1002/cne.902790308>
- Sanes, D.H., Rubel, E.W., 1988. The ontogeny of inhibition and excitation in the gerbil lateral superior olive. *J. Neurosci.* 8, 682–700.
- Sanes, D.H., Siverls, V., 1991. Development and specificity of inhibitory terminal arborizations in the central nervous system. *J. Neurobiol.* 22, 837–854. <https://doi.org/10.1002/neu.480220805>
- Sanes, D.H., Takács, C., 1993. Activity-dependent refinement of inhibitory connections. *Eur. J. Neurosci.* 5, 570–574.
- Saunders, J.C., Dolgin, K.G., Lowry, L.D., 1980. The maturation of frequency selectivity in C57BL/6J mice studied with auditory evoked response tuning curves. *Brain Res.* 187, 69–79.
- Sausbier, U., Sausbier, M., Sailer, C.A., Arntz, C., Knaus, H.-G., Neuhuber, W., Ruth, P., 2006. Ca<sup>2+</sup>-activated K<sup>+</sup> channels of the BK-type in the mouse brain. *Histochem. Cell Biol.* 125, 725–741. <https://doi.org/10.1007/s00418-005-0124-7>
- Schalk, T.B., Sachs, M.B., 1980. Nonlinearities in auditory-nerve fiber responses to bandlimited noise. *J. Acoust. Soc. Am.* 67, 903–913.
- Schmid, S., Brown, T., Simons-Weidenmaier, N., Weber, M., Fendt, M., 2010. Group III metabotropic glutamate receptors inhibit startle-mediating giant neurons in the caudal pontine reticular nucleus but do not mediate synaptic depression/short-term habituation of startle. *J. Neurosci. Off. J. Soc. Neurosci.* 30, 10422–10430. <https://doi.org/10.1523/JNEUROSCI.0024-10.2010>
- Schmidt, P.H., Van Gemert, A.H., De Vries, R.J., Duyff, J.W., 1953. Binaural thresholds for azimuth difference. *Acta Physiol. Pharmacol. Neerl.* 3, 2–18.
- Schneider, A., Leigh, M.J., Adams, P., Nanakul, R., Chechi, T., Olichney, J., Hagerman, R., Hessel, D., 2013. Electrocortical changes associated with minocycline treatment in fragile X syndrome. *J. Psychopharmacol. (Oxf.)* 27, 956–963. <https://doi.org/10.1177/0269881113494105>
- Schnupp, J., Nelken, I., King, A.J., 2012. *Auditory Neuroscience: Making Sense of Sound*. The MIT Press, Cambridge, Mass.
- Sewell, G.D.S., 1972. Ultrasound and mating behaviour in rodents with some observations on other behavioural situations. *J. Zool.* 168, 149–164. <https://doi.org/10.1111/j.1469-7998.1972.tb01345.x>
- Sinclair, D., Oranje, B., Razak, K.A., Siegel, S.J., Schmid, S., 2017. Sensory processing in autism spectrum disorders and Fragile X syndrome—From the clinic to animal models. *Neurosci. Biobehav. Rev.*, SI:IBNS-2015 76, 235–253. <https://doi.org/10.1016/j.neubiorev.2016.05.029>
- Sinclair, D., Oranje, B., Razak, K.A., Siegel, S.J., Schmid, S., 2016. Sensory processing in autism spectrum disorders and Fragile X syndrome—From the clinic to animal models. *Neurosci. Biobehav. Rev.* <https://doi.org/10.1016/j.neubiorev.2016.05.029>
- Siveke, I., Pecka, M., Seidl, A.H., Baudoux, S., Grothe, B., 2006. Binaural Response Properties of Low-Frequency Neurons in the Gerbil Dorsal Nucleus of the Lateral Lemniscus. *J. Neurophysiol.* 96, 1425–1440. <https://doi.org/10.1152/jn.00713.2005>
- Skoe, E., Kraus, N., 2010. Auditory brain stem response to complex sounds: a tutorial. *Ear Hear.* 31, 302–324. <https://doi.org/10.1097/AUD.0b013e3181c8b272>
- Smith, P.H., Joris, P.X., Carney, L.H., Yin, T.C., 1991. Projections of physiologically characterized globular bushy cell axons from the cochlear nucleus of the cat. *J. Comp. Neurol.* 304, 387–407. <https://doi.org/10.1002/cne.903040305>

- Sonntag, M., Englitz, B., Kopp-Scheinpflug, C., Rübsamen, R., 2009. Early Postnatal Development of Spontaneous and Acoustically Evoked Discharge Activity of Principal Cells of the Medial Nucleus of the Trapezoid Body: An In Vivo Study in Mice. *J. Neurosci.* 29, 9510–9520. <https://doi.org/10.1523/JNEUROSCI.1377-09.2009>
- Sourdet, V., Russier, M., Daoudal, G., Ankri, N., Debanne, D., 2003. Long-term enhancement of neuronal excitability and temporal fidelity mediated by metabotropic glutamate receptor subtype 5. *J. Neurosci. Off. J. Soc. Neurosci.* 23, 10238–10248.
- Spitzer, M.W., Semple, M.N., 1995. Neurons sensitive to interaural phase disparity in gerbil superior olive: diverse monaural and temporal response properties. *J. Neurophysiol.* 73, 1668–1690.
- Srinivasan, G., Friauf, E., Löhrike, S., 2004. Functional glutamatergic and glycinergic inputs to several superior olivary nuclei of the rat revealed by optical imaging. *Neuroscience* 128, 617–634. <https://doi.org/10.1016/j.neuroscience.2004.06.012>
- Stiebler, I., Ehret, G., 1985. Inferior colliculus of the house mouse. I. A quantitative study of tonotopic organization, frequency representation, and tone-threshold distribution. *J. Comp. Neurol.* 238, 65–76. <https://doi.org/10.1002/cne.902380106>
- Stiebler, I., Neulist, R., Fichtel, I., Ehret, G., 1997. The auditory cortex of the house mouse: left-right differences, tonotopic organization and quantitative analysis of frequency representation. *J. Comp. Physiol. [A]* 181, 559–571.
- Suga, N., Zhang, Y., Yan, J., 1997. Sharpening of Frequency Tuning by Inhibition in the Thalamic Auditory Nucleus of the Mustached Bat. *J. Neurophysiol.* 77, 2098–2114.
- Sullivan, W.E., 1985. Classification of response patterns in cochlear nucleus of barn owl: correlation with functional response properties. *J. Neurophysiol.* 53, 201–216.
- Sumner, C.J., Palmer, A.R., 2012. Auditory nerve fibre responses in the ferret. *Eur. J. Neurosci.* 36, 2428–2439. <https://doi.org/10.1111/j.1460-9568.2012.08151.x>
- Taberner, A.M., Liberman, M.C., 2005. Response Properties of Single Auditory Nerve Fibers in the Mouse. *J. Neurophysiol.* 93, 557–569. <https://doi.org/10.1152/jn.00574.2004>
- Tabor, K.M., Coleman, W.L., Rubel, E.W., Burger, R.M., 2012. Tonotopic Organization of the Superior Olivary Nucleus in the Chicken Auditory Brainstem. *J. Comp. Neurol.* 520, 1493–1508. <https://doi.org/10.1002/cne.22807>
- Tang, J., Xiao, Z.-J., Shen, J.-X., 2008. Delayed inhibition creates amplitude tuning of mouse inferior collicular neurons. *Neuroreport* 19, 1445–1449. <https://doi.org/10.1097/WNR.0b013e32830dd63a>
- Ting, J.T., Feng, G., 2011. Unfolding neurodevelopmental disorders: Found in translation. *Nat. Med.* 17, 1352–1353. <https://doi.org/10.1038/nm.2553>
- Tollin, D.J., 2003. The Lateral Superior Olive: A Functional Role in Sound Source Localization. *The Neuroscientist* 9, 127–143. <https://doi.org/10.1177/1073858403252228>
- Tollin, D.J., Yin, T.C.T., 2005. Interaural phase and level difference sensitivity in low-frequency neurons in the lateral superior olive. *J. Neurosci. Off. J. Soc. Neurosci.* 25, 10648–10657. <https://doi.org/10.1523/JNEUROSCI.1609-05.2005>
- Tortora, G.J., Nielsen, M., 2013. Principles of Human Anatomy, 13 edition. ed. Wiley, Hoboken, NJ.
- Tsuchitani, C., 1988. The inhibition of cat lateral superior olive unit excitatory responses to binaural tone bursts. I. The transient chopper response. *J. Neurophysiol.* 59, 164–183.
- Tsuchitani, C., Boudreau, J.C., 1966. Single unit analysis of cat superior olive S segment with tonal stimuli. *J. Neurophysiol.* 29, 684–697.
- Typlt, M., Englitz, B., Sonntag, M., Dehmel, S., Kopp-Scheinpflug, C., Rübsamen, R., 2012. Multidimensional characterization and differentiation of neurons in the anteroventral cochlear nucleus. *PloS One* 7, e29965. <https://doi.org/10.1371/journal.pone.0029965>
- Typlt, M., Mirkowski, M., Azzopardi, E., Ruth, P., Pilz, P.K.D., Schmid, S., 2013. Habituation of reflexive and motivated behavior in mice with deficient BK channel function. *Front. Integr. Neurosci.* 7. <https://doi.org/10.3389/fnint.2013.00079>

- Ulanovsky, N., Las, L., Farkas, D., Nelken, I., 2004. Multiple time scales of adaptation in auditory cortex neurons. *J. Neurosci. Off. J. Soc. Neurosci.* 24, 10440–10453.  
<https://doi.org/10.1523/JNEUROSCI.1905-04.2004>
- Ulanovsky, N., Las, L., Nelken, I., 2003. Processing of low-probability sounds by cortical neurons. *Nat. Neurosci.* 6, 391–398. <https://doi.org/10.1038/nn1032>
- Van der Molen, M.J.W., Van der Molen, M.W., Ridderinkhof, K.R., Hamel, B.C.J., Curfs, L.M.G., Ramakers, G.J.A., 2012. Auditory change detection in fragile X syndrome males: A brain potential study. *Clin. Neurophysiol.* 123, 1309–1318.  
<https://doi.org/10.1016/j.clinph.2011.11.039>
- Volkov, I.O., Galazjuk, A.V., 1991. Formation of spike response to sound tones in cat auditory cortex neurons: interaction of excitatory and inhibitory effects. *Neuroscience* 43, 307–321.
- Wakeford, O.S., Robinson, D.E., 1974. Lateralization of tonal stimuli by the cat. *J. Acoust. Soc. Am.* 55, 649–652.
- Walcher, J., Hassfurth, B., Grothe, B., Koch, U., 2011. Comparative posthearing development of inhibitory inputs to the lateral superior olive in gerbils and mice. *J. Neurophysiol.* 106, 1443–1453. <https://doi.org/10.1152/jn.01087.2010>
- Wang, D.O., Martin, K.C., Zukin, R.S., 2010. Spatially restricting gene expression by local translation at synapses. *Trends Neurosci.* 33, 173–182.  
<https://doi.org/10.1016/j.tins.2010.01.005>
- Wang, T., de Kok, L., Willemsen, R., Elgersma, Y., Borst, J.G.G., 2015. In vivo synaptic transmission and morphology in mouse models of Tuberous sclerosis, Fragile X syndrome, Neurofibromatosis type 1, and Costello syndrome. *Front. Cell. Neurosci.* 9, 234.  
<https://doi.org/10.3389/fncel.2015.00234>
- Wang, Y., Sakano, H., Beebe, K., Brown, M.R., de Laat, R., Bothwell, M., Kulesza, R.J., Rubel, E.W., 2014. Intense and specialized dendritic localization of the fragile X mental retardation protein in binaural brainstem neurons: A comparative study in the alligator, chicken, gerbil, and human. *J. Comp. Neurol.* 522, 2107–2128.  
<https://doi.org/10.1002/cne.23520>
- Warr, W.B., Boche, J.B., Neely, S.T., 1997. Efferent innervation of the inner hair cell region: origins and terminations of two lateral olivocochlear systems. *Hear. Res.* 108, 89–111.
- Webb, T.P., Bunday, S.E., Thake, A.I., Todd, J., 1986. Population incidence and segregation ratios in the Martin-Bell syndrome. *Am. J. Med. Genet.* 23, 573–580.
- Weber, M., Schnitzler, H.-U., Schmid, S., 2002. Synaptic plasticity in the acoustic startle pathway: the neuronal basis for short-term habituation? *Eur. J. Neurosci.* 16, 1325–1332.  
<https://doi.org/10.1046/j.1460-9568.2002.02194.x>
- Wehr, M., Zador, A.M., 2005. Synaptic mechanisms of forward suppression in rat auditory cortex. *Neuron* 47, 437–445. <https://doi.org/10.1016/j.neuron.2005.06.009>
- Weiler, I.J., Irwin, S.A., Klintsova, A.Y., Spencer, C.M., Brazelton, A.D., Miyashiro, K., Comery, T.A., Patel, B., Eberwine, J., Greenough, W.T., 1997. Fragile X mental retardation protein is translated near synapses in response to neurotransmitter activation. *Proc. Natl. Acad. Sci. U. S. A.* 94, 5395–5400.
- Weisz, C.J.C., Rubio, M.E., Givens, R.S., Kandler, K., 2016. Excitation by Axon Terminal GABA Spillover in a Sound Localization Circuit. *J. Neurosci. Off. J. Soc. Neurosci.* 36, 911–925.  
<https://doi.org/10.1523/JNEUROSCI.1132-15.2016>
- Westerman, L.A., Smith, R.L., 1984. Rapid and short-term adaptation in auditory nerve responses. *Hear. Res.* 15, 249–260.
- Wisniewski, K.E., Segan, S.M., Mizejeski, C.M., Sersen, E.A., Rudelli, R.D., 1991. The Fra(X) syndrome: neurological, electrophysiological, and neuropathological abnormalities. *Am. J. Med. Genet.* 38, 476–480.
- Wondolowski, J., Dickman, D., 2013. Emerging links between homeostatic synaptic plasticity and neurological disease. *Front. Cell. Neurosci.* 7. <https://doi.org/10.3389/fncel.2013.00223>
- Wu, G.K., Arbuckle, R., Liu, B.-H., Tao, H.W., Zhang, L.I., 2008. Lateral sharpening of cortical frequency tuning by approximately balanced inhibition. *Neuron* 58, 132–143.  
<https://doi.org/10.1016/j.neuron.2008.01.035>

- Wu, S.H., Kelly, J.B., 1992a. Synaptic pharmacology of the superior olivary complex studied in mouse brain slice. *J. Neurosci. Off. J. Soc. Neurosci.* 12, 3084–3097.
- Wu, S.H., Kelly, J.B., 1992b. NMDA, non-NMDA and glycine receptors mediate binaural interaction in the lateral superior olive: physiological evidence from mouse brain slice. *Neurosci. Lett.* 134, 257–260.
- Wu, S.H., Kelly, J.B., 1991. Physiological properties of neurons in the mouse superior olive: membrane characteristics and postsynaptic responses studied in vitro. *J. Neurophysiol.* 65, 230–246.
- Xu, L., Jen, P.H., 2001. The effect of monaural middle ear destruction on postnatal development of auditory response properties of mouse inferior collicular neurons. *Hear. Res.* 159, 1–13.
- Yan, J., Zhang, Y., Ehret, G., 2005. Corticofugal shaping of frequency tuning curves in the central nucleus of the inferior colliculus of mice. *J. Neurophysiol.* 93, 71–83.  
<https://doi.org/10.1152/jn.00348.2004>
- Yates, G.K., Robertson, D., Johnstone, B.M., 1985. Very rapid adaptation in the guinea pig auditory nerve. *Hear. Res.* 17, 1–12.
- Yu, X.-J., Xu, X.-X., He, S., He, J., 2009. Change detection by thalamic reticular neurons. *Nat. Neurosci.* 12, 1165–1170. <https://doi.org/10.1038/nn.2373>
- Zhang, L.I., Tan, A.Y.Y., Schreiner, C.E., Merzenich, M.M., 2003. Topography and synaptic shaping of direction selectivity in primary auditory cortex. *Nature* 424, 201–205.  
<https://doi.org/10.1038/nature01796>
- Zheng, Q.Y., Johnson, K.R., Erway, L.C., 1999. Assessment of hearing in 80 inbred strains of mice by ABR threshold analyses. *Hear. Res.* 130, 94–107.
- Zook, J.M., DiCaprio, R.A., 1988. Intracellular labeling of afferents to the lateral superior olive in the bat, *Eptesicus fuscus*. *Hear. Res.* 34, 141–147.

---

## 9 Abbreviations

ABR	auditory brainstem response
AC	auditory cortex
ANF	auditory nerve fiber
AVCN	anterior ventral cochlear nucleus
CF	characteristic frequency
CN	cochlear nerve
DAB	diaminobenzidine
EEG	electroencephalography
EPSC	excitatory postsynaptic current
ERP	event-related potentials
FIR	finite impulse response
Fmr1	fragile X mental retardation 1
FSL	first spike latency
FXS	fragile X syndrome
GlyT2	glycine transporter 2
HRP	horseradish peroxidase
IC	inferior colliculus
ILD	interaural level difference
ITD	interaural time difference
KO	knock-out
LNTB	lateral nucleus of the trapezoid body
LSO	lateral superior olive
LTD	long-term depression
LTP	long-term potentiation
MAP2	microtubule-associated protein 2
mGluR	metabotropic glutamate receptor
MMN	mismatch negativity
MNTB	medial nucleus of the trapezoid body
MPEP	2-Methyl-6-(phenylethynyl)pyridine
MSO	medial superior olive
NDS	normal donkey serum
PB	phosphate buffer
PBS	phosphate buffered saline
PFA	paraformaldehyde

SD	standard deviation
sEPSC	spontaneous excitatory postsynaptic currents
SNR	signal-to-noise ratio
SOC	superior olivary complex
SPN	superior paraolivary nucleus
SSA	stimulus-specific adaptation
VAS	ventral acoustic stria
vGluT1&2	vesicular glutamate transporter 1 & 2
VNTB	ventral nucleus of the trapezoid body
VS	vector strength
WT	wildtype

## 10 Acknowledgments

First and foremost I want to thank Prof. Dr. Ursula Koch for giving me the chance to work in her group and to realize this thesis. Her support and guidance during my time as her student was of invaluable help. Thanks to her expertise in uncountable aspects in the field of science, it was possible for me to overcome a multitude of everyday research issues.

Moreover, my thanks go to Dr. Daniela Vallentin for taking the time and making the effort to evaluate this work.

I was pleased to share my life in the lab with many dear colleagues. Franziska was always willing to listen to my deliberations and shared her knowledge about ‘the kids’ stuff’ with me. Victor, without you, life was much less purple. Eli comprehensively introduced me to immunohistochemistry and confocal imaging. Yet, you’re awesome. Which also holds true for Julia and Broni, who enriched humdrum office microcosm with excellence and simplicity. Fauve, Conny, Karin, our lab could not survive without your interventions. You taught me so much about quick’n’dirty. And meticulousness. Basement philosopher Peter also contributed decisively to the success of my experiments. Either with calm and tidy animals, or with considerations about ancient vinyls. Last, Waltraud and Angelika, my whole respect goes to you for easing the pain from bureaucracy.

Importantly, I want to thank the SFB 665: Developmental Disturbances in the Nervous System for financing my project.

Tremendous thanks go to my family, including Elisabeth and Rolf. Without your backing, many facets in the struggle of life would have been unbearable.

My deepest gratitude goes to Kathi.